

EUROPEAN ORGANISATION FOR NUCLEAR RESEARCH (CERN)



JHEP 07 (2023) 116
DOI: [10.1007/JHEP07\(2023\)116](https://doi.org/10.1007/JHEP07(2023)116)



CERN-EP-2022-147
20th November 2024

Search for dark matter produced in association with a dark Higgs boson decaying into W^+W^- in the one-lepton final state at $\sqrt{s} = 13 \text{ TeV}$ using 139 fb^{-1} of $p p$ collisions recorded with the ATLAS detector

The ATLAS Collaboration

Several extensions of the Standard Model predict the production of dark matter particles at the LHC. A search for dark matter particles produced in association with a dark Higgs boson decaying into W^+W^- in the $\ell^\pm\nu q\bar{q}'$ final states with $\ell = e, \mu$ is presented. This analysis uses 139 fb^{-1} of $p p$ collisions recorded by the ATLAS detector at a centre-of-mass energy of 13 TeV . The $W^\pm \rightarrow q\bar{q}'$ decays are reconstructed from pairs of calorimeter-measured jets or from track-assisted reclustered jets, a technique aimed at resolving the dense topology from a pair of boosted quarks using jets in the calorimeter and tracking information. The observed data are found to agree with Standard Model predictions. Scenarios with dark Higgs boson masses ranging between 140 and 390 GeV are excluded.

1 Introduction

An overwhelming body of astrophysical evidence [1–4] primarily from galactic rotation velocity measurements, from the gravitational lensing effect and from the spectral analysis of the cosmic microwave background in the context of the Big Bang nucleosynthesis strongly supports the existence of dark matter (DM). The Standard Model of particle physics (SM) does not provide a viable DM candidate. The particle nature of DM is one of the major questions in physics.

Several extensions of the SM postulate a DM candidate χ that is a stable, electrically neutral, and weakly interacting massive particle (WIMP) [4]. Such WIMPs can potentially be produced in high-energy collisions at the CERN Large Hadron Collider (LHC). Their production at the LHC would be characterized by a striking signature with an imbalance in the measured transverse momentum¹ from the WIMPs escaping detection, denoted as missing transverse momentum $\mathbf{p}_T^{\text{miss}}$ with magnitude $E_T^{\text{miss}} \equiv |\mathbf{p}_T^{\text{miss}}|$. Hence, a wide class of DM models probed at the LHC postulate processes where one or more SM particles X are produced recoiling against DM particles, resulting in an ‘ $X + E_T^{\text{miss}}$ ’ signature. Searches at the LHC have considered X to be a hadronic jet [5, 6], top or bottom quarks [7–12], a photon [13, 14], a W or Z boson [15–18], or a Higgs boson [19–21].

Recently, exploration of a new $X + E_T^{\text{miss}}$ DM signature began at the LHC, where X is a hypothetical particle that is produced in proton–proton (pp) collisions and decays into a vector-boson pair $VV = W^+W^-$ or ZZ . It was first probed by the ATLAS Collaboration in the fully hadronic decay channel $VV \rightarrow q\bar{q}'q''\bar{q}'''$, where the invariant mass of the diboson system, m_{VV} , is above 160 GeV [22].

This paper presents an exploration of the hitherto uncharted semileptonic decay channel $W^+W^- \rightarrow \ell^\pm\nu q\bar{q}'$. In the signal region (SR), events are required to have large E_T^{miss} from DM particles escaping detection and the neutrino from the leptonically decaying W boson, an energetic electron or a muon, and a hadronically decaying W boson. Candidate $W \rightarrow q\bar{q}'$ decays are identified as a pair of small-radius jets with an invariant mass consistent with the W boson mass m_W , or, if sufficiently boosted, i.e. with a sufficiently high p_T , as a single large-radius jet with a similar invariant mass requirement. The latter category dominates the sensitivity, due to significantly smaller backgrounds. Large-radius jets are identified using the track-assisted reclustered (TAR) jet reconstruction technique [23] that was first employed in Ref. [22]. The background is dominated by vector-boson production in association with jets, referred to as $V+\text{jets}$ in the following. The analysis employs a control region (CR), defined by requiring a large separation in polar angle between the hadronic W candidate and the charged lepton, to improve the modelling of the $W+\text{jets}$ background by determining its yield from data. Another CR requiring two or more b -quark jets is used to constrain the contribution of the $t\bar{t}$ background and to improve its modelling in the SR.

The discovery of a new boson [24, 25] consistent with the expectations for the SM Higgs boson confirmed the Brout–Englert–Higgs (BEH) mechanism for electroweak symmetry breaking [26–31] that is ultimately responsible for the generation of masses for SM particles. The experimental confirmation of the BEH mechanism motivates a similar mechanism for mass generation in the dark sector that contains the DM particle [32]. In this theoretical paradigm, a fermionic DM particle obtains its mass through Yukawa interactions with a dark Higgs boson, s [33]. Another motivation for this theoretical scenario is the

¹ ATLAS uses a right-handed coordinate system with its origin at the nominal interaction point (IP) in the centre of the detector and the z -axis along the beam pipe. The x -axis points from the IP to the centre of the LHC ring, and the y -axis points upwards. Cylindrical coordinates (r, ϕ) are used in the transverse plane, ϕ being the azimuthal angle around the z -axis. The pseudorapidity is defined in terms of the polar angle θ as $\eta = -\ln \tan(\theta/2)$. Angular distance is measured in units of $\Delta R \equiv \sqrt{(\Delta\eta)^2 + (\Delta\phi)^2}$.

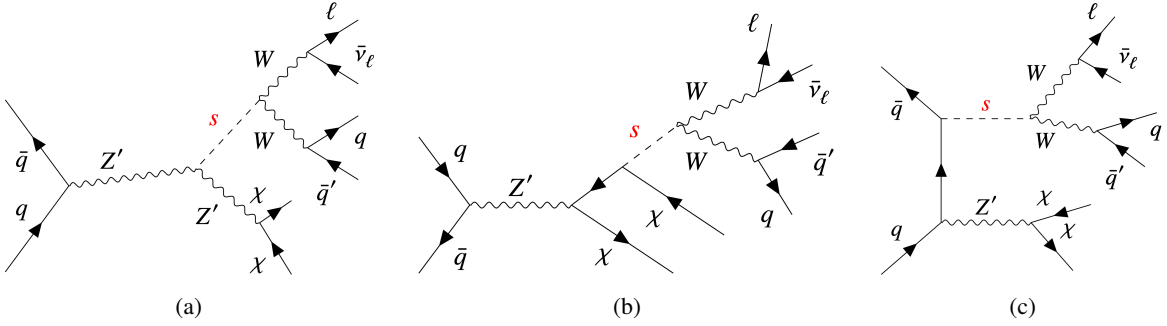


Figure 1: Representative Born-level Feynman diagrams for resonant $q\bar{q} \rightarrow Z' \rightarrow s\chi\chi$ production where the dark Higgs boson decays into semileptonic final states, $s \rightarrow W^-(\ell^-\bar{\nu})W^+(q\bar{q}')$. Diagram (a) typically dominates for high $m_{Z'}$, while diagram (c) contributes most for $m_{Z'} \lesssim 2m_\chi + m_s$. Diagram (b) makes a sizeable contribution throughout the parameter space considered. Charge-conjugated processes are implied.

provision of a new DM annihilation channel into SM particles involving the dark Higgs boson when it, rather than the WIMP DM particle, is the lightest state in the dark sector. This feature addresses the stringent experimental constraints from the observed DM relic density [34]. The dark Higgs boson can be identified with the aforementioned resonance decaying into a pair of massive vector bosons, $s \rightarrow VV$, and produced in association with DM, which strongly motivates exploring the $s(\rightarrow VV) + E_T^{\text{miss}}$ signature presented in this paper. This signature is complementary to the jet + E_T^{miss} signature, which is always present for DM production at the LHC irrespective of the underlying model, since WIMPs result in E_T^{miss} and additional jet(s) can be produced from initial-state radiation.

A two-mediator-based DM model [35] is used for the optimization and interpretation of the search presented in this paper. This model features a new $U(1)'$ gauge symmetry, which yields an additional massive spin-1 vector boson Z' through the BEH mechanism involving a new complex Higgs field and producing the new physical dark Higgs boson s . The characteristic model parameters are the mass m_χ of the Majorana DM particle, which is a singlet under all SM symmetries, the Z' mass $m_{Z'}$, the dark Higgs mass m_s , the Z' couplings g_q to quarks, the Z' couplings g_χ to DM particles, and the mixing angle θ between the SM and dark Higgs bosons [33], which is set to a small value [22]. Representative Born-level Feynman diagrams for the signal processes targeted in this search are shown in Figure 1. The $s + \chi\chi$ signal is produced through the $q\bar{q} \rightarrow Z' \rightarrow s\chi\chi$ process, which requires an off-shell intermediate state such as a Z' or χ . The dark Higgs boson interacts with SM particles only via mixing with the SM Higgs boson, resulting in the same decay branching fractions as a SM Higgs boson with a different mass as long as the $s \rightarrow \chi\chi$ process is kinematically forbidden. The $s \rightarrow W^\pm W^\mp$ and $s \rightarrow ZZ$ processes become important for $m_s \gtrsim 160$ GeV and $m_s \gtrsim 180$ GeV, respectively [36]. The proposed dark Higgs two-mediator DM model framework shares similarities with previously explored spin-1 simplified DM models [37–42], where s is the only new additional particle and χ is a Majorana fermion rather than a Dirac fermion. All choices of common model parameters are made in alignment with Ref. [42] to facilitate comparisons between experiments and between search channels. Other searches in pp collisions for a spin-1 mediator that is identified with the Z' boson in the two-mediator-based DM model provide complementary sensitivity [43]. The strongest limits come from dijet searches, which exclude the full $m_{Z'}$ range investigated in this paper with the chosen parameters [44]. Nevertheless, the exploration of the $s(\rightarrow VV) + E_T^{\text{miss}}$ signature is still strongly motivated, as the aforementioned complementarity relies on the assumptions about the underlying simplified model which may not be realised in a complete model, and on the choice of couplings like g_χ and g_q .

The paper is organized as follows. The ATLAS detector and the analysed data set together with simulations

are discussed in Sections 2 and 3. The reconstruction of events is covered in Section 4, which is followed by a description of the track-assisted reclustering algorithm in Section 5. The data analysis procedures are summarized in Section 6 and the corresponding systematic uncertainties are estimated in Section 7. The results are presented in Section 8 and conclusions are drawn in Section 9.

2 ATLAS detector

The ATLAS detector [45] at the LHC covers nearly the entire solid angle around the collision point. It consists of an inner tracking detector (ID) surrounded by a thin superconducting solenoid, electromagnetic and hadronic calorimeters, and a muon spectrometer incorporating three superconducting toroidal magnets.

The ID system is immersed in a 2 T axial magnetic field and provides charged-particle tracking in the range $|\eta| < 2.5$. The high-granularity silicon pixel detector covers the vertex region and typically provides four measurements per track [46, 47]. It is followed by the silicon microstrip tracker, which usually provides eight measurements per track for central $|\eta|$. These silicon detectors are complemented by the transition radiation tracker, which enables radially extended track reconstruction up to $|\eta| = 2.0$. This detector also provides electron identification information based on the fraction of hits (typically 30 in total) above a higher energy-deposit threshold corresponding to transition radiation.

The calorimeter system covers the pseudorapidity range $|\eta| < 4.9$. Within the region $|\eta| < 3.2$, electromagnetic calorimetry is provided by barrel and endcap high-granularity lead/liquid-argon (LAr) calorimeters, with an additional thin LAr presampler covering $|\eta| < 1.8$ to correct for energy loss in material upstream of the calorimeters. Hadronic calorimetry is provided by the steel/scintillator-tile calorimeter, segmented into three barrel structures within $|\eta| < 1.7$, and two copper/LAr hadronic endcap calorimeters. The solid angle coverage is completed with forward copper/LAr and tungsten/LAr calorimeter modules optimized for electromagnetic and hadronic measurements respectively.

The muon spectrometer comprises separate trigger and high-precision tracking chambers measuring the deflection of muons in a magnetic field generated by the superconducting air-core toroids. The field integral of the toroids ranges between 2.0 and 6.0 T m across most of the detector. A set of precision chambers covers the region $|\eta| < 2.7$ with three layers of monitored drift tubes, complemented by cathode-strip chambers in the forward region, where the background is highest. The muon trigger system covers the range $|\eta| < 2.4$ with resistive-plate chambers in the barrel, and thin-gap chambers in the endcap regions.

Events are selected to be recorded by the first-level (L1) trigger system implemented in custom hardware, followed by selections made by algorithms implemented in software in the high-level trigger (HLT) [48]. The L1 trigger accepts events from the 40 MHz bunch crossings at a rate below 100 kHz, which the HLT reduces in order to record events to disk at about 1 kHz.

An extensive software suite [49] is used in the reconstruction and analysis of real and simulated data, in detector operations, and in the trigger and data acquisition systems of the experiment.

3 Data and simulated events

The data used in this analysis are proton–proton collisions provided by the LHC during 2015–2018 and recorded by the ATLAS detector. The data were taken at a centre-of-mass energy of $\sqrt{s} = 13$ TeV with a

minimum separation of 25 ns between consecutive crossings of proton bunches from the two beams. The data set corresponds to an integrated luminosity of 139 fb^{-1} , determined by using the LUCID-2 detector [50] for the primary luminosity measurement. The corresponding uncertainty is 1.7% [51]. The data were collected using a missing transverse momentum trigger in combination with single-muon triggers [52–54]. The missing transverse momentum trigger is based on $\mathbf{p}_T^{\text{miss, trigger}}$ as computed from calorimeter information. Depending on the data-taking period, the missing transverse momentum trigger was one of a set with thresholds ranging from $E_T^{\text{miss, trigger}} = 70 \text{ GeV}$ to $E_T^{\text{miss, trigger}} = 110 \text{ GeV}$. In the absence of muons, this set of triggers was measured to be fully efficient for events with $E_T^{\text{miss}} > 200 \text{ GeV}$, as reconstructed using offline algorithms. Events with muons can escape the E_T^{miss} triggers. This is because muons tend to deposit negligible amounts of energy in the calorimeters and hence contribute to $\mathbf{p}_T^{\text{miss, trigger}}$ that is reconstructed using exclusively calorimeter information. This can result in a lower $E_T^{\text{miss, trigger}}$ for signal events in kinematic configurations where the muon counterbalances the p_T from the neutrino and the WIMPs. To compensate for the decreased efficiency of the E_T^{miss} trigger, which is particularly pronounced for high- p_T muons, a combination of single-muon triggers was added. Some of these with an isolation criterion applied a low p_T threshold ranging from 20 GeV to 26 GeV in different data-taking periods, while others without an isolation criterion applied a p_T threshold ranging from 50 GeV to 60 GeV. In events selected by a muon trigger, an offline reconstructed muon is required to match the trigger-level muon. This combination of a missing transverse momentum trigger and single-muon triggers was measured to be fully efficient for the examined final states after the selections described in Section 6.1.

Monte Carlo (MC) simulations were used to model the expected kinematic behaviour of SM background processes as well as the investigated signal. They are described in the following, starting with the SM background processes relevant to this analysis.

The $W + \text{jets}$ production process was simulated with the SHERPA 2.2.10 generator [55] using next-to-leading-order (NLO) matrix elements for up to two partons, and leading-order (LO) matrix elements for up to four partons, calculated with the Comix [56] and OPENLOOPS [57–59] libraries. They were matched with the SHERPA parton shower [60] using the MEPS@NLO prescription [61–64] and the set of tuned parameters developed by the SHERPA authors. The samples were normalized to a next-to-next-to-leading-order (NNLO) prediction [65]. The $Z + \text{jets}$ process was generated using an identical set-up, except that SHERPA 2.2.11 was used and LO matrix elements were calculated for up to five partons.

Samples of diboson final states (VV) were simulated with the SHERPA 2.2.1 or 2.2.2 generator depending on the process, including off-shell effects and Higgs boson contributions where appropriate. Fully leptonic final states and semileptonic final states, where one boson decays leptonically and the other hadronically, were generated using matrix elements at NLO accuracy in QCD for up to one additional parton and at LO accuracy for up to three additional parton emissions. Samples for the loop-induced processes $gg \rightarrow VV$ were generated using LO-accurate matrix elements for up to one additional parton emission. The matrix element calculations were matched and merged with the SHERPA parton shower based on Catani–Seymour dipole factorization [56, 60] using the MEPS@NLO prescription. The virtual QCD corrections were provided by the OPENLOOPS library.

The electroweak $VVjj$ production processes, which include vector-boson scattering, vector-boson fusion Higgs production, and triboson processes with this final state when taking interference into account, as well as triboson (VVV) processes with other final states, were simulated with the SHERPA 2.2.2 generator using factorized gauge-boson decays. To account for interference, the two sets of triboson processes are treated together and labelled ‘triboson’ in the following. Matrix elements, accurate to NLO for the inclusive process and to LO for up to two additional parton emissions (VVV) or accurate to LO ($VVjj$),

were matched and merged with the **SHERPA** parton shower based on Catani–Seymour dipole factorization using the **MEPS@NLO** prescription. The virtual QCD corrections for matrix elements at NLO accuracy were provided by the **OPENLOOPS** library.

All **SHERPA** weak-boson samples were generated using the NNPDF3.0NNLO set of parton distribution functions (PDFs) [66], along with the dedicated set of tuned parton-shower parameters developed by the **SHERPA** authors. For all weak-boson processes, uncertainties from missing higher orders were evaluated [67] using seven variations of the QCD factorization and renormalization scales in the matrix elements by factors of 0.5 and 2, excluding variations in opposite directions. Uncertainties associated with the PDF set were evaluated according to the PDF4LHC recommendations [68]: uncertainties in the nominal PDF set were calculated using 100 replica variations. The effect of the uncertainty in the strong coupling constant α_s was assessed by variations of ± 0.001 . Uncertainties arise from the scale choices for the matching of the matrix elements (CKKW) [69] and the resummation calculations to the **SHERPA** parton-shower algorithm. These uncertainties are evaluated by changing the nominal CKKW scale of 20 GeV to either 15 GeV or 30 GeV and by varying the resummation scale by a factor of 0.5 or 2. The same relative uncertainties were assumed for VVV and $VVjj$ backgrounds per analysis region. For $Z+jets$, all uncertainties were extrapolated from $W+jets$ in order to avoid large effects from statistical fluctuations.

The production of $t\bar{t}$ events was modelled using the Powheg Box v2 [70–73] generator at NLO with the NNPDF3.0NLO PDF set and the h_{damp} parameter set to $1.5 m_{\text{top}}$ [74]. The h_{damp} parameter is a resummation damping factor and one of the parameters that controls the matching of Powheg matrix elements to the parton shower and thus effectively regulates the high- p_T radiation against which the $t\bar{t}$ system recoils. The events were interfaced to Pythia 8.230 [75] to model the parton shower, hadronization, and underlying event, with parameter values set according to the A14 tune [76] and using the NNPDF2.3LO set of PDFs [77]. The decays of bottom and charm hadrons in all MC samples involving top quarks were performed by EvtGen 1.6.0 [78].

The production of top quarks in association with W bosons (tW) was modelled by the Powheg Box v2 [71–73, 79] generator at NLO in QCD, using the five-flavour scheme and the NNPDF3.0NLO set of PDFs. The diagram removal scheme [80] was used to remove interference and overlap with $t\bar{t}$ production. The related uncertainty was estimated by comparing these events with an alternative sample generated using the diagram subtraction scheme [74, 80]. The events were interfaced to Pythia 8.230, which used the A14 tune and the NNPDF2.3LO set of PDFs.

Single-top t -channel production was modelled by the Powheg Box v2 [71–73, 81] generator at NLO in QCD, using the four-flavour scheme and the corresponding NNPDF3.0NLO set of PDFs. The events were interfaced with Pythia 8.230, which used the A14 tune and the NNPDF2.3LO set of PDFs. Single-top s -channel production was studied and found to be negligible.

For all processes involving top quarks, the uncertainty due to initial-state radiation was estimated by simultaneously varying the h_{damp} parameter and the renormalization and factorization scales μ_r and μ_f , and choosing the Var3c up/down variants of the A14 tune as described in Ref. [82]. The impact of final-state radiation was evaluated by raising or lowering the renormalization scale for emissions from the parton shower by a factor two. To evaluate the PDF uncertainties for the nominal PDF, the 100 variations for NNPDF3.0NLO were taken into account; for $t\bar{t}$ the effect of a ± 0.001 change in α_s was also evaluated. The uncertainty due to the parton-shower and hadronization model was evaluated by comparing the nominal samples of events with samples where events generated by Powheg Box v2 [71–73, 79] were interfaced to Herwig 7.04 [83, 84], using the H7UE set of tuned parameters [84] and the MMHT2014LO PDF set [85]. To assess the uncertainty in the matching of NLO matrix elements to the parton shower, the Powheg Box

samples were compared with samples of events generated with `MADGRAPH5_AMC@NLO` 2.6.0 interfaced with `PYTHIA` 8.230. The `MADGRAPH5_AMC@NLO` calculation used the NNPDF3.0NLO set of PDFs, and `PYTHIA` 8 used the A14 tune and the NNPDF2.3LO set of PDFs.

Simulated event samples for the $pp \rightarrow Z' \rightarrow s\chi\chi \rightarrow W^+W^-\chi\chi \rightarrow q\bar{q}'\ell^\pm\nu\chi\chi$ process were generated at LO in QCD with up to one additional parton in the event, using `MADGRAPH5_AMC@NLO` 2.8.1 [86] with the NNPDF3.0NLO PDF set. Other processes arising from the dark Higgs model could also contribute to the analysis regions of this search but were not considered. These include the $s \rightarrow hh$ decay channel, which contributes a small fraction of the signal for $m_s > 250$ GeV. The parton-showering process was simulated with `PYTHIA` 8.244 using the A14 tune and the NNPDF2.3LO set of PDFs. Samples were generated in the $(m_{Z'}, m_s)$ plane for $0.3 \leq m_{Z'} \leq 3.3$ TeV and for $115 \leq m_s \leq 385$ GeV. Other dark Higgs model parameter values were chosen as $m_\chi = 200$ GeV to avoid $s \rightarrow \chi\chi$ decays in the m_s range considered, $g_\chi = 1.0$, $g_q = 0.25$ [40, 42], and $\sin\theta = 0.01$ [22]. Uncertainties due to QCD factorization and renormalization were estimated using seven variations of the scales by factors of 0.5 and 2, avoiding variations in opposite directions. Uncertainties from the PDF set were estimated using 100 replica variations. The uncertainties due to the parton-shower and hadronization model were estimated by comparing the nominal samples with alternative samples from the same matrix element generator but interfaced with `HERWIG` 7.2.1, using the H7UE set of tuned parameters and the NNPDF3.0NLO PDF set.

The effect of multiple interactions in the same and neighbouring bunch crossings (pile-up) was modelled by overlaying the simulated hard-scattering event with inelastic pp events generated with `PYTHIA` 8.186 [87] using the NNPDF2.3LO set of PDFs and the A3 tune [88]. The detector response for all MC samples was modelled with a full detector simulation [89] based on `GEANT4` [90].

4 Event reconstruction

Each event requires the presence of at least one pp collision vertex that is reconstructed from at least two ID tracks with $p_T^{\text{track}} > 0.5$ GeV. The vertex with the highest $\sum(p_T^{\text{track}})^2$ in the event is designated the primary vertex (PV). The ID tracks must have at least seven hits and satisfy $p_T > 0.5$ GeV and $|\eta| < 2.5$ requirements [91, 92]. Their transverse and longitudinal impact parameters relative to the PV must satisfy $|d_0| < 2$ mm and $|z_0 \sin(\theta)| < 3$ mm, respectively, where θ is the polar angle of the track.

Charged leptons $\ell = e, \mu$ are used to identify events with leptonic final states produced in decays of W bosons. This includes τ -lepton decays into ℓ . Hadronic τ -lepton decays are not considered due to their small contribution to the overall sensitivity of the analysis. Electrons [93] are reconstructed by matching clusters of energy deposited in the calorimeter to an ID track. Candidate electrons are identified using a likelihood-based method, and must satisfy the ‘Medium’ requirement and be matched to the PV of the event. Furthermore, they must fall within $|\eta| < 2.47$, have $p_T > 7$ GeV, and be isolated from additional activity reconstructed in the calorimeter and the tracker, following the ‘Loose’ isolation requirement. To veto additional electrons in the event, the identification requirement is relaxed to satisfy the ‘Loose’ working point and have a hit in the innermost layer of the pixel detector, while the isolation requirement remains unchanged. Muons [94] are reconstructed by matching a track or track segment detected in the muon spectrometer, depending on the p_T and $|\eta|$ range, to an ID track that is matched to the PV. Muon candidates must satisfy ‘Medium’ requirements, have $p_T > 7$ GeV and fall within $|\eta| < 2.5$. Furthermore, they must be isolated from additional activity reconstructed in the tracker within a cone of p_T -dependent angular size ΔR around the muon, following the ‘FixedCutTightTrackOnly’ isolation requirement. To veto additional muons, the identification requirement is relaxed to satisfy the ‘Loose’ working point and

Table 1: Overview of the electron and muon selection criteria.

Feature	Electron	Veto electron	Muon	Veto muon
Pseudorapidity range	$ \eta < 2.47$	$ \eta < 2.47$	$ \eta < 2.5$	$ \eta < 2.7$
Transverse momentum	$p_T > 7 \text{ GeV}$	$p_T > 7 \text{ GeV}$	$p_T > 7 \text{ GeV}$	$p_T > 7 \text{ GeV}$
Identification	Medium	Loose	Medium	Loose
Isolation	Loose	Loose	FixedCutTightTrackOnly	-

the muon is required to fall within $|\eta| < 2.7$, which corresponds to the acceptance region of the muon spectrometer, while the isolation requirement is dropped. The selections for leptons are summarized in Table 1. Electrons and muons which satisfy only the relaxed definition are labelled as ‘veto leptons’.

To avoid reconstruction ambiguities, if a muon candidate and an electron candidate share a track, the muon candidate is ignored from further analysis if it is calorimeter-tagged, and the electron candidate otherwise. Calorimeter-tagged muons are identified as an ID track that can be matched only to an energy deposit in the calorimeter compatible with a minimum-ionizing particle. Since muons of this type have no muon spectrometer information, they have lower purity than other muon types [94].

Jets of hadrons are used to identify the hadronically decaying W bosons and other hadronic activity in the event. Particle-flow (PFlow) jets are constructed from charged constituents associated with the PV and neutral constituents [95] using the anti- k_t algorithm [96, 97] with a radius parameter of $R = 0.4$. The energy of PFlow jets is calibrated to the particle scale using a sequence of corrections, including pile-up subtraction and in situ calibration [98], and the energy resolution in MC simulations is calibrated to match that found in data. PFlow jets are required to have $p_T > 20 \text{ GeV}$ and fall within the acceptance region of the ID, i.e. $|\eta| < 2.5$. The jet vertex tagger (JVT) discriminant is applied to reject jets with $p_T < 60 \text{ GeV}$ and $|\eta| < 2.4$ originating from pile-up interactions through the use of tracking and vertexing information [99]. PFlow jets closer than $\Delta R = 0.2$ to an electron are rejected. A similar requirement is applied to PFlow jets with fewer than three tracks in the vicinity of a muon. Electrons or muons at an angular distance of less than $\Delta R = \min(0.4, 0.04 + 10 \text{ GeV}/p_T^\ell)$ from a jet are rejected, as they are likely to originate from hadron decays within jets. Here, $\Delta R \propto 1/p_T^\ell$ accounts for tighter collimation of electromagnetic showers from electrons and final-state radiation from electrons and muons with increasing p_T .

The decay products of boosted W bosons with $p_T \gtrsim 150 \text{ GeV}$ are collimated, which makes the matching of the energy deposits to the individual quarks from the $W \rightarrow q\bar{q}'$ decay challenging. This is addressed through jets that are formed from the energy in three-dimensional clusters of calorimeter cells using the anti- k_t algorithm with a small radius parameter of $R = 0.2$. The energy of the input calorimeter cells is corrected for dead material, out-of-cluster losses for pions, and calorimeter response to hadronic energy clusters, which are identified using their topology and energy density. These corrections are implemented with a local cell signal weighting (LCW) method [100]. Corrections for pile-up and the energy scale and resolution—following methodologies similar to those in Ref. [101]—are subsequently applied to $R = 0.2$ jets. The $R = 0.2$ jets must have $p_T > 20 \text{ GeV}$ and fall within the acceptance region of the ID, i.e. $|\eta| < 2.5$. The reconstruction of highly boosted, hadronically decaying W bosons is discussed in Section 5.

In order to suppress contributions from background processes that involve top quarks, which decay almost exclusively to b -quarks, a multivariate deep-learning algorithm, DL1r, is used to identify (b -tag) jets containing b -hadrons. The b -tagging is performed using PFlow jets with a working point corresponding to an efficiency of 77% [102] for jets containing b -hadrons. Events containing b -tagged jets are rejected.

The $\mathbf{p}_T^{\text{miss}}$ vector is computed as the negative vector sum of the transverse momenta of the veto electrons, veto muons, PFlow jet candidates, and ID tracks not associated with the aforementioned objects [103]. Hadronically decaying τ -leptons and photons are not explicitly considered in the $\mathbf{p}_T^{\text{miss}}$ calculation. In addition, an object-based E_T^{miss} significance \mathcal{S} is used to reject multijet background events. The \mathcal{S} observable is computed from the expected resolutions for all the objects used in the E_T^{miss} calculation [104].

5 Track-assisted reclustering

With increasing momenta of the dark Higgs boson, its decay products and ultimately the products of the $W \rightarrow q\bar{q}'$ decay become more boosted and hence more collimated. The track-assisted reclustering (TAR) algorithm [23] is employed to reconstruct the topological substructure of boosted $W \rightarrow q\bar{q}'$ decays. This algorithm improves the resolution of jet substructure observables by considering both tracking and calorimeter information, combined with the flexibility of jet reclustering. The TAR jets are formed from $R = 0.2$ jets reclustered into larger jets with $R = 1$ using trimming parameters optimized for the ATLAS experiment [105]. The trimming procedure was shown to improve the mass resolution of W decay jets despite the pile-up corrections to the input $R = 0.2$ jets. Any $R = 0.2$ jets overlapping with an electron within $\Delta R = 0.2$ are not considered in the reclustering process. The mass and other substructure observables of TAR jets are reconstructed using ID tracks. For this, ID tracks are first matched to the $R = 0.2$ jets that constitute the $R = 1$ jets using a two-step procedure. First, ID tracks are matched to $R = 0.2$ jets using ghost association [106]. Second, any remaining tracks closer than $\Delta R = 0.3$ to $R = 0.2$ jets are matched to the closest $R = 0.2$ jet in ΔR . Tracks associated with electrons or muons are not considered in the matching procedure. Subsequently, the p_T of tracks matched to a given $R = 0.2$ jet are rescaled such that their sum equals the p_T of that jet:

$$p_T^{\text{track, new}} = p_T^{\text{track, old}} \times \frac{p_T^{R=0.2}}{\sum_i p_{T,i}^{\text{track, old}}},$$

where the sum in i runs over all tracks matched to a given $R = 0.2$ jet. The jet mass and other jet substructure observables of a reclustered $R = 1$ jet are then reconstructed from these rescaled tracks. This procedure compensates for the neutral jet components missed by the tracker and improves the reconstruction of jet substructure observables, which is limited by the angular resolution of the detector [23]. Furthermore, the TAR algorithm provides a straightforward method to calibrate and assign uncertainties to jet substructure observables by propagating calibrations and uncertainties from the well-defined constituent $R = 0.2$ jets and tracks, as is detailed in Section 7.

As already mentioned above, TAR jets with $R = 1$ are used to reconstruct $W \rightarrow q\bar{q}'$ candidate decays, leading to a two-prong jet signature. When the final-state particles from the $s \rightarrow WW \rightarrow \ell\nu q\bar{q}'$ decays are collimated due to a significant boost of the dark Higgs boson, this leads to a dense environment with the charged lepton often being very close to the hadronic W decay products, as schematically shown in Figure 2. In this situation, additional tracks from charged leptons and calorimetric energy clusters from electrons tend to fall into the catchment area of the $R = 1$ jet used to reconstruct the $W \rightarrow q\bar{q}'$ decay. For ‘standard’ large- R jets [107], this was shown to distort the kinematic properties and substructure of W boson candidate jets, resulting in a significant reduction of their identification efficiency. This effect is particularly pronounced in the $s \rightarrow WW \rightarrow e\nu_e q\bar{q}'$ decay channel. With the TAR algorithm, this challenge can be met by appropriately preselecting the input tracks and $R = 0.2$ jets, rejecting those associated with

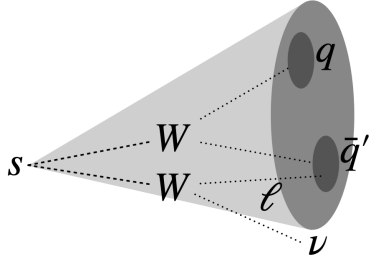


Figure 2: Sketch of the $s \rightarrow WW \rightarrow \ell\nu q\bar{q}'$ decay where the dark Higgs boson is significantly boosted, reconstructed as a large- R jet in the detector. The collimation due to the boost of the dark Higgs decay products often leads to an overlap of the charged lepton ℓ and the large- R jet from the $W \rightarrow q\bar{q}'$ decay.

leptons, as described above. This ensures that only hadronic objects are considered in the reconstruction of the $W \rightarrow q\bar{q}'$ candidates using TAR jets. Hence, the typical two-prong structure with a reconstructed mass near the W boson mass is preserved. The small radius parameter of $R = 0.2$ used for the reconstruction of anti- k_t subjets forming TAR jets prevents significant numbers of hadronic components from being removed because of their proximity to electrons.

The criteria used to identify W candidates in this search are the TAR jet mass and the ratio of energy correlation functions $D_2^{\beta=1}$ [108], which is a measure for judging whether the topological substructure of a jet is consistent with a two-prong decay. The identification criteria are chosen to optimize the $W \rightarrow q\bar{q}'$ identification efficiency while effectively rejecting fake W candidates from QCD jets present in the dominant W +jets background processes. This is further described in Section 6.2.

6 Analysis

As a reminder, the target signature of this analysis, $s \rightarrow WW \rightarrow \ell\nu q\bar{q}'$, is characterized by a single charged lepton ℓ , missing transverse momentum, and a hadronically decaying W boson candidate W_{had} . The SR is split into two categories based on the reconstruction method used for W_{had} : a *merged* category, where the hadronically decaying W boson candidate is reconstructed as a single $R = 1$ TAR jet, and a *resolved* category, where the candidate consists of two $R = 0.4$ jets. The merged reconstruction method is characterized by its excellent background rejection, but also a relatively low signal efficiency. This motivates the addition of the resolved category to accept signal events that fail to meet the strict criteria for the merged category but still contribute to the overall sensitivity. The orthogonality of the merged and resolved categories is ensured by prioritizing the more sensitive merged category: events fulfilling its selection criteria are not considered for the resolved category.

Dedicated control regions (CR) are constructed to improve the modelling of the W +jets and $t\bar{t}$ background processes by determining their normalizations from data. These CRs are referred to as CRW and CRTT, respectively. Each CR is split into a merged and a resolved category using the same approach as in the SR to closely match its kinematics. The final discriminant to separate signal from background in the SR is m_s^{\min} , which represents the minimum possible mass of the dark Higgs boson that is compatible with the signal process given the kinematic properties of the measured reconstructed objects; this observable is introduced in detail in Section 6.3. No m_s^{\min} information is used in the CRs that are used to constrain the overall yield of the W +jets and $t\bar{t}$ processes. The individual data analysis steps are described in greater detail in the following.

6.1 Preselection

Events that are found to contain any jets with properties consistent with beam-induced backgrounds, cosmic-ray showers, or noisy calorimeter cells are rejected [109]. All events are required to have exactly one lepton and no additional veto leptons. A missing transverse momentum of $E_T^{\text{miss}} > 200 \text{ GeV}$ is required, with a significance of $\mathcal{S} > 5$. At least one TAR jet or at least two $R = 0.4$ jets are required. Since a majority of SM background events with this signature originate from events where a single neutrino from a $W \rightarrow \ell\nu$ decay is the only source of $\mathbf{p}_T^{\text{miss}}$, a leptonic transverse mass of $m_T > 150 \text{ GeV}$ is required. The leptonic transverse mass is defined as

$$m_T = \sqrt{2p_{T,\ell}E_T^{\text{miss}} \left(1 - \cos(\phi_\ell - \phi_{\mathbf{p}_T^{\text{miss}}})\right)},$$

where the subscript ℓ indicates kinematic observables of the charged lepton. Stricter criteria are applied depending on the analysis region, as described in the following sections.

6.2 Signal regions

The selection requirements for the SR are summarized in Table 2 for the merged category and in Table 3 for the resolved category. In the following, a qualitative description of the used observables and the motivation for their use is given.

Table 2: Selection criteria for the merged category. The two CRs are analysed inclusively, i.e. not considering any m_s^{min} information. In this category the W boson candidate W_{cand} is the p_T -leading TAR jet.

Requirement	SR	CRW	CRTT
Trigger	E_T^{miss} or single muon		
N_ℓ	= 1		
$m_T [\text{GeV}]$	> 220		
$E_T^{\text{miss}} [\text{GeV}]$	> 200		
$N_{b\text{-Jets}}$	0	0	≥ 2
$N_{\text{TAR Jets}}$		≥ 1	
$m_{W_{\text{cand}}} [\text{GeV}]$		[68, 89]	
\mathcal{S}	> 16	> 12	> 12
$\Delta R(W_{\text{cand}}, \ell)$	< 1.2	> 1.8	< 1.2
$D_2^{\beta=1}$		< 1.1	
m_s^{min} binning [GeV]	[125, 165, 190, 225, 375]	incl.	incl.

In the merged category, the p_T -leading TAR jet is used to reconstruct the hadronically decaying W boson candidate W_{cand} . The invariant mass of the TAR jet, $m_{W_{\text{cand}}}$, is required to be close to the W boson mass m_W , which is taken to be 80.4 GeV [110]. Additionally, the topological jet substructure observable $D_2^{\beta=1}$ [108] is employed to select for a two-prong structure consistent with a $W \rightarrow q\bar{q}'$ decay. Figure 3(a) shows the efficiency of this reconstruction method, defined as the fraction of events with at least one TAR jet, where the p_T -leading TAR jet passes the $m_{W_{\text{cand}}}$ and $D_2^{\beta=1}$ requirements as described in Table 2, in a sample

Table 3: Selection criteria for the resolved category. The two CRs are analysed inclusively, i.e. not considering any m_s^{\min} information. In this category the W boson candidate W_{cand} is a combination of two $R = 0.4$ PFlow jets

Requirement	SR	CRW	CRTT
Orthogonality	Fails merged category selections		
Trigger	E_T^{miss} or single muon		
N_ℓ	= 1		
m_T [GeV]	> 200		
E_T^{miss} [GeV]	> 250		
$N_{b\text{-Jets}}$	0	0	≥ 2
N_{Jets}		≥ 2	
$m_{W_{\text{cand}}}$ [GeV]	[65, 95]		
S		> 16	
$\Delta R(W_{\text{cand}}, \ell)$	< 1.4	> 1.4	< 1.4
$p_{T,W_{\text{cand}}}$ [GeV]			> 150
m_s^{\min} binning [GeV]	[125, 175, 225, 275, 325, 375]	incl.	incl.

of signal events passing the preselection requirements from Section 6.1. This efficiency ranges between 5% and 30% as a function of m_s . For the dominant W +jets background, the corresponding efficiency is $(1.35 \pm 0.38)\%$, where the uncertainties are statistical only.

In the resolved category, the W_{had} candidate is reconstructed as a combination of two $R = 0.4$ PFlow jets. If several combinations of jets are possible, the pair whose invariant mass is closest to m_W is chosen. Since the W boson is expected to be significantly boosted due to the recoil from the DM particles, a high transverse momentum $p_{T,W_{\text{had}}}$ is required for the W_{had} candidate. As in the merged category, the invariant mass $m_{W_{\text{had}}}$ of the W_{had} candidate is required to be close to m_W . The efficiency of finding a W_{had} candidate fulfilling these criteria as summarized in Table 3 is shown in Figure 3(b). This efficiency is determined in a sample of events passing the preselections from Section 6.1 but not all of the requirements of the merged category, and ranges between 55% and 65% as a function of m_s . For the dominant W +jets background, the corresponding efficiency is $(31.3 \pm 2.7)\%$ considering only statistical uncertainties.

The mass distributions of the respective W_{had} candidates in the merged and resolved categories are shown in Figure 4. The $m_{W_{\text{cand}}}$ window in the merged category is tighter than in the resolved category to maximize the sensitivity.

An important kinematic feature of signal events that distinguishes them from SM background events is that the momenta of the two W bosons are almost collinear because they recoil against an energetic pair of DM particles. This leads to a small angular separation between the charged lepton and the hadronic W candidate. By contrast, that angular separation is expected to be large for W +jets or diboson processes or other backgrounds where the hadronic W candidate does not originate from a real W boson. Hence, an upper bound is placed on $\Delta R(W_{\text{cand}}, \ell)$, as shown in Tables 2 and 3 for the merged and resolved categories, respectively. The distributions of this observable in both categories are shown in Figure 5.

Events containing any b -jets are rejected in order to suppress the background contribution from $t\bar{t}$ production. The exact requirements on the observables described here and in Section 6.1 were optimized by maximizing

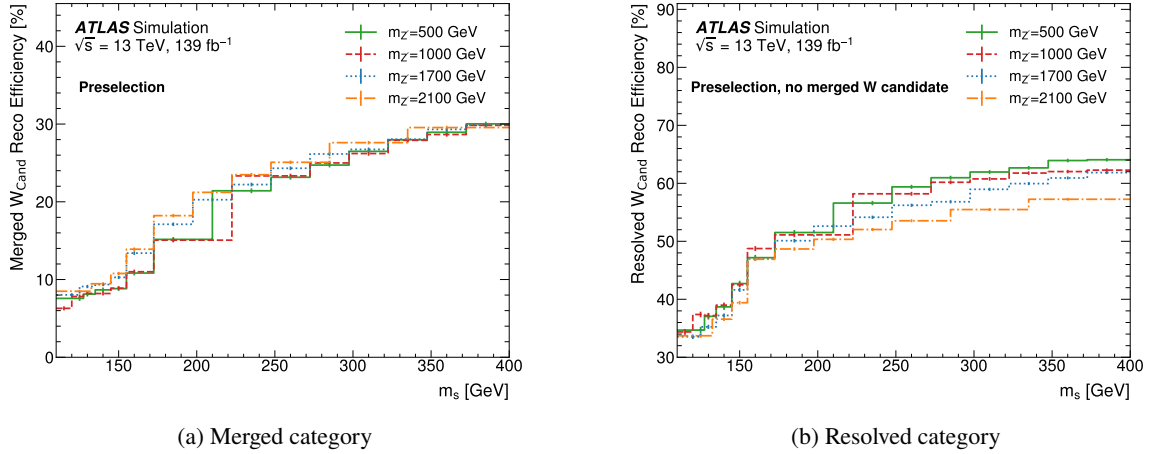


Figure 3: Probability of finding (a) at least one TAR jet, where the p_T -leading TAR jet passes the $m_{W_{\text{cand}}}$ and $D_2^{\beta=1}$ requirements in Table 2, as a function of m_s . The probability is determined in a sample of signal events passing the preselections from Section 6.1. Probability of finding (b) a W_{had} candidate reconstructed as a pair of $R = 0.4$ PFflow jets following requirements in Table 3, as a function of m_s . The probability is determined in a sample of signal events passing the preselections from Section 6.1 but not all of the requirements of the merged category. The statistical uncertainties due to finite MC samples are indicated as vertical error bars.

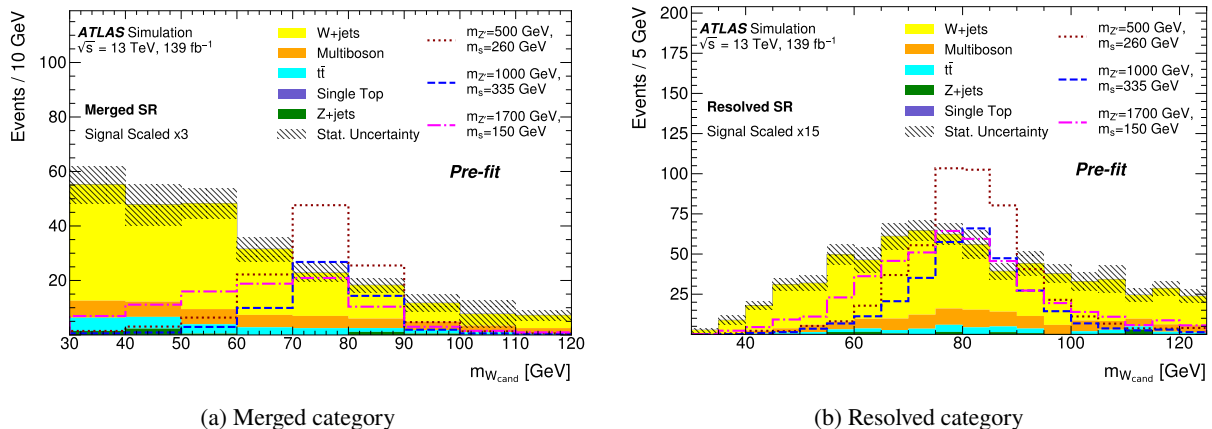


Figure 4: Distributions of $m_{W_{\text{cand}}}$ in the signal region for the merged (a) and resolved (b) category, before any fit ('Pre-fit'). The contributions from all SM backgrounds are shown as a histogram stack. The 'multiboson' category includes contributions from VV , VVV , and electroweak $VVjj$ production. The hatched bands represent the total MC statistical uncertainty of the SM expectation. The expected signal from a representative set of dark Higgs models with $g_q = 0.25$, $g_\chi = 1$, $m_\chi = 200$ GeV, and $\sin \theta = 0.01$ scaled for presentation purposes is also shown for reference. All selection criteria for the corresponding category (see Tables 2 and 3) are applied, except the one for the displayed observable.

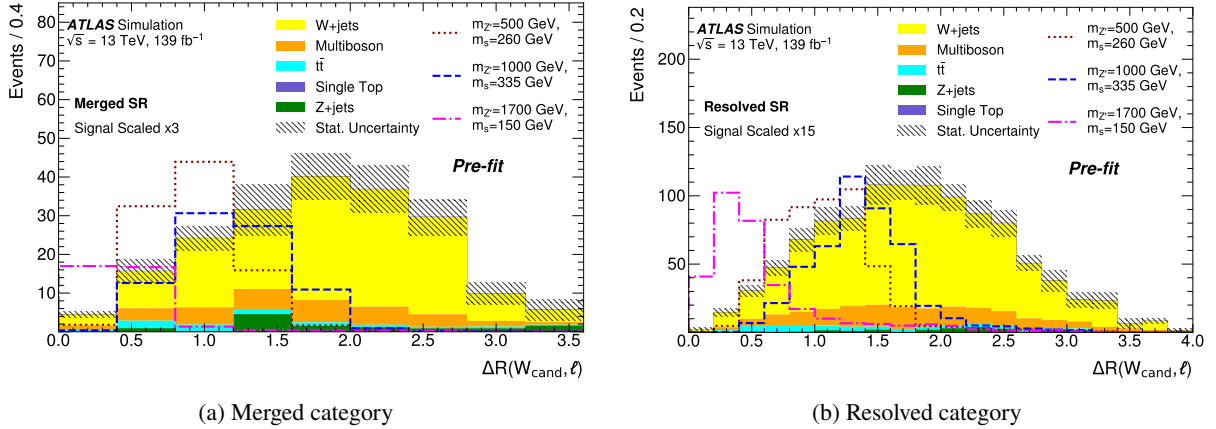


Figure 5: Distributions of $\Delta R(W_{\text{cand}}, \ell)$ in the signal region for the merged (a) and resolved (b) category, before any fit ('Pre-fit'). The contributions from all SM backgrounds are shown as a histogram stack. The 'multiboson' category includes contributions from VV , VVV , and electroweak $VVjj$ production. The hatched bands represent the total MC statistical uncertainty of the SM expectation. The expected signal from a representative set of dark Higgs models with $g_q = 0.25$, $g_\chi = 1$, $m_\chi = 200 \text{ GeV}$, and $\sin \theta = 0.01$ scaled for presentation purposes is also shown for reference. All selection criteria for the corresponding category (see Tables 2 and 3) are applied, except the one for the displayed observable.

the expected Asimov discovery significance [111], which is calculated as

$$Z_{\text{sign}} \equiv \left[2(s+b) \left(\ln \left[\frac{(s+b)(b+\sigma_b^2)}{b^2 + (s+b)\sigma_b^2} \right] - \frac{b^2}{\sigma_b^2} \ln \left[1 + \frac{\sigma_b^2 s}{b(b+\sigma_b^2)} \right] \right) \right]^{\frac{1}{2}},$$

where s and b are the expected total number of signal events and background events, respectively, and σ_b is the statistical uncertainty of the expected total number of background events. The optimization was performed within the merged and resolved categories separately. The typical acceptance \times efficiency of this analysis for the studied dark Higgs model is about 1% in both the merged and resolved categories.

6.3 Dark Higgs reconstruction strategy

An exact kinematic reconstruction of the four-momentum of the dark Higgs particle s is not possible because three invisible particles in the final state contribute to p_T^{miss} : the neutrino from the $W \rightarrow \ell\nu$ decay and the two DM particles χ . Hence, a dedicated method is used to calculate the minimum possible dark Higgs mass m_s^{\min} given the four-momentum of the hadronically decaying W boson candidate W_{cand} , the lepton four-momentum, and the invariant mass of the charged lepton and neutrino being equal to m_W . Neglecting the lepton mass, the solution for the neutrino energy in this approach is

$$E_\nu = \frac{m_W^2}{2E_\ell(1 - \cos \theta_{\ell\nu})}. \quad (1)$$

After a rotation into a coordinate system where the charged lepton travels along the z -axis and the W_{cand} momentum is in the xz -plane, the neutrino four-momentum becomes

$$p_\nu = \frac{m_W^2}{2E_\ell(1 - \cos \theta_{\ell\nu})} (\sin \theta_{\ell\nu} \cos \phi_\nu, \sin \theta_{\ell\nu} \sin \phi_\nu, \cos \theta_{\ell\nu}, 1).$$

The invariant mass of the $s \rightarrow WW$ system is then

$$\begin{aligned} m_s^2 &= (p_{W_{\text{cand}}} + p_\ell + p_\nu)^2 \\ &= (E_{W_{\text{cand}}} + E_\ell + E_\nu)^2 - (p_{x,W_{\text{cand}}} + E_\nu \sin \theta_{\ell\nu} \cos \phi_\nu)^2 \\ &\quad - (E_\nu \sin \theta_{\ell\nu} \sin \phi_\nu)^2 - (E_\ell + p_{z,W_{\text{cand}}} + E_\nu \cos \theta_{\ell\nu})^2. \end{aligned} \quad (2)$$

It can be shown that the minimum occurs when $\phi_\nu = 0$. Using this and Eq. (1), Eq. (2) can be written as

$$m_s^2 = \left(E_\ell + \frac{m_W^2}{2E_\ell(1-\cos\theta_{\ell\nu})} + E_{W_{\text{cand}}} \right)^2 - \left(\left| \vec{p}_{W_{\text{cand}}} \right| \sin \theta_{W_{\text{cand}}\ell} + \frac{m_W^2 \sqrt{1-\cos^2\theta_{\ell\nu}}}{2E_\ell(1-\cos\theta_{\ell\nu})} \right)^2 - \left(E_\ell + \left| \vec{p}_{W_{\text{cand}}} \right| \cos \theta_{W_{\text{cand}}\ell} + \frac{m_W^2 \cos \theta_{\ell\nu}}{2E_\ell(1-\cos\theta_{\ell\nu})} \right)^2,$$

which leaves only $\cos \theta_{\ell\nu}$ as an unknown. Minimizing this function over $\cos \theta_{\ell\nu}$ leads therefore to the desired observable m_s^{\min} :

$$m_s^{\min} \equiv \min_{\cos \theta_{\ell\nu}} (m_s).$$

The distributions of m_s^{\min} in the merged and resolved categories of the SR are shown in Figure 6.

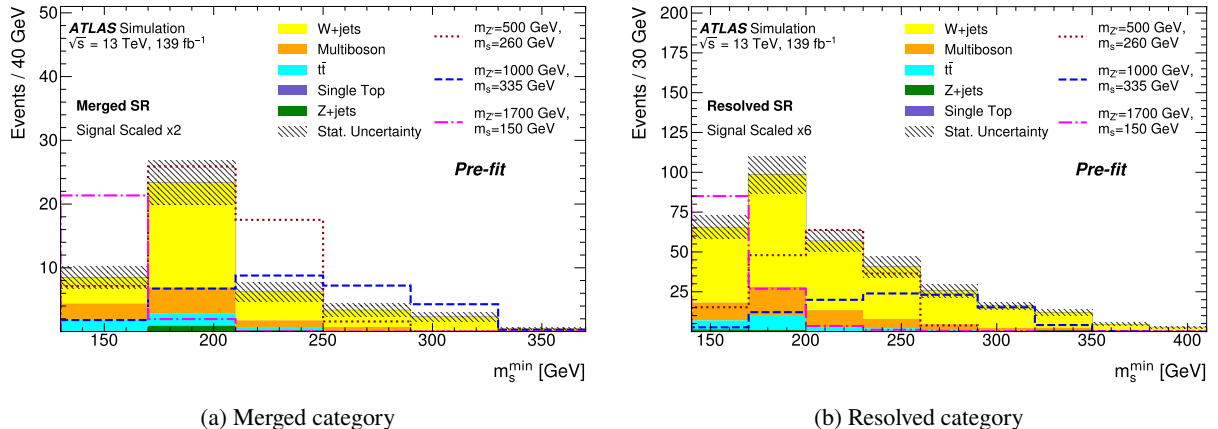


Figure 6: Distributions of m_s^{\min} in the signal region for the merged (a) and resolved (b) category, before any fit ('Pre-fit'). The contributions from all SM backgrounds are shown as a histogram stack. 'Multiboson' includes contributions from VV , VVV , and electroweak $VVjj$ production. The hatched bands represent the total MC statistical uncertainty of the SM expectation. The expected signal from a representative set of dark Higgs models with $g_q = 0.25$, $g_\chi = 1$, $m_\chi = 200$ GeV, and $\sin \theta = 0.01$ scaled for presentation purposes is also shown for reference. All selection criteria for the corresponding category (see Tables 2 and 3) are applied except for the binning in m_s^{\min} .

The m_s^{\min} observable is used as the final discriminant in the SR to separate the signal, which is resonant in m_s^{\min} , from the backgrounds, which tend to be non-resonant in m_s^{\min} . To effectively use the m_s^{\min} information, both the merged and resolved categories of the SR are split into bins. Taking into account the expected number of events and their predicted distribution in m_s^{\min} , the merged category is split into four m_s^{\min} bins of unequal width, as indicated in Table 2. In a similar spirit, the resolved category is divided into five equal-width bins of 50 GeV in m_s^{\min} , as displayed in Table 3.

6.4 Background estimation

Control regions are used to improve the modelling of dominant backgrounds. The CRs are split into merged and resolved categories in analogy with the SR to mimic its kinematic properties. In order to obtain a sufficient number of events in the CRs for the merged category, the requirement on S is lowered to $S > 12$, while all other selection requirements remain identical to those for the SR. It was confirmed that with this change the events in the CRs still closely mimic the kinematic properties of the SRs.

In order to improve the MC prediction for the dominant $W+\text{jets}$ background, a dedicated control region is used to normalize this process. This CR with suppressed signal contribution is defined by requiring $\Delta R(\text{TAR Jet}, \ell) > 1.8$ in the merged category and $\Delta R(W_{\text{cand}}, \ell) > 1.4$ in the resolved category. In a similar fashion, a CR is used for the sub-dominant $t\bar{t}$ process, and requires at least two b -tagged jets. The exact definitions of the CRs can be found in Tables 2 and 3. Other sub-dominant and minor backgrounds include $Z+\text{jets}$, diboson, triboson and single-top processes. The predictions for these backgrounds are based purely on MC simulations, normalized to their respective theoretical cross sections. About 20% of the total background is contributed by multiboson production, of which about 90% is diboson production. Generally, good agreement between data and MC simulation is found in the CRs, given the uncertainties. A potential contribution from QCD multijet production was studied and found negligible.

To predict the SM background yields in the SR, a simultaneous profile likelihood fit [112] is performed to constrain the MC yields with the observed data in the CRs, using standard minimization algorithms [113, 114]. Four background normalization factors are used separately for the $W+\text{jets}$ and $t\bar{t}$ processes in the merged and resolved regimes, and are allowed to float freely in the fit. The systematic uncertainties discussed in Section 7 are parameterized as nuisance parameters with Gaussian or log-normal prior probabilities in the fit.

7 Systematic uncertainties

In the following, the estimation of the relevant systematic uncertainties for background and signal processes is discussed. The systematic effects are studied coherently across all analysis regions. The impact of the uncertainties is quantified as the fractional effect relative to the total background yield in the merged (resolved) category of the SR before any fit, using an X% (Y%) format.

A major source of uncertainty is the statistical uncertainty of the MC simulation, which amounts to 9% (5%). This is due to the very low acceptance of the analysis to dominant SM backgrounds like $W+\text{jets}$, which is the main contributor to this uncertainty category. Theoretical uncertainties of the $W+\text{jets}$ and $t\bar{t}$ backgrounds that affect their normalization are significantly reduced through the use of CRs and are limited by the statistical uncertainty of the data and the extrapolation to the SR. The evaluation of theoretical modelling uncertainties is described in Section 3. The leading theoretical uncertainties are the uncertainties related to the matrix element generator for the $t\bar{t}$ sample, amounting to 4% (1%), as well as for the single-top sample, amounting to 3% (1%), the diboson scale uncertainty, amounting to 3% (2%), and the $W+\text{jets}$ scale uncertainty, contributing 2% (6%). The leading experimental systematic uncertainties are related to the jet energy scale (JES) and jet energy resolution (JER). These uncertainties are derived as a function of the p_T and η of the jet, the pile-up conditions, and the jet-flavour composition of the selected sample. They are estimated separately for $R = 0.4$ PFlow jets [98] and $R = 0.2$ LCW jets, following methodologies similar to those in Ref. [115]. The JES and JER uncertainties for $R=0.2$ jets are propagated to the observables related to TAR jets like $m_{W_{\text{cand}}}$, m_s^{\min} and $D_2^{\beta=1}$. The effect of the JER uncertainty amounts to 9% (5%), and that

of the JES uncertainty to 7% (5%). Sub-dominant experimental uncertainties considered are associated with the modelling of E_T^{miss} [103], amounting to 3% (1%), the track reconstruction efficiency [116] (3% in the merged category) and the luminosity uncertainty [51] (2% in the both categories). Other considered, but less important, uncertainties are associated with the modelling of b -tagging efficiencies [102], the reconstruction efficiency, energy scale, energy resolution, and trigger efficiency of leptons [48, 54, 93, 94], the pile-up reweighting, and the tagging and suppression of pile-up jets [117].

While quantifying the impact of a given systematic uncertainty as the fractional effect relative to the total background yield in each SR category is useful, it does not capture effects that are differential in m_s^{\min} . Hence, the effect of systematic uncertainties is quantified in Table 4 in terms of their contribution to the fitted signal uncertainty relative to the theory prediction. In this procedure, each systematic uncertainty's squared contribution is given by the difference between the squares of the total uncertainty and the uncertainty obtained by neglecting the systematic uncertainty source in question, where in the latter fit the signal value is fixed to its value considering all uncertainties. This is done for three representative signal models that span the range of the dark Higgs model parameter space that this analysis is sensitive to.

Table 4: Dominant sources of uncertainty for three dark Higgs scenarios after the fit to data. The uncertainties are quantified in terms of their contribution to the fitted signal uncertainty, which is expressed relative to the theory prediction. Three representative dark Higgs signal scenarios with $g_q = 0.25$, $g_\chi = 1.0$, $\sin \theta = 0.01$ and $m_\chi = 200$ GeV are considered, which are indicated using the $(m_{Z'}, m_s)$ format in units of GeV in the table columns. ‘Total uncertainty’ is the quadrature sum of statistical and total systematic uncertainties, which consider correlations. Only the largest systematic uncertainties are shown.

Source of uncertainty	Uncertainty [%]		
	(2100, 210)	(1000, 140)	(1000, 360)
$W + \text{jets}$ modelling	4	5	2
Diboson modelling	5	4	1
$t\bar{t}$ modelling	7	4	1
Single top modelling	9	5	11
Signal modelling	1	3	0
Statistical uncertainty of MC	26	15	29
$R = 0.4$ jet energy scale	11	12	14
$R = 0.4$ jet energy resolution	9	4	7
$R = 0.2$ jet energy scale	9	9	14
$R = 0.2$ jet energy resolution	13	10	16
E_T^{miss}	7	1	7
Track reconstruction	5	2	2
Lepton reconstruction	2	3	1
Systematic uncertainty	38	28	40
Statistical uncertainty of data	38	32	37
Total uncertainty	53	43	55

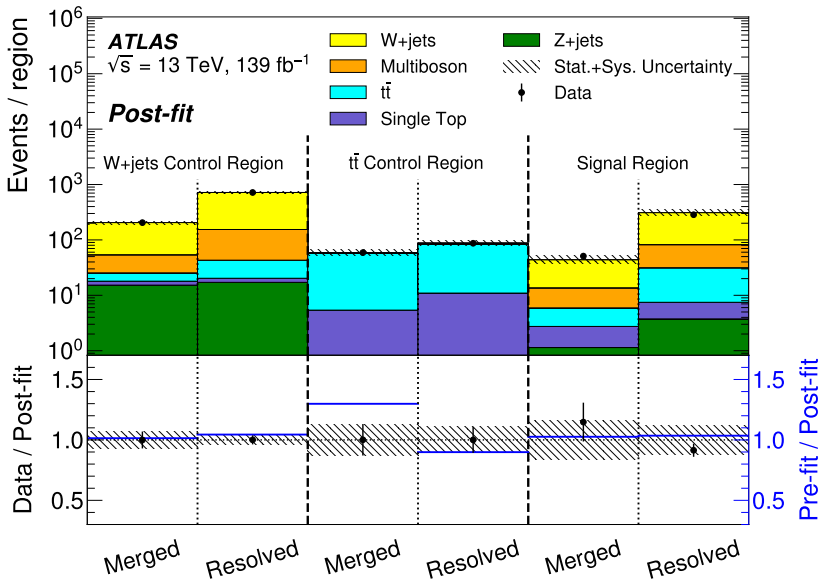


Figure 7: Data overlaid on SM background yields stacked in each SR and CR category after the fit to data ('Post-fit'). The maximum-likelihood estimators are set to the conditional values of the CR-only fit, and propagated to the SR and CRs. The lower panel displays the ratio of data to SM expectations after the fit, with its systematic uncertainty considering correlations between individual contributions indicated by the hatched band. The lower panel also displays the blue line representing the ratio of pre-fit to post-fit background predictions.

8 Results

The data analysis is performed in several steps and with the SR initially blinded to minimize any human bias. First, a fit to the SM backgrounds is performed only with data from the $W+jets$ and $t\bar{t}$ CRs, split into the merged and resolved categories analogously to the SR. The resulting observed and fitted yields in the CR categories are shown in Figure 7. To demonstrate the propagation of constraints on the $W+jets$ and $t\bar{t}$ backgrounds and experimental uncertainties from the CRs to the SR, Figure 7 also shows the yields of background processes predicted in the SR when using the observed parameter values from the CR-only fit. This fit slightly reduces the overall $V+jets$ contribution. The fitted normalization of the dominant $W+jets$ background is 0.99 ± 0.17 (0.94 ± 0.07) in the merged (resolved) category. The $t\bar{t}$ background normalization falls to 0.75 ± 0.13 in the merged category, and rises to 1.14 ± 0.22 in the resolved category. Given the uncertainties, no significant discrepancy between the yields in the SR categories is observed.

Finally, a simultaneous fit to the SR and the CRs is performed considering both the merged and resolved categories. The reconstructed dark Higgs candidate mass m_s^{\min} is used as the main discriminant between signal and background in the SR in this fit set-up. Figure 8 shows the m_s^{\min} distributions of the dark Higgs candidate in the merged and resolved SR categories, obtained after a simultaneous fit to the SR and the CRs under the hypothesis that only the SM predictions are present. In the combined SR and CR fit the data distributions are found to be well described by MC simulations within the estimated uncertainties, similarly to the CR-only fit. The data are found to be one standard deviation above the MC simulations in the merged category for $m_s^{\min} < 165$ GeV, but this trend is not reproduced in the resolved category. A data event deficit of about 1.5 standard deviations is observed for $m_s^{\min} > 325$ GeV in the resolved category.

The results of this search are interpreted by setting upper limits on the product of the $pp \rightarrow s\chi\chi$

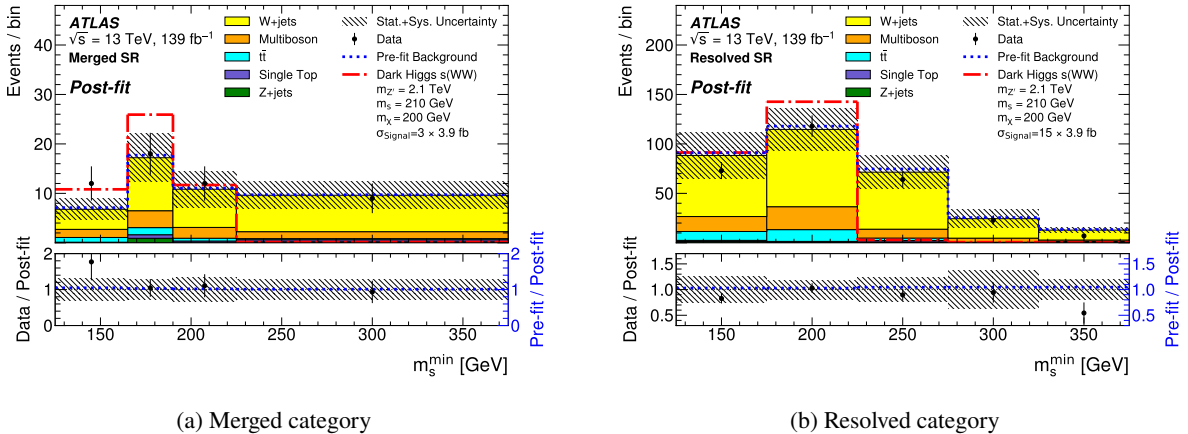


Figure 8: Distributions of the invariant mass of the dark Higgs candidates in the signal region for the merged (a) and resolved (b) category, after the fit to data ('Post-fit'). The upper panels compare the data with the SM expectation before (blue dashed line) and after the background-only fit (histogram stack). The lower panels display the ratio of data to SM expectations after the fit, with its systematic uncertainty. Also shown is the ratio of SM expectations before and after the fit (blue dashed line). The expected signal from a representative dark Higgs model with $g_q = 0.25$, $g_\chi = 1$, $m_\chi = 200$ GeV, and $\sin \theta = 0.01$ assuming $m_{Z'} = 2.1$ TeV and $m_s = 210$ GeV, with a cross section of 3.9 fb for the $s \rightarrow W^-(\ell^-\bar{\nu})W^+(q\bar{q}')$ decay mode, is shown as the dash-dotted line and scaled for presentation purposes.

production cross section and the decay branching fraction $\mathcal{B}(s \rightarrow W^+W^-)$, using a modified frequentist approach (CL_s) [118] with a test statistic based on the profile likelihood in the asymptotic approximation [112]. Upper limits on the ratio of the measured signal cross section to its theoretically predicted value are determined at 95% confidence level (CL). Exclusion contours in the $(m_{Z'}, m_s)$ plane for the dark Higgs model with $g_q = 0.25$, $g_\chi = 1.0$, and $\sin \theta = 0.01$ are presented in Figure 9. Consistency with the observed relic density can indicate the preferred model parameters if it is assumed that no additional particles beyond s and Z' are present. For $m_s \lesssim 200$ GeV, the relic density suggests $m_{Z'}$ masses of about 850 GeV, and increases with growing $m_{Z'}$. For $m_s \gtrsim 200$ GeV, a lower $m_{Z'}$ value of about 760 GeV is preferred for consistency with the observed relic density; this is due to annihilation of WIMP pairs into pairs of on-shell dark Higgs bosons becoming kinematically impossible. The sensitivity of the search is highest for $m_{Z'} \approx 750$ GeV and for this $m_{Z'}$ value a wide range of dark Higgs boson masses from 140 GeV to 390 GeV can be excluded. The existence of a hypothetical Z' boson with a mass of up to 1.8 TeV is excluded for $150 \lesssim m_s \lesssim 250$ GeV at 95% CL. In this dark Higgs boson mass range, the observed exclusion at high $m_{Z'}$ is weaker than expected owing to the small excess in data at $m_s^{\min} < 165$ GeV in the merged region that was discussed above. For $m_s \gtrsim 300$ GeV, the exclusion limits are somewhat stronger than expected owing to the deficit in data at $m_s^{\min} > 325$ GeV in the resolved region.

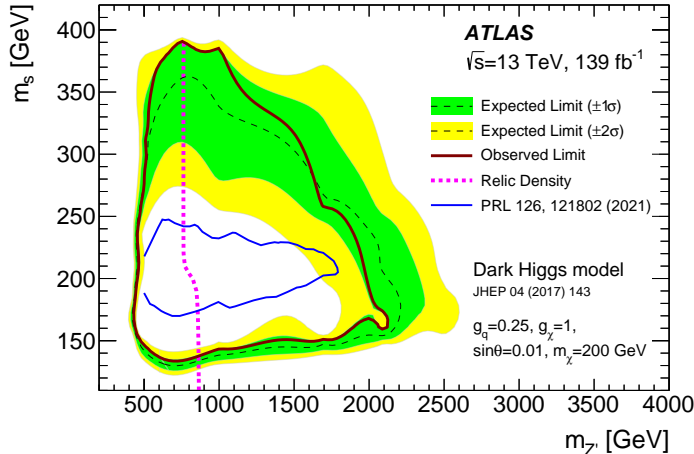


Figure 9: Exclusion contours for the dark Higgs model in the $(m_{Z'}, m_s)$ plane for $g_q = 0.25$, $g_\chi = 1$, $m_\chi = 200$ GeV, and $\sin \theta = 0.01$. The observed (expected) 95% CL exclusion is represented by the solid line (dashed line), along with the $\pm 1\sigma$ ($\pm 2\sigma$) expected uncertainty as the filled green (yellow) band. The area within the contour curve is excluded. The parameter values where the relic density value, as calculated with MadDM [119], matches the observed relic density [34] are shown by the short-dashed line. Values of $m_{Z'}$ above this line correspond to an overabundance of DM. The observed exclusion contour from the analysis of the $s \rightarrow VV \rightarrow q\bar{q}'q''\bar{q}'''$ decay channel [22], where $VV = W^+W^-$ or ZZ , is also shown.

9 Conclusion

A search for dark matter in final states with large E_T^{miss} and semileptonic decays of resonantly produced $W^\pm W^\mp$ pairs is presented. The search uses the full Run 2 data set recorded with the ATLAS detector at the LHC in 2015–2018, which corresponds to 139 fb^{-1} of pp collisions at $\sqrt{s} = 13 \text{ TeV}$. A new technique of track-assisted reclustering was used to identify merged hadronic W boson candidates as a single large-radius jet, in addition to a resolved method using a combination of small-radius jets. The data are found to be consistent with the Standard Model predictions. The result is interpreted as upper limits at 95% confidence level on the dark Higgs model parameters. The most stringent limits on $m_{Z'}$ can be set for $m_s = 160$ GeV, excluding the range $500 < m_{Z'} < 2100$ GeV, and the most stringent limits on m_s can be set for $m_{Z'} = 750$ GeV, excluding the range $140 < m_s < 390$ GeV. This result substantially extends the sensitivity into mass regions beyond the reach of previous analyses by the ATLAS and CMS collaborations in fully hadronic final states and fully leptonic final states for dark Higgs boson masses above 140 GeV.

Acknowledgements

We thank CERN for the very successful operation of the LHC, as well as the support staff from our institutions without whom ATLAS could not be operated efficiently.

We acknowledge the support of ANPCyT, Argentina; YerPhI, Armenia; ARC, Australia; BMWFW and FWF, Austria; ANAS, Azerbaijan; CNPq and FAPESP, Brazil; NSERC, NRC and CFI, Canada; CERN; ANID, Chile; CAS, MOST and NSFC, China; Minciencias, Colombia; MEYS CR, Czech Republic; DNRF and DNSRC, Denmark; IN2P3-CNRS and CEA-DRF/IRFU, France; SRNSFG, Georgia; BMBF, HGF and

MPG, Germany; GSRI, Greece; RGC and Hong Kong SAR, China; ISF and Benoziyo Center, Israel; INFN, Italy; MEXT and JSPS, Japan; CNRST, Morocco; NWO, Netherlands; RCN, Norway; MEiN, Poland; FCT, Portugal; MNE/IFA, Romania; MESTD, Serbia; MSSR, Slovakia; ARRS and MIZŠ, Slovenia; DS/ NRF, South Africa; MICINN, Spain; SRC and Wallenberg Foundation, Sweden; SERI, SNSF and Cantons of Bern and Geneva, Switzerland; MOST, Taiwan; TENMAK, Türkiye; STFC, United Kingdom; DOE and NSF, United States of America. In addition, individual groups and members have received support from BCKDF, CANARIE, Compute Canada and CRC, Canada; PRIMUS 21/SCI/017 and UNCE SCI/013, Czech Republic; COST, ERC, ERDF, Horizon 2020 and Marie Skłodowska-Curie Actions, European Union; Investissements d’Avenir Labex, Investissements d’Avenir Idex and ANR, France; DFG and AvH Foundation, Germany; Herakleitos, Thales and Aristeia programmes co-financed by EU-ESF and the Greek NSRF, Greece; BSF-NSF and MINERVA, Israel; Norwegian Financial Mechanism 2014-2021, Norway; NCN and NAWA, Poland; La Caixa Banking Foundation, CERCA Programme Generalitat de Catalunya and PROMETEO and GenT Programmes Generalitat Valenciana, Spain; Göran Gustafssons Stiftelse, Sweden; The Royal Society and Leverhulme Trust, United Kingdom.

The crucial computing support from all WLCG partners is acknowledged gratefully, in particular from CERN, the ATLAS Tier-1 facilities at TRIUMF (Canada), NDGF (Denmark, Norway, Sweden), CC-IN2P3 (France), KIT/GridKA (Germany), INFN-CNAF (Italy), NL-T1 (Netherlands), PIC (Spain), ASGC (Taiwan), RAL (UK) and BNL (USA), the Tier-2 facilities worldwide and large non-WLCG resource providers. Major contributors of computing resources are listed in Ref. [120].

References

- [1] J. Silk et al., *Particle Dark Matter: Observations, Models and Searches*, ed. by G. Bertone, Cambridge: Cambridge Univ. Press, 2010, ISBN: 978-1-107-65392-4.
- [2] J. L. Feng, *Dark Matter Candidates from Particle Physics and Methods of Detection*, *Ann. Rev. Astron. Astrophys.* **48** (2010) 495, arXiv: [1003.0904 \[astro-ph.CO\]](#).
- [3] T. A. Porter, R. P. Johnson and P. W. Graham, *Dark Matter Searches with Astroparticle Data*, *Ann. Rev. Astron. Astrophys.* **49** (2011) 155, arXiv: [1104.2836 \[astro-ph.HE\]](#).
- [4] G. Bertone et al., *Identifying WIMP dark matter from particle and astroparticle data*, *JCAP* **03** (2018) 026, arXiv: [1712.04793 \[hep-ph\]](#).
- [5] ATLAS Collaboration, *Search for new phenomena in events with an energetic jet and missing transverse momentum in pp collisions at $\sqrt{s} = 13 \text{ TeV}$ with the ATLAS detector*, *Phys. Rev. D* **103** (2021) 112006, arXiv: [2102.10874 \[hep-ex\]](#).
- [6] CMS Collaboration, *Search for new particles in events with energetic jets and large missing transverse momentum in proton–proton collisions at $\sqrt{s} = 13 \text{ TeV}$* , *JHEP* **11** (2021) 153, arXiv: [2107.13021 \[hep-ex\]](#).
- [7] ATLAS Collaboration, *Search for dark matter produced in association with a single top quark in $\sqrt{s} = 13 \text{ TeV}$ pp collisions with the ATLAS detector*, *Eur. Phys. J. C* **81** (2020) 860, arXiv: [2011.09308 \[hep-ex\]](#).
- [8] ATLAS Collaboration, *Search for new phenomena in final states with b-jets and missing transverse momentum in $\sqrt{s} = 13 \text{ TeV}$ pp collisions with the ATLAS detector*, *JHEP* **05** (2021) 093, arXiv: [2101.12527 \[hep-ex\]](#).
- [9] ATLAS Collaboration, *Search for new phenomena in events with two opposite-charge leptons, jets and missing transverse momentum in pp collisions at $\sqrt{s} = 13 \text{ TeV}$ with the ATLAS detector*, *JHEP* **04** (2021) 165, arXiv: [2102.01444 \[hep-ex\]](#).
- [10] ATLAS Collaboration, *Search for new phenomena with top quark pairs in final states with one lepton, jets, and missing transverse momentum in pp collisions at $\sqrt{s} = 13 \text{ TeV}$ with the ATLAS detector*, *JHEP* **04** (2020) 174, arXiv: [2012.03799 \[hep-ex\]](#).
- [11] CMS Collaboration, *Search for Dark Matter Particles Produced in Association with a Top Quark Pair at $\sqrt{s} = 13 \text{ TeV}$* , *Phys. Rev. Lett.* **122** (2019) 011803, arXiv: [1807.06522 \[hep-ex\]](#).
- [12] CMS Collaboration, *Search for dark matter produced in association with a single top quark or a top quark pair in proton–proton collisions at $\sqrt{s} = 13 \text{ TeV}$* , *JHEP* **03** (2019) 141, arXiv: [1901.01553 \[hep-ex\]](#).
- [13] ATLAS Collaboration, *Search for dark matter in association with an energetic photon in pp collisions at $\sqrt{s} = 13 \text{ TeV}$ with the ATLAS detector*, *JHEP* **02** (2021) 226, arXiv: [2011.05259 \[hep-ex\]](#).
- [14] CMS Collaboration, *Search for new physics in the monophoton final state in proton–proton collisions at $\sqrt{s} = 13 \text{ TeV}$* , *JHEP* **10** (2017) 073, arXiv: [1706.03794 \[hep-ex\]](#).

- [15] ATLAS Collaboration, *Search for dark matter in events with a hadronically decaying vector boson and missing transverse momentum in pp collisions at $\sqrt{s} = 13$ TeV with the ATLAS detector*, *JHEP* **10** (2018) 180, arXiv: [1807.11471 \[hep-ex\]](#).
- [16] ATLAS Collaboration, *Search for an invisibly decaying Higgs boson or dark matter candidates produced in association with a Z boson in pp collisions at $\sqrt{s} = 13$ TeV with the ATLAS detector*, *Phys. Lett. B* **776** (2018) 318, arXiv: [1708.09624 \[hep-ex\]](#).
- [17] CMS Collaboration, *Search for dark matter produced in association with a leptonically decaying Z boson in proton–proton collisions at $\sqrt{s} = 13$ TeV*, *Eur. Phys. J. C* **81** (2021) 13, arXiv: [2008.04735 \[hep-ex\]](#).
- [18] CMS Collaboration, *Search for new physics in final states with an energetic jet or a hadronically decaying W or Z boson and transverse momentum imbalance at $\sqrt{s} = 13$ TeV*, *Phys. Rev. D* **97** (2018) 092005, arXiv: [1712.02345 \[hep-ex\]](#).
- [19] ATLAS Collaboration, *Search for dark matter produced in association with a Standard Model Higgs boson decaying into b-quarks using the full Run 2 dataset from the ATLAS detector*, *JHEP* **11** (2021) 209, arXiv: [2108.13391 \[hep-ex\]](#).
- [20] CMS Collaboration, *Search for dark matter particles produced in association with a Higgs boson in proton–proton collisions at $\sqrt{s} = 13$ TeV*, *JHEP* **03** (2020) 025, arXiv: [1908.01713 \[hep-ex\]](#).
- [21] CMS Collaboration, *Search for dark matter produced in association with a Higgs boson decaying to $\gamma\gamma$ or $\tau^+\tau^-$ at $\sqrt{s} = 13$ TeV*, *JHEP* **09** (2018) 046, arXiv: [1806.04771 \[hep-ex\]](#).
- [22] ATLAS Collaboration, *Search for Dark Matter Produced in Association with a Dark Higgs Boson Decaying into $W^\pm W^\mp$ or ZZ in Fully Hadronic Final States from $\sqrt{s} = 13$ TeV pp Collisions Recorded with the ATLAS Detector*, *Phys. Rev. Lett.* **126** (2021) 121802, arXiv: [2010.06548 \[hep-ex\]](#).
- [23] ATLAS Collaboration, *Track assisted techniques for jet substructure*, ATL-PHYS-PUB-2018-012, 2018, URL: <https://cds.cern.ch/record/2630864>.
- [24] ATLAS Collaboration, *Observation of a new particle in the search for the Standard Model Higgs boson with the ATLAS detector at the LHC*, *Phys. Lett. B* **716** (2012) 1, arXiv: [1207.7214 \[hep-ex\]](#).
- [25] CMS Collaboration, *Observation of a new boson at a mass of 125 GeV with the CMS experiment at the LHC*, *Phys. Lett. B* **716** (2012) 30, arXiv: [1207.7235 \[hep-ex\]](#).
- [26] F. Englert and R. Brout, *Broken Symmetry and the Mass of Gauge Vector Mesons*, *Phys. Rev. Lett.* **13** (1964) 321.
- [27] P. W. Higgs, *Broken symmetries, massless particles and gauge fields*, *Phys. Lett.* **12** (1964) 132.
- [28] P. W. Higgs, *Broken Symmetries and the Masses of Gauge Bosons*, *Phys. Rev. Lett.* **13** (1964) 508.
- [29] G. Guralnik, C. Hagen and T. Kibble, *Global Conservation Laws and Massless Particles*, *Phys. Rev. Lett.* **13** (1964) 585.
- [30] P. W. Higgs, *Spontaneous Symmetry Breakdown without Massless Bosons*, *Phys. Rev.* **145** (1966) 1156.
- [31] T. Kibble, *Symmetry Breaking in Non-Abelian Gauge Theories*, *Phys. Rev.* **155** (1967) 1554.

- [32] F. Kahlhoefer, K. Schmidt-Hoberg, T. Schwetz and S. Vogl,
Implications of unitarity and gauge invariance for simplified dark matter models,
JHEP **02** (2016) 016, arXiv: [1510.02110 \[hep-ph\]](#).
- [33] M. Duerr et al., *Hunting the dark Higgs*, **JHEP** **04** (2017) 143, arXiv: [1701.08780 \[hep-ph\]](#).
- [34] Planck Collaboration, *Planck 2018 results. VI. Cosmological parameters*,
Astron. Astrophys. **641** (2020) A6, arXiv: [1807.06209 \[astro-ph.CO\]](#),
 Erratum: P. Collaboration, **Astron. Astrophys.** **652** (2021) C4.
- [35] M. Duerr, F. Kahlhoefer, K. Schmidt-Hoberg, T. Schwetz and S. Vogl,
How to save the WIMP: global analysis of a dark matter model with two s-channel mediators,
JHEP **09** (2016) 042, arXiv: [1606.07609 \[hep-ph\]](#).
- [36] J. R. Andersen et al., *Handbook of LHC Higgs Cross Sections: 3. Higgs Properties*,
 (2013), ed. by S. Heinemeyer, C. Mariotti, G. Passarino and R. Tanaka,
 arXiv: [1307.1347 \[hep-ph\]](#).
- [37] O. Buchmueller, M. J. Dolan and C. McCabe,
Beyond effective field theory for dark matter searches at the LHC, **JHEP** **01** (2014) 025,
 arXiv: [1308.6799 \[hep-ph\]](#).
- [38] P. Harris, V. V. Khoze, M. Spannowsky and C. Williams,
Constraining dark sectors at colliders: Beyond the effective theory approach,
Phys. Rev. D **91** (2015) 055009, arXiv: [1411.0535 \[hep-ph\]](#).
- [39] M. R. Buckley, D. Feld and D. Goncalves, *Scalar simplified models for dark matter*,
Phys. Rev. D **91** (2015) 015017, arXiv: [1410.6497 \[hep-ph\]](#).
- [40] D. Abercrombie et al., *Dark Matter benchmark models for early LHC Run-2 searches: Report of the ATLAS/CMS Dark Matter Forum*, **Phys. Dark Univ.** **27** (2020) 100371,
 arXiv: [1507.00966 \[hep-ex\]](#).
- [41] J. Abdallah et al., *Simplified models for dark matter searches at the LHC*,
Phys. Dark Univ. **9-10** (2015) 8, arXiv: [1506.03116 \[hep-ph\]](#).
- [42] A. Albert et al., *Recommendations of the LHC Dark Matter Working Group: Comparing LHC searches for dark matter mediators in visible and invisible decay channels and calculations of the thermal relic density*, **Phys. Dark Univ.** **26** (2019) 100377, arXiv: [1703.05703 \[hep-ex\]](#).
- [43] ATLAS Collaboration, *Constraints on mediator-based dark matter and scalar dark energy models using $\sqrt{s} = 13\text{ TeV}$ pp collision data collected by the ATLAS detector*, **JHEP** **05** (2019) 142,
 arXiv: [1903.01400 \[hep-ex\]](#).
- [44] S. Argyropoulos, O. Brandt and U. Haisch,
Collider Searches for Dark Matter through the Higgs Lens, **Symmetry** **2021** (2021) 13,
 arXiv: [2109.13597 \[hep-ph\]](#).
- [45] ATLAS Collaboration, *The ATLAS Experiment at the CERN Large Hadron Collider*,
JINST **3** (2008) S08003.
- [46] ATLAS Collaboration, *ATLAS Insertable B-Layer Technical Design Report*,
 ATLAS-TDR-19; CERN-LHCC-2010-013, 2010,
 URL: <https://cds.cern.ch/record/1291633>, Addendum: ATLAS-TDR-19-ADD-1;
 CERN-LHCC-2012-009, 2012, URL: <https://cds.cern.ch/record/1451888>.

- [47] B. Abbott et al., *Production and integration of the ATLAS Insertable B-Layer*, JINST **13** (2018) T05008, arXiv: [1803.00844 \[physics.ins-det\]](#).
- [48] ATLAS Collaboration, *Performance of the ATLAS trigger system in 2015*, Eur. Phys. J. C **77** (2017) 317, arXiv: [1611.09661 \[hep-ex\]](#).
- [49] ATLAS Collaboration, *The ATLAS Collaboration Software and Firmware*, ATL-SOFT-PUB-2021-001, 2021, URL: <https://cds.cern.ch/record/2767187>.
- [50] G. Avoni et al., *The new LUCID-2 detector for luminosity measurement and monitoring in ATLAS*, JINST **13** (2018) P07017.
- [51] ATLAS Collaboration, *Luminosity determination in pp collisions at $\sqrt{s} = 13\text{ TeV}$ using the ATLAS detector at the LHC*, ATLAS-CONF-2019-021, 2019, URL: <https://cds.cern.ch/record/2677054>.
- [52] ATLAS Collaboration, *Operation of the ATLAS trigger system in Run 2*, JINST **15** (2020) P10004, arXiv: [2007.12539 \[hep-ex\]](#).
- [53] ATLAS Collaboration, *Performance of the missing transverse momentum triggers for the ATLAS detector during Run-2 data taking*, JHEP **08** (2020) 080, arXiv: [2005.09554 \[hep-ex\]](#).
- [54] ATLAS Collaboration, *Performance of the ATLAS muon triggers in Run 2*, JINST **15** (2020) P09015, arXiv: [2004.13447 \[hep-ex\]](#).
- [55] E. Bothmann et al., *Event generation with Sherpa 2.2*, SciPost Phys. **7** (2019) 034, arXiv: [1905.09127 \[hep-ph\]](#).
- [56] T. Gleisberg and S. Höche, *Comix, a new matrix element generator*, JHEP **12** (2008) 039, arXiv: [0808.3674 \[hep-ph\]](#).
- [57] F. Buccioni et al., *OpenLoops 2*, Eur. Phys. J. C **79** (2019) 866, arXiv: [1907.13071 \[hep-ph\]](#).
- [58] F. Cascioli, P. Maierhofer and S. Pozzorini, *Scattering Amplitudes with Open Loops*, Phys. Rev. Lett. **108** (2012) 111601, arXiv: [1111.5206 \[hep-ph\]](#).
- [59] A. Denner, S. Dittmaier and L. Hofer, *Collier: a fortran-based Complex One-Loop Library in Extended Regularizations*, Comput. Phys. Commun. **212** (2017) 220, arXiv: [1604.06792 \[hep-ph\]](#).
- [60] S. Schumann and F. Krauss, *A Parton shower algorithm based on Catani-Seymour dipole factorisation*, JHEP **03** (2008) 038, arXiv: [0709.1027 \[hep-ph\]](#).
- [61] S. Höche, F. Krauss, M. Schönherr and F. Siegert, *A critical appraisal of NLO+PS matching methods*, JHEP **09** (2012) 049, arXiv: [1111.1220 \[hep-ph\]](#).
- [62] S. Höche, F. Krauss, M. Schönherr and F. Siegert, *QCD matrix elements + parton showers: The NLO case*, JHEP **04** (2013) 027, arXiv: [1207.5030 \[hep-ph\]](#).
- [63] S. Catani, F. Krauss, B. R. Webber and R. Kuhn, *QCD Matrix Elements + Parton Showers*, JHEP **11** (2001) 063, arXiv: [hep-ph/0109231](#).
- [64] S. Höche, F. Krauss, S. Schumann and F. Siegert, *QCD matrix elements and truncated showers*, JHEP **05** (2009) 053, arXiv: [0903.1219 \[hep-ph\]](#).

- [65] C. Anastasiou, L. J. Dixon, K. Melnikov and F. Petriello,
High precision QCD at hadron colliders: Electroweak gauge boson rapidity distributions at NNLO,
Phys. Rev. D **69** (2004) 094008, arXiv: [hep-ph/0312266](#).
- [66] NNPDF Collaboration, R.D. Ball et al., *Parton distributions for the LHC Run II*,
JHEP **04** (2015) 040, arXiv: [1410.8849 \[hep-ph\]](#).
- [67] E. Bothmann, M. Schönherr and S. Schumann,
Reweighting QCD matrix-element and parton-shower calculations, *Eur. Phys. J. C* **76** (2016) 590,
arXiv: [1606.08753 \[hep-ph\]](#).
- [68] J. Butterworth et al., *PDF4LHC recommendations for LHC Run II*, *J. Phys. G* **43** (2016) 023001,
arXiv: [1510.03865 \[hep-ph\]](#).
- [69] L. Lönnblad and S. Prestel, *Matching Tree-Level Matrix Elements with Interleaved Showers*,
JHEP **03** (2012) 019, arXiv: [1109.4829 \[hep-ph\]](#).
- [70] S. Frixione, G. Ridolfi and P. Nason,
A positive-weight next-to-leading-order Monte Carlo for heavy flavour hadroproduction,
JHEP **09** (2007) 126, arXiv: [0707.3088 \[hep-ph\]](#).
- [71] P. Nason, *A new method for combining NLO QCD with shower Monte Carlo algorithms*,
JHEP **11** (2004) 040, arXiv: [hep-ph/0409146](#).
- [72] S. Frixione, P. Nason and C. Oleari,
Matching NLO QCD computations with Parton Shower simulations: the POWHEG method,
JHEP **11** (2007) 070, arXiv: [0709.2092 \[hep-ph\]](#).
- [73] S. Alioli, P. Nason, C. Oleari and E. Re, *A general framework for implementing NLO calculations in shower Monte Carlo programs: the POWHEG BOX*, *JHEP* **06** (2010) 043,
arXiv: [1002.2581 \[hep-ph\]](#).
- [74] ATLAS Collaboration, *Studies on top-quark Monte Carlo modelling for Top2016*,
ATL-PHYS-PUB-2016-020, 2016, URL: <https://cds.cern.ch/record/2216168>.
- [75] T. Sjöstrand et al., *An Introduction to PYTHIA 8.2*, *Comput. Phys. Commun.* **191** (2015) 159,
arXiv: [1410.3012 \[hep-ph\]](#).
- [76] ATLAS Collaboration, *ATLAS Pythia 8 tunes to 7 TeV data*, ATL-PHYS-PUB-2014-021, 2014,
URL: <https://cds.cern.ch/record/1966419>.
- [77] R. D. Ball, V. Bertone, S. Carrazza, C. S. Deans, L. Del Debbio et al.,
Parton distributions with LHC data, *Nucl. Phys. B* **867** (2013) 244, arXiv: [1207.1303 \[hep-ph\]](#).
- [78] D. J. Lange, *The EvtGen particle decay simulation package*,
Nucl. Instrum. Meth. A **462** (2001) 152.
- [79] E. Re,
Single-top Wt-channel production matched with parton showers using the POWHEG method,
Eur. Phys. J. C **71** (2011) 1547, arXiv: [1009.2450 \[hep-ph\]](#).
- [80] S. Frixione, E. Laenen, P. Motylinski, C. White and B. R. Webber,
Single-top hadroproduction in association with a W boson, *JHEP* **07** (2008) 029,
arXiv: [0805.3067 \[hep-ph\]](#).
- [81] R. Frederix, E. Re and P. Torrielli,
Single-top t-channel hadroproduction in the four-flavour scheme with POWHEG and aMC@NLO,
JHEP **09** (2012) 130, arXiv: [1207.5391 \[hep-ph\]](#).

- [82] ATLAS Collaboration,
Studies on top-quark Monte Carlo modelling with Sherpa and MG5_aMC@NLO,
ATL-PHYS-PUB-2017-007, 2017, URL: <https://cds.cern.ch/record/2261938>.
- [83] M. Bähr et al., *Herwig++ physics and manual*, Eur. Phys. J. C **58** (2008) 639,
arXiv: [0803.0883 \[hep-ph\]](#).
- [84] J. Bellm et al., *Herwig 7.0/Herwig++ 3.0 release note*, Eur. Phys. J. C **76** (2016) 196,
arXiv: [1512.01178 \[hep-ph\]](#).
- [85] L. A. Harland-Lang, A. D. Martin, P. Motylinski and R. S. Thorne,
Parton distributions in the LHC era: MMHT 2014 PDFs, Eur. Phys. J. C **75** (2015) 204,
arXiv: [1412.3989 \[hep-ph\]](#).
- [86] J. Alwall et al., *The automated computation of tree-level and next-to-leading order differential cross sections, and their matching to parton shower simulations*, JHEP **07** (2014) 079,
arXiv: [1405.0301 \[hep-ph\]](#).
- [87] T. Sjostrand, S. Mrenna and P. Skands, *A brief introduction to PYTHIA 8.1*,
Comput. Phys. Commun. **178** (2008) 852, arXiv: [0710.3820 \[hep-ph\]](#).
- [88] ATLAS Collaboration, *The Pythia 8 A3 tune description of ATLAS minimum bias and inelastic measurements incorporating the Donnachie–Landshoff diffractive model*,
ATL-PHYS-PUB-2016-017, 2016, URL: <https://cds.cern.ch/record/2206965>.
- [89] ATLAS Collaboration, *The ATLAS Simulation Infrastructure*, Eur. Phys. J. C **70** (2010) 823,
arXiv: [1005.4568 \[physics.ins-det\]](#).
- [90] GEANT4 Collaboration, S. Agostinelli et al., *GEANT4 – a simulation toolkit*,
Nucl. Instrum. Meth. A **506** (2003) 250.
- [91] ATLAS Collaboration, *The Optimization of ATLAS Track Reconstruction in Dense Environments*,
ATL-PHYS-PUB-2015-006, 2015, URL: <https://cds.cern.ch/record/2002609>.
- [92] ATLAS Collaboration,
Early Inner Detector Tracking Performance in the 2015 Data at $\sqrt{s} = 13 \text{ TeV}$,
ATL-PHYS-PUB-2015-051, 2015, URL: <https://cds.cern.ch/record/2110140>.
- [93] ATLAS Collaboration, *Electron and photon performance measurements with the ATLAS detector using the 2015–2017 LHC proton–proton collision data*, JINST **14** (2019) P12006,
arXiv: [1908.00005 \[hep-ex\]](#).
- [94] ATLAS Collaboration, *Muon reconstruction and identification efficiency in ATLAS using the full Run 2 pp collision data set at $\sqrt{s} = 13 \text{ TeV}$* , Eur. Phys. J. C **81** (2021) 578,
arXiv: [2012.00578 \[hep-ex\]](#).
- [95] ATLAS Collaboration,
Jet reconstruction and performance using particle flow with the ATLAS Detector,
Eur. Phys. J. C **77** (2017) 466, arXiv: [1703.10485 \[hep-ex\]](#).
- [96] M. Cacciari, G. P. Salam and G. Soyez, *The anti- k_t jet clustering algorithm*, JHEP **04** (2008) 063,
arXiv: [0802.1189 \[hep-ph\]](#).
- [97] M. Cacciari, G. P. Salam and G. Soyez, *FastJet user manual*, Eur. Phys. J. C **72** (2012) 1896,
arXiv: [1111.6097 \[hep-ph\]](#).

- [98] ATLAS Collaboration, *Jet energy scale and resolution measured in proton–proton collisions at $\sqrt{s} = 13\text{ TeV}$ with the ATLAS detector*, *Eur. Phys. J. C* **81** (2020) 689, arXiv: [2007.02645 \[hep-ex\]](#).
- [99] ATLAS Collaboration, *Performance of pile-up mitigation techniques for jets in pp collisions at $\sqrt{s} = 8\text{ TeV}$ using the ATLAS detector*, *Eur. Phys. J. C* **76** (2016) 581, arXiv: [1510.03823 \[hep-ex\]](#).
- [100] ATLAS Collaboration, *Topological cell clustering in the ATLAS calorimeters and its performance in LHC Run 1*, *Eur. Phys. J. C* **77** (2017) 490, arXiv: [1603.02934 \[hep-ex\]](#).
- [101] ATLAS Collaboration, *Jet energy scale measurements and their systematic uncertainties in proton–proton collisions at $\sqrt{s} = 13\text{ TeV}$ with the ATLAS detector*, *Phys. Rev. D* **96** (2017) 072002, arXiv: [1703.09665 \[hep-ex\]](#).
- [102] ATLAS Collaboration, *Measurements of b -jet tagging efficiency with the ATLAS detector using $t\bar{t}$ events at $\sqrt{s} = 13\text{ TeV}$* , *JHEP* **08** (2018) 089, arXiv: [1805.01845 \[hep-ex\]](#).
- [103] ATLAS Collaboration, *Performance of missing transverse momentum reconstruction with the ATLAS detector using proton–proton collisions at $\sqrt{s} = 13\text{ TeV}$* , *Eur. Phys. J. C* **78** (2018) 903, arXiv: [1802.08168 \[hep-ex\]](#).
- [104] ATLAS Collaboration, *Object-based missing transverse momentum significance in the ATLAS Detector*, ATLAS-CONF-2018-038, 2018, URL: <https://cds.cern.ch/record/2630948>.
- [105] ATLAS Collaboration, *Identification of Boosted, Hadronically-Decaying W and Z Bosons in $\sqrt{s} = 13\text{ TeV}$ Monte Carlo Simulations for ATLAS*, ATL-PHYS-PUB-2015-033, 2015, URL: <https://cds.cern.ch/record/2041461>.
- [106] M. Cacciari, G. P. Salam and G. Soyez, *The catchment area of jets*, *JHEP* **04** (2008) 005, arXiv: [0802.1188 \[hep-ph\]](#).
- [107] ATLAS Collaboration, *In situ calibration of large-radius jet energy and mass in 13 TeV proton–proton collisions with the ATLAS detector*, *Eur. Phys. J. C* **79** (2019) 135, arXiv: [1807.09477 \[hep-ex\]](#).
- [108] A. J. Larkoski, I. Moult and D. Neill, *Power counting to better jet observables*, *JHEP* **12** (2014) 009, arXiv: [1409.6298 \[hep-ph\]](#).
- [109] ATLAS Collaboration, *ATLAS data quality operations and performance for 2015–2018 data-taking*, *JINST* **15** (2020) P04003, arXiv: [1911.04632 \[physics.ins-det\]](#).
- [110] Particle Data Group, *Review of Particle Physics*, *PTEP* **2020** (2020) 083C01.
- [111] ATLAS Collaboration, *Formulae for Estimating Significance*, ATL-PHYS-PUB-2020-025, 2020, URL: <https://cds.cern.ch/record/2736148>.
- [112] G. Cowan, K. Cranmer, E. Gross and O. Vitells, *Asymptotic formulae for likelihood-based tests of new physics*, *Eur. Phys. J. C* **71** (2011) 1554, arXiv: [1007.1727 \[physics.data-an\]](#), Erratum: *Eur. Phys. J. C* **73** (2013) 2501.
- [113] W. Verkerke and D. Kirkby, *The RooFit toolkit for data modeling*, 2003, arXiv: [physics/0306116 \[physics.data-an\]](#).

- [114] M. Baak et al., *HistFitter software framework for statistical data analysis*, *Eur. Phys. J. C* **75** (2015) 153, arXiv: [1410.1280 \[hep-ex\]](https://arxiv.org/abs/1410.1280).
- [115] ATLAS Collaboration, *Jet Calibration and Systematic Uncertainties for Jets Reconstructed in the ATLAS Detector at $\sqrt{s} = 13$ TeV*, ATL-PHYS-PUB-2015-015, 2015, URL: <https://cds.cern.ch/record/2037613>.
- [116] ATLAS Collaboration, *Performance of the ATLAS track reconstruction algorithms in dense environments in LHC Run 2*, *Eur. Phys. J. C* **77** (2017) 673, arXiv: [1704.07983 \[hep-ex\]](https://arxiv.org/abs/1704.07983).
- [117] ATLAS Collaboration, *Tagging and suppression of pileup jets with the ATLAS detector*, ATL-CONF-2014-018, 2014, URL: <https://cds.cern.ch/record/1700870>.
- [118] A. L. Read, *Presentation of search results: the CL_S technique*, *J. Phys. G* **28** (2002) 2693.
- [119] C. Arina, J. Heisig, F. Maltoni, D. Massaro and O. Mattelaer, *Indirect dark-matter detection with MadDM v3.2 – Lines and Loops*, (2021), arXiv: [2107.04598 \[hep-ph\]](https://arxiv.org/abs/2107.04598).
- [120] ATLAS Collaboration, *ATLAS Computing Acknowledgements*, ATL-SOFT-PUB-2021-003, 2021, URL: <https://cds.cern.ch/record/2776662>.

The ATLAS Collaboration

G. Aad [ID¹⁰¹](#), B. Abbott [ID¹¹⁹](#), D.C. Abbott [ID¹⁰²](#), K. Abeling [ID⁵⁵](#), S.H. Abidi [ID²⁹](#), A. Aboulhorma [ID^{35e}](#), H. Abramowicz [ID¹⁵⁰](#), H. Abreu [ID¹⁴⁹](#), Y. Abulaiti [ID¹¹⁶](#), A.C. Abusleme Hoffman [ID^{136a}](#), B.S. Acharya [ID^{68a,68b,p}](#), B. Achkar [ID⁵⁵](#), C. Adam Bourdarios [ID⁴](#), L. Adamczyk [ID^{84a}](#), L. Adamek [ID¹⁵⁴](#), S.V. Addepalli [ID²⁶](#), J. Adelman [ID¹¹⁴](#), A. Adiguzel [ID^{21c}](#), S. Adorni [ID⁵⁶](#), T. Adye [ID¹³³](#), A.A. Affolder [ID¹³⁵](#), Y. Afik [ID³⁶](#), M.N. Agaras [ID¹³](#), J. Agarwala [ID^{72a,72b}](#), A. Aggarwal [ID⁹⁹](#), C. Agheorghiesei [ID^{27c}](#), J.A. Aguilar-Saavedra [ID^{129f}](#), A. Ahmad [ID³⁶](#), F. Ahmadov [ID^{38,y}](#), W.S. Ahmed [ID¹⁰³](#), S. Ahuja [ID⁹⁴](#), X. Ai [ID⁴⁸](#), G. Aielli [ID^{75a,75b}](#), I. Aizenberg [ID¹⁶⁸](#), M. Akbiyik [ID⁹⁹](#), T.P.A. Åkesson [ID⁹⁷](#), A.V. Akimov [ID³⁷](#), K. Al Khoury [ID⁴¹](#), G.L. Alberghi [ID^{23b}](#), J. Albert [ID¹⁶⁴](#), P. Albicocco [ID⁵³](#), M.J. Alconada Verzini [ID⁸⁹](#), S. Alderweireldt [ID⁵²](#), M. Aleksa [ID³⁶](#), I.N. Aleksandrov [ID³⁸](#), C. Alexa [ID^{27b}](#), T. Alexopoulos [ID¹⁰](#), A. Alfonsi [ID¹¹³](#), F. Alfonsi [ID^{23b}](#), M. Althroob [ID¹¹⁹](#), B. Ali [ID¹³¹](#), S. Ali [ID¹⁴⁷](#), M. Aliev [ID³⁷](#), G. Alimonti [ID^{70a}](#), W. Alkakhi [ID⁵⁵](#), C. Allaire [ID³⁶](#), B.M.M. Allbrooke [ID¹⁴⁵](#), P.P. Allport [ID²⁰](#), A. Aloisio [ID^{71a,71b}](#), F. Alonso [ID⁸⁹](#), C. Alpigiani [ID¹³⁷](#), E. Alunno Camelia [ID^{75a,75b}](#), M. Alvarez Estevez [ID⁹⁸](#), M.G. Alvaggi [ID^{71a,71b}](#), Y. Amaral Coutinho [ID^{81b}](#), A. Ambler [ID¹⁰³](#), C. Amelung [ID³⁶](#), C.G. Ames [ID¹⁰⁸](#), D. Amidei [ID¹⁰⁵](#), S.P. Amor Dos Santos [ID^{129a}](#), S. Amoroso [ID⁴⁸](#), K.R. Amos [ID¹⁶²](#), C.S. Amrouche [ID⁵⁶](#), V. Ananiev [ID¹²⁴](#), C. Anastopoulos [ID¹³⁸](#), T. Andeen [ID¹¹](#), J.K. Anders [ID¹⁹](#), S.Y. Andrean [ID^{47a,47b}](#), A. Andreazza [ID^{70a,70b}](#), S. Angelidakis [ID⁹](#), A. Angerami [ID^{41,ab}](#), A.V. Anisenkov [ID³⁷](#), A. Annovi [ID^{73a}](#), C. Antel [ID⁵⁶](#), M.T. Anthony [ID¹³⁸](#), E. Antipov [ID¹²⁰](#), M. Antonelli [ID⁵³](#), D.J.A. Antrim [ID^{17a}](#), F. Anulli [ID^{74a}](#), M. Aoki [ID⁸²](#), T. Aoki [ID¹⁵²](#), J.A. Aparisi Pozo [ID¹⁶²](#), M.A. Aparo [ID¹⁴⁵](#), L. Aperio Bella [ID⁴⁸](#), C. Appelt [ID¹⁸](#), N. Aranzabal [ID³⁶](#), V. Araujo Ferraz [ID^{81a}](#), C. Arcangeletti [ID⁵³](#), A.T.H. Arce [ID⁵¹](#), E. Arena [ID⁹¹](#), J-F. Arguin [ID¹⁰⁷](#), S. Argyropoulos [ID⁵⁴](#), J.-H. Arling [ID⁴⁸](#), A.J. Armbruster [ID³⁶](#), O. Arnaez [ID¹⁵⁴](#), H. Arnold [ID¹¹³](#), Z.P. Arrubarrena Tame [ID¹⁰⁸](#), G. Artoni [ID^{74a,74b}](#), H. Asada [ID¹¹⁰](#), K. Asai [ID¹¹⁷](#), S. Asai [ID¹⁵²](#), N.A. Asbah [ID⁶¹](#), J. Assahsah [ID^{35d}](#), K. Assamagan [ID²⁹](#), R. Astalos [ID^{28a}](#), R.J. Atkin [ID^{33a}](#), M. Atkinson [ID¹⁶¹](#), N.B. Atlay [ID¹⁸](#), H. Atmani [ID^{62b}](#), P.A. Atmasiddha [ID¹⁰⁵](#), K. Augsten [ID¹³¹](#), S. Auricchio [ID^{71a,71b}](#), A.D. Auriol [ID²⁰](#), V.A. Aastrup [ID¹⁷⁰](#), G. Avner [ID¹⁴⁹](#), G. Avolio [ID³⁶](#), K. Axiotis [ID⁵⁶](#), M.K. Ayoub [ID^{14c}](#), G. Azuelos [ID^{107,af}](#), D. Babal [ID^{28a}](#), H. Bachacou [ID¹³⁴](#), K. Bachas [ID^{151,s}](#), A. Bachiu [ID³⁴](#), F. Backman [ID^{47a,47b}](#), A. Badea [ID⁶¹](#), P. Bagnaia [ID^{74a,74b}](#), M. Bahmani [ID¹⁸](#), A.J. Bailey [ID¹⁶²](#), V.R. Bailey [ID¹⁶¹](#), J.T. Baines [ID¹³³](#), C. Bakalis [ID¹⁰](#), O.K. Baker [ID¹⁷¹](#), P.J. Bakker [ID¹¹³](#), E. Bakos [ID¹⁵](#), D. Bakshi Gupta [ID⁸](#), S. Balaji [ID¹⁴⁶](#), R. Balasubramanian [ID¹¹³](#), E.M. Baldin [ID³⁷](#), P. Balek [ID¹³²](#), E. Ballabene [ID^{70a,70b}](#), F. Balli [ID¹³⁴](#), L.M. Baltes [ID^{63a}](#), W.K. Balunas [ID³²](#), J. Balz [ID⁹⁹](#), E. Banas [ID⁸⁵](#), M. Bandieramonte [ID¹²⁸](#), A. Bandyopadhyay [ID²⁴](#), S. Bansal [ID²⁴](#), L. Barak [ID¹⁵⁰](#), E.L. Barberio [ID¹⁰⁴](#), D. Barberis [ID^{57b,57a}](#), M. Barbero [ID¹⁰¹](#), G. Barbour [ID⁹⁵](#), K.N. Barends [ID^{33a}](#), T. Barillari [ID¹⁰⁹](#), M-S. Barisits [ID³⁶](#), T. Barklow [ID¹⁴²](#), R.M. Barnett [ID^{17a}](#), P. Baron [ID¹²¹](#), D.A. Baron Moreno [ID¹⁰⁰](#), A. Baroncelli [ID^{62a}](#), G. Barone [ID²⁹](#), A.J. Barr [ID¹²⁵](#), L. Barranco Navarro [ID^{47a,47b}](#), F. Barreiro [ID⁹⁸](#), J. Barreiro Guimaraes da Costa [ID^{14a}](#), U. Barron [ID¹⁵⁰](#), M.G. Barros Teixeira [ID^{129a}](#), S. Barsov [ID³⁷](#), F. Bartels [ID^{63a}](#), R. Bartoldus [ID¹⁴²](#), A.E. Barton [ID⁹⁰](#), P. Bartos [ID^{28a}](#), A. Basalaev [ID⁴⁸](#), A. Basan [ID⁹⁹](#), M. Baselga [ID⁴⁹](#), I. Bashta [ID^{76a,76b}](#), A. Bassalat [ID^{66,b}](#), M.J. Basso [ID¹⁵⁴](#), C.R. Basson [ID¹⁰⁰](#), R.L. Bates [ID⁵⁹](#), S. Batlamous [ID^{35e}](#), J.R. Batley [ID³²](#), B. Batool [ID¹⁴⁰](#), M. Battaglia [ID¹³⁵](#), D. Battulga [ID¹⁸](#), M. Bauce [ID^{74a,74b}](#), P. Bauer [ID²⁴](#), A. Bayirli [ID^{21a}](#), J.B. Beacham [ID⁵¹](#), T. Beau [ID¹²⁶](#), P.H. Beauchemin [ID¹⁵⁷](#), F. Becherer [ID⁵⁴](#), P. Bechtle [ID²⁴](#), H.P. Beck [ID^{19,r}](#), K. Becker [ID¹⁶⁶](#), C. Becot [ID⁴⁸](#), A.J. Beddall [ID^{21d}](#), V.A. Bednyakov [ID³⁸](#), C.P. Bee [ID¹⁴⁴](#), L.J. Beemster [ID¹⁵](#), T.A. Beermann [ID³⁶](#), M. Begallie [ID^{81d}](#), M. Begel [ID²⁹](#), A. Behera [ID¹⁴⁴](#), J.K. Behr [ID⁴⁸](#), C. Beirao Da Cruz E Silva [ID³⁶](#), J.F. Beirer [ID^{55,36}](#), F. Beisiegel [ID²⁴](#), M. Belfkir [ID¹⁵⁸](#), G. Bella [ID¹⁵⁰](#), L. Bellagamba [ID^{23b}](#), A. Bellerive [ID³⁴](#), P. Bellos [ID²⁰](#), K. Beloborodov [ID³⁷](#), K. Belotskiy [ID³⁷](#), N.L. Belyaev [ID³⁷](#), D. Benchekroun [ID^{35a}](#), F. Bendebba [ID^{35a}](#), Y. Benhammou [ID¹⁵⁰](#), D.P. Benjamin [ID²⁹](#),

M. Benoit [ID²⁹](#), J.R. Bensinger [ID²⁶](#), S. Bentvelsen [ID¹¹³](#), L. Beresford [ID³⁶](#), M. Beretta [ID⁵³](#), D. Berge [ID¹⁸](#), E. Bergeaas Kuutmann [ID¹⁶⁰](#), N. Berger [ID⁴](#), B. Bergmann [ID¹³¹](#), J. Beringer [ID^{17a}](#), S. Berlendis [ID⁷](#), G. Bernardi [ID⁵](#), C. Bernius [ID¹⁴²](#), F.U. Bernlochner [ID²⁴](#), T. Berry [ID⁹⁴](#), P. Berta [ID¹³²](#), A. Berthold [ID⁵⁰](#), I.A. Bertram [ID⁹⁰](#), S. Bethke [ID¹⁰⁹](#), A. Betti [ID^{74a,74b}](#), A.J. Bevan [ID⁹³](#), M. Bhamjee [ID^{33c}](#), S. Bhatta [ID¹⁴⁴](#), D.S. Bhattacharya [ID¹⁶⁵](#), P. Bhattacharai [ID²⁶](#), V.S. Bhopatkar [ID¹²⁰](#), R. Bi [ID^{29,ai}](#), R.M. Bianchi [ID¹²⁸](#), O. Biebel [ID¹⁰⁸](#), R. Bielski [ID¹²²](#), M. Biglietti [ID^{76a}](#), T.R.V. Billoud [ID¹³¹](#), M. Bindu [ID⁵⁵](#), A. Bingul [ID^{21b}](#), C. Bini [ID^{74a,74b}](#), S. Biondi [ID^{23b,23a}](#), A. Biondini [ID⁹¹](#), C.J. Birch-sykes [ID¹⁰⁰](#), G.A. Bird [ID^{20,133}](#), M. Birman [ID¹⁶⁸](#), T. Bisanz [ID³⁶](#), E. Bisceglie [ID^{43b,43a}](#), D. Biswas [ID^{169,1}](#), A. Bitadze [ID¹⁰⁰](#), K. Bjørke [ID¹²⁴](#), I. Bloch [ID⁴⁸](#), C. Blocker [ID²⁶](#), A. Blue [ID⁵⁹](#), U. Blumenschein [ID⁹³](#), J. Blumenthal [ID⁹⁹](#), G.J. Bobbink [ID¹¹³](#), V.S. Bobrovnikov [ID³⁷](#), M. Boehler [ID⁵⁴](#), D. Bogavac [ID³⁶](#), A.G. Bogdanchikov [ID³⁷](#), C. Bohm [ID^{47a}](#), V. Boisvert [ID⁹⁴](#), P. Bokan [ID⁴⁸](#), T. Bold [ID^{84a}](#), M. Bomben [ID⁵](#), M. Bona [ID⁹³](#), M. Boonekamp [ID¹³⁴](#), C.D. Booth [ID⁹⁴](#), A.G. Borbely [ID⁵⁹](#), H.M. Borecka-Bielska [ID¹⁰⁷](#), L.S. Borgna [ID⁹⁵](#), G. Borissov [ID⁹⁰](#), D. Bortoletto [ID¹²⁵](#), D. Boscherini [ID^{23b}](#), M. Bosman [ID¹³](#), J.D. Bossio Sola [ID³⁶](#), K. Bouaouda [ID^{35a}](#), J. Boudreau [ID¹²⁸](#), E.V. Bouhova-Thacker [ID⁹⁰](#), D. Boumediene [ID⁴⁰](#), R. Bouquet [ID⁵](#), A. Boveia [ID¹¹⁸](#), J. Boyd [ID³⁶](#), D. Boye [ID²⁹](#), I.R. Boyko [ID³⁸](#), J. Bracinik [ID²⁰](#), N. Brahimi [ID^{62d}](#), G. Brandt [ID¹⁷⁰](#), O. Brandt [ID³²](#), F. Braren [ID⁴⁸](#), B. Brau [ID¹⁰²](#), J.E. Brau [ID¹²²](#), K. Brendlinger [ID⁴⁸](#), R. Brener [ID¹⁶⁸](#), L. Brenner [ID³⁶](#), R. Brenner [ID¹⁶⁰](#), S. Bressler [ID¹⁶⁸](#), B. Brickwedde [ID⁹⁹](#), D. Britton [ID⁵⁹](#), D. Britzger [ID¹⁰⁹](#), I. Brock [ID²⁴](#), G. Brooijmans [ID⁴¹](#), W.K. Brooks [ID^{136f}](#), E. Brost [ID²⁹](#), T.L. Bruckler [ID¹²⁵](#), P.A. Bruckman de Renstrom [ID⁸⁵](#), B. Brüers [ID⁴⁸](#), D. Bruncko [ID^{28b,*}](#), A. Brunni [ID^{23b}](#), G. Brunni [ID^{23b}](#), M. Bruschi [ID^{23b}](#), N. Bruscino [ID^{74a,74b}](#), L. Bryngemark [ID¹⁴²](#), T. Buanes [ID¹⁶](#), Q. Buat [ID¹³⁷](#), P. Buchholz [ID¹⁴⁰](#), A.G. Buckley [ID⁵⁹](#), I.A. Budagov [ID^{38,*}](#), M.K. Bugge [ID¹²⁴](#), O. Bulekov [ID³⁷](#), B.A. Bullard [ID⁶¹](#), S. Burdin [ID⁹¹](#), C.D. Burgard [ID⁴⁸](#), A.M. Burger [ID⁴⁰](#), B. Burghgrave [ID⁸](#), J.T.P. Burr [ID³²](#), C.D. Burton [ID¹¹](#), J.C. Burzynski [ID¹⁴¹](#), E.L. Busch [ID⁴¹](#), V. Büscher [ID⁹⁹](#), P.J. Bussey [ID⁵⁹](#), J.M. Butler [ID²⁵](#), C.M. Buttar [ID⁵⁹](#), J.M. Butterworth [ID⁹⁵](#), W. Buttinger [ID¹³³](#), C.J. Buxo Vazquez [ID¹⁰⁶](#), A.R. Buzykaev [ID³⁷](#), G. Cabras [ID^{23b}](#), S. Cabrera Urbán [ID¹⁶²](#), D. Caforio [ID⁵⁸](#), H. Cai [ID¹²⁸](#), Y. Cai [ID^{14a,14d}](#), V.M.M. Cairo [ID³⁶](#), O. Cakir [ID^{3a}](#), N. Calace [ID³⁶](#), P. Calafiura [ID^{17a}](#), G. Calderini [ID¹²⁶](#), P. Calfayan [ID⁶⁷](#), G. Callea [ID⁵⁹](#), L.P. Caloba [ID^{81b}](#), D. Calvet [ID⁴⁰](#), S. Calvet [ID⁴⁰](#), T.P. Calvet [ID¹⁰¹](#), M. Calvetti [ID^{73a,73b}](#), R. Camacho Toro [ID¹²⁶](#), S. Camarda [ID³⁶](#), D. Camarero Munoz [ID²⁶](#), P. Camarri [ID^{75a,75b}](#), M.T. Camerlingo [ID^{76a,76b}](#), D. Cameron [ID¹²⁴](#), C. Camincher [ID¹⁶⁴](#), M. Campanelli [ID⁹⁵](#), A. Camplani [ID⁴²](#), V. Canale [ID^{71a,71b}](#), A. Canesse [ID¹⁰³](#), M. Cano Bret [ID⁷⁹](#), J. Cantero [ID¹⁶²](#), Y. Cao [ID¹⁶¹](#), F. Capocasa [ID²⁶](#), M. Capua [ID^{43b,43a}](#), A. Carbone [ID^{70a,70b}](#), R. Cardarelli [ID^{75a}](#), J.C.J. Cardenas [ID⁸](#), F. Cardillo [ID¹⁶²](#), T. Carli [ID³⁶](#), G. Carlino [ID^{71a}](#), J.I. Carlotto [ID¹³](#), B.T. Carlson [ID^{128,t}](#), E.M. Carlson [ID^{164,155a}](#), L. Carminati [ID^{70a,70b}](#), M. Carnesale [ID^{74a,74b}](#), S. Caron [ID¹¹²](#), E. Carquin [ID^{136f}](#), S. Carrá [ID^{70a,70b}](#), G. Carratta [ID^{23b,23a}](#), F. Carrio Argos [ID^{33g}](#), J.W.S. Carter [ID¹⁵⁴](#), T.M. Carter [ID⁵²](#), M.P. Casado [ID^{13,i}](#), A.F. Casha [ID¹⁵⁴](#), E.G. Castiglia [ID¹⁷¹](#), F.L. Castillo [ID^{63a}](#), L. Castillo Garcia [ID¹³](#), V. Castillo Gimenez [ID¹⁶²](#), N.F. Castro [ID^{129a,129e}](#), A. Catinaccio [ID³⁶](#), J.R. Catmore [ID¹²⁴](#), V. Cavalieri [ID²⁹](#), N. Cavalli [ID^{23b,23a}](#), V. Cavasinni [ID^{73a,73b}](#), E. Celebi [ID^{21a}](#), F. Celli [ID¹²⁵](#), M.S. Centonze [ID^{69a,69b}](#), K. Cerny [ID¹²¹](#), A.S. Cerqueira [ID^{81a}](#), A. Cerri [ID¹⁴⁵](#), L. Cerrito [ID^{75a,75b}](#), F. Cerutti [ID^{17a}](#), A. Cervelli [ID^{23b}](#), S.A. Cetin [ID^{21d}](#), Z. Chadi [ID^{35a}](#), D. Chakraborty [ID¹¹⁴](#), M. Chala [ID^{129f}](#), J. Chan [ID¹⁶⁹](#), W.Y. Chan [ID¹⁵²](#), J.D. Chapman [ID³²](#), B. Chargeishvili [ID^{148b}](#), D.G. Charlton [ID²⁰](#), T.P. Charman [ID⁹³](#), M. Chatterjee [ID¹⁹](#), S. Chekanov [ID⁶](#), S.V. Chekulaev [ID^{155a}](#), G.A. Chelkov [ID^{38,a}](#), A. Chen [ID¹⁰⁵](#), B. Chen [ID¹⁵⁰](#), B. Chen [ID¹⁶⁴](#), C. Chen [ID^{62a}](#), H. Chen [ID^{14c}](#), H. Chen [ID²⁹](#), J. Chen [ID^{62c}](#), J. Chen [ID²⁶](#), S. Chen [ID¹⁵²](#), S.J. Chen [ID^{14c}](#), X. Chen [ID^{62c}](#), X. Chen [ID^{14b,ae}](#), Y. Chen [ID^{62a}](#), C.L. Cheng [ID¹⁶⁹](#), H.C. Cheng [ID^{64a}](#), A. Cheplakov [ID³⁸](#), E. Cheremushkina [ID⁴⁸](#), E. Cherepanova [ID¹¹³](#), R. Cherkaoui El Moursli [ID^{35e}](#), E. Cheu [ID⁷](#), K. Cheung [ID⁶⁵](#), L. Chevalier [ID¹³⁴](#), V. Chiarella [ID⁵³](#), G. Chiarelli [ID^{73a}](#), N. Chiedde [ID¹⁰¹](#), G. Chiodini [ID^{69a}](#), A.S. Chisholm [ID²⁰](#), A. Chitan [ID^{27b}](#), M. Chitishvili [ID¹⁶²](#), Y.H. Chiu [ID¹⁶⁴](#), M.V. Chizhov [ID³⁸](#), K. Choi [ID¹¹](#), A.R. Chomont [ID^{74a,74b}](#), Y. Chou [ID¹⁰²](#), E.Y.S. Chow [ID¹¹³](#), T. Chowdhury [ID^{33g}](#), L.D. Christopher [ID^{33g}](#),

K.L. Chu^{64a}, M.C. Chu^{ID_{64a}}, X. Chu^{ID_{14a,14d}}, J. Chudoba^{ID₁₃₀}, J.J. Chwastowski^{ID₈₅}, D. Cieri^{ID₁₀₉},
 K.M. Ciesla^{ID_{84a}}, V. Cindro^{ID₉₂}, A. Ciocio^{ID_{17a}}, F. Cirotto^{ID_{71a,71b}}, Z.H. Citron^{ID_{168,m}}, M. Citterio^{ID_{70a}},
 D.A. Ciubotaru^{ID_{27b}}, B.M. Ciungu^{ID₁₅₄}, A. Clark^{ID₅₆}, P.J. Clark^{ID₅₂}, J.M. Clavijo Columbie^{ID₄₈},
 S.E. Clawson^{ID₁₀₀}, C. Clement^{ID_{47a,47b}}, J. Clercx^{ID₄₈}, L. Clissa^{ID_{23b,23a}}, Y. Coadou^{ID₁₀₁},
 M. Cobal^{ID_{68a,68c}}, A. Coccaro^{ID_{57b}}, R.F. Coelho Barrue^{ID_{129a}}, R. Coelho Lopes De Sa^{ID₁₀₂},
 S. Coelli^{ID_{70a}}, H. Cohen^{ID₁₅₀}, A.E.C. Coimbra^{ID_{70a,70b}}, B. Cole^{ID₄₁}, J. Collot^{ID₆₀},
 P. Conde Muiño^{ID_{129a,129g}}, M.P. Connell^{ID_{33c}}, S.H. Connell^{ID_{33c}}, I.A. Connelly^{ID₅₉}, E.I. Conroy^{ID₁₂₅},
 F. Conventi^{ID_{71a,ag}}, H.G. Cooke^{ID₂₀}, A.M. Cooper-Sarkar^{ID₁₂₅}, F. Cormier^{ID₁₆₃}, L.D. Corpe^{ID₃₆},
 M. Corradi^{ID_{74a,74b}}, E.E. Corrigan^{ID₉₇}, F. Corriveau^{ID_{103,x}}, A. Cortes-Gonzalez^{ID₁₈}, M.J. Costa^{ID₁₆₂},
 F. Costanza^{ID₄}, D. Costanzo^{ID₁₃₈}, B.M. Cote^{ID₁₁₈}, G. Cowan^{ID₉₄}, J.W. Cowley^{ID₃₂}, K. Cranmer^{ID₁₁₆},
 S. Crépé-Renaudin^{ID₆₀}, F. Crescioli^{ID₁₂₆}, M. Cristinziani^{ID₁₄₀}, M. Cristoforetti^{ID_{77a,77b,d}}, V. Croft^{ID₁₅₇},
 G. Crosetti^{ID_{43b,43a}}, A. Cueto^{ID₃₆}, T. Cuhadar Donszelmann^{ID₁₅₉}, H. Cui^{ID_{14a,14d}}, Z. Cui^{ID₇},
 A.R. Cukierman^{ID₁₄₂}, W.R. Cunningham^{ID₅₉}, F. Curcio^{ID_{43b,43a}}, P. Czodrowski^{ID₃₆}, M.M. Czurylo^{ID_{63b}},
 M.J. Da Cunha Sargedas De Sousa^{ID_{62a}}, J.V. Da Fonseca Pinto^{ID_{81b}}, C. Da Via^{ID₁₀₀}, W. Dabrowski^{ID_{84a}},
 T. Dado^{ID₄₉}, S. Dahbi^{ID_{33g}}, T. Dai^{ID₁₀₅}, C. Dallapiccola^{ID₁₀₂}, M. Dam^{ID₄₂}, G. D'amen^{ID₂₉},
 V. D'Amico^{ID₁₀₈}, J. Damp^{ID₉₉}, J.R. Dandoy^{ID₁₂₇}, M.F. Daneri^{ID₃₀}, M. Danninger^{ID₁₄₁}, V. Dao^{ID₃₆},
 G. Darbo^{ID_{57b}}, S. Darmora^{ID₆}, S.J. Das^{ID_{29,ai}}, S. D'Auria^{ID_{70a,70b}}, C. David^{ID_{155b}}, T. Davidek^{ID₁₃₂},
 D.R. Davis^{ID₅₁}, B. Davis-Purcell^{ID₃₄}, I. Dawson^{ID₉₃}, K. De^{ID₈}, R. De Asmundis^{ID_{71a}},
 M. De Beurs^{ID₁₁₃}, N. De Biase^{ID₄₈}, S. De Castro^{ID_{23b,23a}}, N. De Groot^{ID₁₁₂}, P. de Jong^{ID₁₁₃},
 H. De la Torre^{ID₁₀₆}, A. De Maria^{ID_{14c}}, A. De Salvo^{ID_{74a}}, U. De Sanctis^{ID_{75a,75b}}, A. De Santo^{ID₁₄₅},
 J.B. De Vivie De Regie^{ID₆₀}, D.V. Dedovich³⁸, J. Degens^{ID₁₁₃}, A.M. Deiana^{ID₄₄}, F. Del Corso^{ID_{23b,23a}},
 J. Del Peso^{ID₉₈}, F. Del Rio^{ID_{63a}}, F. Deliot^{ID₁₃₄}, C.M. Delitzsch^{ID₄₉}, M. Della Pietra^{ID_{71a,71b}},
 D. Della Volpe^{ID₅₆}, A. Dell'Acqua^{ID₃₆}, L. Dell'Asta^{ID_{70a,70b}}, M. Delmastro^{ID₄}, P.A. Delsart^{ID₆₀},
 S. Demers^{ID₁₇₁}, M. Demichev^{ID₃₈}, S.P. Denisov^{ID₃₇}, L. D'Eramo^{ID₁₁₄}, D. Derendarz^{ID₈₅}, F. Derue^{ID₁₂₆},
 P. Dervan^{ID₉₁}, K. Desch^{ID₂₄}, K. Dette^{ID₁₅₄}, C. Deutsch^{ID₂₄}, P.O. Deviveiros^{ID₃₆}, F.A. Di Bello^{ID_{74a,74b}},
 A. Di Ciacco^{ID_{75a,75b}}, L. Di Ciacco^{ID₄}, A. Di Domenico^{ID_{74a,74b}}, C. Di Donato^{ID_{71a,71b}},
 A. Di Girolamo^{ID₃₆}, G. Di Gregorio^{ID_{73a,73b}}, A. Di Luca^{ID_{77a,77b}}, B. Di Micco^{ID_{76a,76b}},
 R. Di Nardo^{ID_{76a,76b}}, C. Diaconu^{ID₁₀₁}, F.A. Dias^{ID₁₁₃}, T. Dias Do Vale^{ID₁₄₁}, M.A. Diaz^{ID_{136a,136b}},
 F.G. Diaz Capriles^{ID₂₄}, M. Didenko^{ID₁₆₂}, E.B. Diehl^{ID₁₀₅}, L. Diehl^{ID₅₄}, S. Díez Cornell^{ID₄₈},
 C. Diez Pardos^{ID₁₄₀}, C. Dimitriadi^{ID_{24,160}}, A. Dimitrievska^{ID_{17a}}, W. Ding^{ID_{14b}}, J. Dingfelder^{ID₂₄},
 I-M. Dinu^{ID_{27b}}, S.J. Dittmeier^{ID_{63b}}, F. Dittus^{ID₃₆}, F. Djama^{ID₁₀₁}, T. Djobava^{ID_{148b}}, J.I. Djuvsland^{ID₁₆},
 C. Doglioni^{ID_{100,97}}, J. Dolejsi^{ID₁₃₂}, Z. Dolezal^{ID₁₃₂}, M. Donadelli^{ID_{81c}}, B. Dong^{ID_{62c}}, J. Donini^{ID₄₀},
 A. D'Onofrio^{ID_{14c}}, M. D'Onofrio^{ID₉₁}, J. Dopke^{ID₁₃₃}, A. Doria^{ID_{71a}}, M.T. Dova^{ID₈₉}, A.T. Doyle^{ID₅₉},
 M.A. Draguet^{ID₁₂₅}, E. Drechsler^{ID₁₄₁}, E. Dreyer^{ID₁₆₈}, I. Drivas-koulouris^{ID₁₀}, A.S. Drobac^{ID₁₅₇},
 M. Drozdova^{ID₅₆}, D. Du^{ID_{62a}}, T.A. du Pree^{ID₁₁₃}, F. Dubinin^{ID₃₇}, M. Dubovsky^{ID_{28a}}, E. Duchovni^{ID₁₆₈},
 G. Duckeck^{ID₁₀₈}, O.A. Ducu^{ID_{27b}}, D. Duda^{ID₁₀₉}, A. Dudarev^{ID₃₆}, M. D'uffizi^{ID₁₀₀}, L. Duflot^{ID₆₆},
 M. Dührssen^{ID₃₆}, C. Dülsen^{ID₁₇₀}, A.E. Dumitriu^{ID_{27b}}, M. Dunford^{ID_{63a}}, S. Dungs^{ID₄₉},
 K. Dunne^{ID_{47a,47b}}, A. Duperrin^{ID₁₀₁}, H. Duran Yildiz^{ID_{3a}}, M. Düren^{ID₅₈}, A. Durglishvili^{ID_{148b}},
 B.L. Dwyer^{ID₁₁₄}, G.I. Dyckes^{ID_{17a}}, M. Dyndal^{ID_{84a}}, S. Dysch^{ID₁₀₀}, B.S. Dziedzic^{ID₈₅},
 Z.O. Earnshaw^{ID₁₄₅}, B. Eckerova^{ID_{28a}}, M.G. Eggleston⁵¹, E. Egidio Purcino De Souza^{ID_{81b}},
 L.F. Ehrke^{ID₅₆}, G. Eigen^{ID₁₆}, K. Einsweiler^{ID_{17a}}, T. Ekelof^{ID₁₆₀}, P.A. Ekman^{ID₉₇}, Y. El Ghazali^{ID_{35b}},
 H. El Jarrari^{ID_{35e,147}}, A. El Moussaoui^{ID_{35a}}, V. Ellajosyula^{ID₁₆₀}, M. Ellert^{ID₁₆₀}, F. Ellinghaus^{ID₁₇₀},
 A.A. Elliot^{ID₉₃}, N. Ellis^{ID₃₆}, J. Elmsheuser^{ID₂₉}, M. Elsing^{ID₃₆}, D. Emeliyanov^{ID₁₃₃}, A. Emerman^{ID₄₁},
 Y. Enari^{ID₁₅₂}, I. Ene^{ID_{17a}}, S. Epari^{ID₁₃}, J. Erdmann^{ID₄₉}, A. Ereditato^{ID₁₉}, P.A. Erland^{ID₈₅},
 M. Errenst^{ID₁₇₀}, M. Escalier^{ID₆₆}, C. Escobar^{ID₁₆₂}, E. Etzion^{ID₁₅₀}, G. Evans^{ID_{129a}}, H. Evans^{ID₆₇},
 M.O. Evans^{ID₁₄₅}, A. Ezhilov^{ID₃₇}, S. Ezzarqtouni^{ID_{35a}}, F. Fabbri^{ID₅₉}, L. Fabbri^{ID_{23b,23a}}, G. Facini^{ID₉₅},
 V. Fadeyev^{ID₁₃₅}, R.M. Fakhrutdinov^{ID₃₇}, S. Falciano^{ID_{74a}}, P.J. Falke^{ID₂₄}, S. Falke^{ID₃₆}, J. Faltova^{ID₁₃₂},

Y. Fan **ID**^{14a}, Y. Fang **ID**^{14a,14d}, G. Fanourakis **ID**⁴⁶, M. Fanti **ID**^{70a,70b}, M. Faraj **ID**^{68a,68b}, A. Farbin **ID**⁸,
 A. Farilla **ID**^{76a}, T. Farooque **ID**¹⁰⁶, S.M. Farrington **ID**⁵², F. Fassi **ID**^{35e}, D. Fassouliotis **ID**⁹,
 M. Faucci Giannelli **ID**^{75a,75b}, W.J. Fawcett **ID**³², L. Fayard **ID**⁶⁶, P. Federicova **ID**¹³⁰, O.L. Fedin **ID**^{37,a},
 G. Fedotov **ID**³⁷, M. Feickert **ID**¹⁶¹, L. Feligioni **ID**¹⁰¹, A. Fell **ID**¹³⁸, D.E. Fellers **ID**¹²², C. Feng **ID**^{62b},
 M. Feng **ID**^{14b}, Z. Feng **ID**¹¹³, M.J. Fenton **ID**¹⁵⁹, A.B. Fenyuk ³⁷, L. Ferencz **ID**⁴⁸, S.W. Ferguson **ID**⁴⁵,
 J. Ferrando **ID**⁴⁸, A. Ferrari **ID**¹⁶⁰, P. Ferrari **ID**¹¹³, R. Ferrari **ID**^{72a}, D. Ferrere **ID**⁵⁶, C. Ferretti **ID**¹⁰⁵,
 F. Fiedler **ID**⁹⁹, A. Filipčič **ID**⁹², E.K. Filmer **ID**¹, F. Filthaut **ID**¹¹², M.C.N. Fiolhais **ID**^{129a,129c,c},
 L. Fiorini **ID**¹⁶², F. Fischer **ID**¹⁴⁰, W.C. Fisher **ID**¹⁰⁶, T. Fitschen **ID**²⁰, I. Fleck **ID**¹⁴⁰, P. Fleischmann **ID**¹⁰⁵,
 T. Flick **ID**¹⁷⁰, L. Flores **ID**¹²⁷, M. Flores **ID**^{33d,ac}, L.R. Flores Castillo **ID**^{64a}, F.M. Follega **ID**^{77a,77b},
 N. Fomin **ID**¹⁶, J.H. Foo **ID**¹⁵⁴, B.C. Forland ⁶⁷, A. Formica **ID**¹³⁴, A.C. Forti **ID**¹⁰⁰, E. Fortin **ID**¹⁰¹,
 A.W. Fortman **ID**⁶¹, M.G. Foti **ID**^{17a}, L. Fountas **ID**^{9,j}, D. Fournier **ID**⁶⁶, H. Fox **ID**⁹⁰, P. Francavilla **ID**^{73a,73b},
 S. Francescato **ID**⁶¹, M. Franchini **ID**^{23b,23a}, S. Franchino **ID**^{63a}, D. Francis ³⁶, L. Franco **ID**¹¹²,
 L. Franconi **ID**¹⁹, M. Franklin **ID**⁶¹, G. Frattari **ID**²⁶, A.C. Freegard **ID**⁹³, P.M. Freeman ²⁰, W.S. Freund **ID**^{81b},
 N. Fritzsche **ID**⁵⁰, A. Froch **ID**⁵⁴, D. Froidevaux **ID**³⁶, J.A. Frost **ID**¹²⁵, Y. Fu **ID**^{62a}, M. Fujimoto **ID**¹¹⁷,
 E. Fullana Torregrosa **ID**^{162,*}, J. Fuster **ID**¹⁶², A. Gabrielli **ID**^{23b,23a}, A. Gabrielli **ID**¹⁵⁴, P. Gadow **ID**⁴⁸,
 G. Gagliardi **ID**^{57b,57a}, L.G. Gagnon **ID**^{17a}, G.E. Gallardo **ID**¹²⁵, E.J. Gallas **ID**¹²⁵, B.J. Gallop **ID**¹³³,
 R. Gamboa Goni **ID**⁹³, K.K. Gan **ID**¹¹⁸, S. Ganguly **ID**¹⁵², J. Gao **ID**^{62a}, Y. Gao **ID**⁵²,
 F.M. Garay Walls **ID**^{136a,136b}, B. Garcia ^{29,ai}, C. Garcia **ID**¹⁶², J.E. García Navarro **ID**¹⁶²,
 J.A. García Pascual **ID**^{14a}, M. Garcia-Sciveres **ID**^{17a}, R.W. Gardner **ID**³⁹, D. Garg **ID**⁷⁹, R.B. Garg **ID**^{142,q},
 S. Gargiulo **ID**⁵⁴, C.A. Garner ¹⁵⁴, V. Garonne **ID**²⁹, S.J. Gasiorowski **ID**¹³⁷, P. Gaspar **ID**^{81b}, G. Gaudio **ID**^{72a},
 V. Gautam ¹³, P. Gauzzi **ID**^{74a,74b}, I.L. Gavrilenko **ID**³⁷, A. Gavrilyuk **ID**³⁷, C. Gay **ID**¹⁶³, G. Gaycken **ID**⁴⁸,
 E.N. Gazis **ID**¹⁰, A.A. Geanta **ID**^{27b,27e}, C.M. Gee **ID**¹³⁵, J. Geisen **ID**⁹⁷, M. Geisen **ID**⁹⁹, C. Gemme **ID**^{57b},
 M.H. Genest **ID**⁶⁰, S. Gentile **ID**^{74a,74b}, S. George **ID**⁹⁴, W.F. George **ID**²⁰, T. Geralis **ID**⁴⁶, L.O. Gerlach ⁵⁵,
 P. Gessinger-Befurt **ID**³⁶, M. Ghasemi Bostanabad **ID**¹⁶⁴, M. Ghneimat **ID**¹⁴⁰, A. Ghosal **ID**¹⁴⁰,
 A. Ghosh **ID**¹⁵⁹, A. Ghosh **ID**⁷, B. Giacobbe **ID**^{23b}, S. Giagu **ID**^{74a,74b}, N. Giangiocomi **ID**¹⁵⁴,
 P. Giannetti **ID**^{73a}, A. Giannini **ID**^{62a}, S.M. Gibson **ID**⁹⁴, M. Gignac **ID**¹³⁵, D.T. Gil **ID**^{84b}, A.K. Gilbert **ID**^{84a},
 B.J. Gilbert **ID**⁴¹, D. Gillberg **ID**³⁴, G. Gilles **ID**¹¹³, N.E.K. Gillwald **ID**⁴⁸, L. Ginabat **ID**¹²⁶,
 D.M. Gingrich **ID**^{2,af}, M.P. Giordani **ID**^{68a,68c}, P.F. Giraud **ID**¹³⁴, G. Giugliarelli **ID**^{68a,68c}, D. Giugni **ID**^{70a},
 F. Giuli **ID**³⁶, I. Gkialas **ID**^{9,j}, L.K. Gladilin **ID**³⁷, C. Glasman **ID**⁹⁸, G.R. Gledhill **ID**¹²², M. Glisic ¹²²,
 I. Gnesi **ID**^{43b,f}, Y. Go **ID**^{29,ai}, M. Goblirsch-Kolb **ID**²⁶, D. Godin ¹⁰⁷, S. Goldfarb **ID**¹⁰⁴, T. Golling **ID**⁵⁶,
 M.G.D. Gololo ^{33g}, D. Golubkov **ID**³⁷, J.P. Gombas **ID**¹⁰⁶, A. Gomes **ID**^{129a,129b}, G. Gomes Da Silva **ID**¹⁴⁰,
 A.J. Gomez Delegido **ID**¹⁶², R. Goncalves Gama **ID**⁵⁵, R. Gonçalo **ID**^{129a,129c}, G. Gonella **ID**¹²²,
 L. Gonella **ID**²⁰, A. Gongadze **ID**³⁸, F. Gonnella **ID**²⁰, J.L. Gonski **ID**⁴¹, R.Y. González Andana **ID**⁵²,
 S. González de la Hoz **ID**¹⁶², S. Gonzalez Fernandez **ID**¹³, R. Gonzalez Lopez **ID**⁹¹,
 C. Gonzalez Renteria **ID**^{17a}, R. Gonzalez Suarez **ID**¹⁶⁰, S. Gonzalez-Sevilla **ID**⁵⁶,
 G.R. Gonzalez Rodriguez **ID**¹⁶², L. Goossens **ID**³⁶, N.A. Gorasia **ID**²⁰, P.A. Gorbounov **ID**³⁷, B. Gorini **ID**³⁶,
 E. Gorini **ID**^{69a,69b}, A. Gorišek **ID**⁹², A.T. Goshaw **ID**⁵¹, M.I. Gostkin **ID**³⁸, C.A. Gottardo **ID**³⁶,
 M. Gouighri **ID**^{35b}, V. Goumarre **ID**⁴⁸, A.G. Goussiou **ID**¹³⁷, N. Govender **ID**^{33c}, C. Goy **ID**⁴,
 I. Grabowska-Bold **ID**^{84a}, K. Graham **ID**³⁴, E. Gramstad **ID**¹²⁴, S. Grancagnolo **ID**¹⁸, M. Grandi **ID**¹⁴⁵,
 V. Gratchev ^{37,*}, P.M. Gravila **ID**^{27f}, F.G. Gravili **ID**^{69a,69b}, H.M. Gray **ID**^{17a}, M. Greco **ID**^{69a,69b},
 C. Grefe **ID**²⁴, I.M. Gregor **ID**⁴⁸, P. Grenier **ID**¹⁴², C. Grieco **ID**¹³, A.A. Grillo **ID**¹³⁵, K. Grimm **ID**^{31,n},
 S. Grinstein **ID**^{13,v}, J.-F. Grivaz **ID**⁶⁶, E. Gross **ID**¹⁶⁸, J. Grosse-Knetter **ID**⁵⁵, C. Grud ¹⁰⁵, A. Grummer **ID**¹¹¹,
 J.C. Grundy **ID**¹²⁵, L. Guan **ID**¹⁰⁵, W. Guan **ID**¹⁶⁹, C. Gubbels **ID**¹⁶³, J.G.R. Guerrero Rojas **ID**¹⁶²,
 G. Guerrieri **ID**^{68a,68b}, F. Guescini **ID**¹⁰⁹, R. Gugel **ID**⁹⁹, J.A.M. Guhit **ID**¹⁰⁵, A. Guida **ID**⁴⁸, T. Guillemin **ID**⁴,
 E. Guilloton **ID**^{166,133}, S. Guindon **ID**³⁶, F. Guo **ID**^{14a,14d}, J. Guo **ID**^{62c}, L. Guo **ID**⁶⁶, Y. Guo **ID**¹⁰⁵,
 R. Gupta **ID**⁴⁸, S. Gurbuz **ID**²⁴, S.S. Gurdasani **ID**⁵⁴, G. Gustavino **ID**³⁶, M. Guth **ID**⁵⁶, P. Gutierrez **ID**¹¹⁹,
 L.F. Gutierrez Zagazeta **ID**¹²⁷, C. Gutschow **ID**⁹⁵, C. Guyot **ID**¹³⁴, C. Gwenlan **ID**¹²⁵, C.B. Gwilliam **ID**⁹¹,

E.S. Haaland [ID¹²⁴](#), A. Haas [ID¹¹⁶](#), M. Habedank [ID⁴⁸](#), C. Haber [ID^{17a}](#), H.K. Hadavand [ID⁸](#), A. Hadef [ID⁹⁹](#), S. Hadzic [ID¹⁰⁹](#), M. Haleem [ID¹⁶⁵](#), J. Haley [ID¹²⁰](#), J.J. Hall [ID¹³⁸](#), G.D. Hallewell [ID¹⁰¹](#), L. Halser [ID¹⁹](#), K. Hamano [ID¹⁶⁴](#), H. Hamdaoui [ID^{35e}](#), M. Hamer [ID²⁴](#), G.N. Hamity [ID⁵²](#), J. Han [ID^{62b}](#), K. Han [ID^{62a}](#), L. Han [ID^{14c}](#), L. Han [ID^{62a}](#), S. Han [ID^{17a}](#), Y.F. Han [ID¹⁵⁴](#), K. Hanagaki [ID⁸²](#), M. Hance [ID¹³⁵](#), D.A. Hangal [ID^{41,ab}](#), H. Hanif [ID¹⁴¹](#), M.D. Hank [ID³⁹](#), R. Hankache [ID¹⁰⁰](#), J.B. Hansen [ID⁴²](#), J.D. Hansen [ID⁴²](#), P.H. Hansen [ID⁴²](#), K. Hara [ID¹⁵⁶](#), D. Harada [ID⁵⁶](#), T. Harenberg [ID¹⁷⁰](#), S. Harkusha [ID³⁷](#), Y.T. Harris [ID¹²⁵](#), N.M. Harrison [ID¹¹⁸](#), P.F. Harrison [ID¹⁶⁶](#), N.M. Hartman [ID¹⁴²](#), N.M. Hartmann [ID¹⁰⁸](#), Y. Hasegawa [ID¹³⁹](#), A. Hasib [ID⁵²](#), S. Haug [ID¹⁹](#), R. Hauser [ID¹⁰⁶](#), M. Havranek [ID¹³¹](#), C.M. Hawkes [ID²⁰](#), R.J. Hawkings [ID³⁶](#), S. Hayashida [ID¹¹⁰](#), D. Hayden [ID¹⁰⁶](#), C. Hayes [ID¹⁰⁵](#), R.L. Hayes [ID¹⁶³](#), C.P. Hays [ID¹²⁵](#), J.M. Hays [ID⁹³](#), H.S. Hayward [ID⁹¹](#), F. He [ID^{62a}](#), Y. He [ID¹⁵³](#), Y. He [ID¹²⁶](#), M.P. Heath [ID⁵²](#), V. Hedberg [ID⁹⁷](#), A.L. Heggelund [ID¹²⁴](#), N.D. Hehir [ID⁹³](#), C. Heidegger [ID⁵⁴](#), K.K. Heidegger [ID⁵⁴](#), W.D. Heidorn [ID⁸⁰](#), J. Heilman [ID³⁴](#), S. Heim [ID⁴⁸](#), T. Heim [ID^{17a}](#), J.G. Heinlein [ID¹²⁷](#), J.J. Heinrich [ID¹²²](#), L. Heinrich [ID^{109,ad}](#), J. Hejbal [ID¹³⁰](#), L. Helaryl [ID⁴⁸](#), A. Held [ID¹⁶⁹](#), S. Hellesund [ID¹²⁴](#), C.M. Helling [ID¹⁶³](#), S. Hellman [ID^{47a,47b}](#), C. Helsens [ID³⁶](#), R.C.W. Henderson [ID⁹⁰](#), L. Henkelmann [ID³²](#), A.M. Henriques Correia [ID³⁶](#), H. Herde [ID¹⁴²](#), Y. Hernández Jiménez [ID¹⁴⁴](#), M.G. Herrmann [ID¹⁰⁸](#), T. Herrmann [ID⁵⁰](#), G. Herten [ID⁵⁴](#), R. Hertenberger [ID¹⁰⁸](#), L. Hervas [ID³⁶](#), N.P. Hessey [ID^{155a}](#), H. Hibi [ID⁸³](#), E. Higón-Rodríguez [ID¹⁶²](#), S.J. Hillier [ID²⁰](#), I. Hinchliffe [ID^{17a}](#), F. Hinterkeuser [ID²⁴](#), M. Hirose [ID¹²³](#), S. Hirose [ID¹⁵⁶](#), D. Hirschbuehl [ID¹⁷⁰](#), T.G. Hitchings [ID¹⁰⁰](#), B. Hiti [ID⁹²](#), J. Hobbs [ID¹⁴⁴](#), R. Hobincu [ID^{27e}](#), N. Hod [ID¹⁶⁸](#), M.C. Hodgkinson [ID¹³⁸](#), B.H. Hodgkinson [ID³²](#), A. Hoecker [ID³⁶](#), J. Hofer [ID⁴⁸](#), D. Hohn [ID⁵⁴](#), T. Holm [ID²⁴](#), M. Holzbock [ID¹⁰⁹](#), L.B.A.H. Hommels [ID³²](#), B.P. Honan [ID¹⁰⁰](#), J. Hong [ID^{62c}](#), T.M. Hong [ID¹²⁸](#), Y. Hong [ID⁵⁵](#), J.C. Honig [ID⁵⁴](#), A. Hönlé [ID¹⁰⁹](#), B.H. Hooberman [ID¹⁶¹](#), W.H. Hopkins [ID⁶](#), Y. Horii [ID¹¹⁰](#), S. Hou [ID¹⁴⁷](#), A.S. Howard [ID⁹²](#), J. Howarth [ID⁵⁹](#), J. Hoya [ID⁶](#), M. Hrabovsky [ID¹²¹](#), A. Hrynevich [ID³⁷](#), T. Hrynov'ova [ID⁴](#), P.J. Hsu [ID⁶⁵](#), S.-C. Hsu [ID¹³⁷](#), Q. Hu [ID^{41,ab}](#), Y.F. Hu [ID^{14a,14d,ah}](#), D.P. Huang [ID⁹⁵](#), S. Huang [ID^{64b}](#), X. Huang [ID^{14c}](#), Y. Huang [ID^{62a}](#), Y. Huang [ID^{14a}](#), Z. Huang [ID¹⁰⁰](#), Z. Hubacek [ID¹³¹](#), M. Huebner [ID²⁴](#), F. Huegging [ID²⁴](#), T.B. Huffman [ID¹²⁵](#), M. Huhtinen [ID³⁶](#), S.K. Huiberts [ID¹⁶](#), R. Hulskens [ID¹⁰³](#), N. Huseynov [ID^{12,a}](#), J. Huston [ID¹⁰⁶](#), J. Huth [ID⁶¹](#), R. Hyneman [ID¹⁴²](#), S. Hyrych [ID^{28a}](#), G. Iacobucci [ID⁵⁶](#), G. Iakovidis [ID²⁹](#), I. Ibragimov [ID¹⁴⁰](#), L. Iconomidou-Fayard [ID⁶⁶](#), P. Iengo [ID^{71a,71b}](#), R. Iguchi [ID¹⁵²](#), T. Iizawa [ID⁵⁶](#), Y. Ikegami [ID⁸²](#), A. Ilg [ID¹⁹](#), N. Ilic [ID¹⁵⁴](#), H. Imam [ID^{35a}](#), T. Ingebretsen Carlson [ID^{47a,47b}](#), G. Introzzi [ID^{72a,72b}](#), M. Iodice [ID^{76a}](#), V. Ippolito [ID^{74a,74b}](#), M. Ishino [ID¹⁵²](#), W. Islam [ID¹⁶⁹](#), C. Issever [ID^{18,48}](#), S. Istin [ID^{21a,ak}](#), H. Ito [ID¹⁶⁷](#), J.M. Iturbe Ponce [ID^{64a}](#), R. Iuppa [ID^{77a,77b}](#), A. Ivina [ID¹⁶⁸](#), J.M. Izen [ID⁴⁵](#), V. Izzo [ID^{71a}](#), P. Jacka [ID^{130,131}](#), P. Jackson [ID¹](#), R.M. Jacobs [ID⁴⁸](#), B.P. Jaeger [ID¹⁴¹](#), C.S. Jagfeld [ID¹⁰⁸](#), G. Jäkel [ID¹⁷⁰](#), K. Jakobs [ID⁵⁴](#), T. Jakoubek [ID¹⁶⁸](#), J. Jamieson [ID⁵⁹](#), K.W. Janas [ID^{84a}](#), G. Jarlskog [ID⁹⁷](#), A.E. Jaspan [ID⁹¹](#), M. Javurkova [ID¹⁰²](#), F. Jeanneau [ID¹³⁴](#), L. Jeanty [ID¹²²](#), J. Jejelava [ID^{148a,z}](#), P. Jenni [ID^{54,g}](#), C.E. Jessiman [ID³⁴](#), S. Jézéquel [ID⁴](#), J. Jia [ID¹⁴⁴](#), X. Jia [ID⁶¹](#), X. Jia [ID^{14a,14d}](#), Z. Jia [ID^{14c}](#), Y. Jiang [ID^{62a}](#), S. Jiggins [ID⁵²](#), J. Jimenez Pena [ID¹⁰⁹](#), S. Jin [ID^{14c}](#), A. Jinaru [ID^{27b}](#), O. Jinnouchi [ID¹⁵³](#), P. Johansson [ID¹³⁸](#), K.A. Johns [ID⁷](#), D.M. Jones [ID³²](#), E. Jones [ID¹⁶⁶](#), P. Jones [ID³²](#), R.W.L. Jones [ID⁹⁰](#), T.J. Jones [ID⁹¹](#), R. Joshi [ID¹¹⁸](#), J. Jovicevic [ID¹⁵](#), X. Ju [ID^{17a}](#), J.J. Junggeburth [ID³⁶](#), A. Juste Rozas [ID^{13,v}](#), S. Kabana [ID^{136e}](#), A. Kaczmarska [ID⁸⁵](#), M. Kado [ID^{74a,74b}](#), H. Kagan [ID¹¹⁸](#), M. Kagan [ID¹⁴²](#), A. Kahn [ID⁴¹](#), A. Kahn [ID¹²⁷](#), C. Kahra [ID⁹⁹](#), T. Kaji [ID¹⁶⁷](#), E. Kajomovitz [ID¹⁴⁹](#), N. Kakati [ID¹⁶⁸](#), C.W. Kalderon [ID²⁹](#), A. Kamenshchikov [ID¹⁵⁴](#), S. Kanayama [ID¹⁵³](#), N.J. Kang [ID¹³⁵](#), Y. Kano [ID¹¹⁰](#), D. Kar [ID^{33g}](#), K. Karava [ID¹²⁵](#), M.J. Kareem [ID^{155b}](#), E. Karentzos [ID⁵⁴](#), I. Karkanias [ID¹⁵¹](#), S.N. Karpov [ID³⁸](#), Z.M. Karpova [ID³⁸](#), V. Kartvelishvili [ID⁹⁰](#), A.N. Karyukhin [ID³⁷](#), E. Kasimi [ID¹⁵¹](#), C. Kato [ID^{62d}](#), J. Katzy [ID⁴⁸](#), S. Kaur [ID³⁴](#), K. Kawade [ID¹³⁹](#), K. Kawagoe [ID⁸⁸](#), T. Kawamoto [ID¹³⁴](#), G. Kawamura [ID⁵⁵](#), E.F. Kay [ID¹⁶⁴](#), F.I. Kaya [ID¹⁵⁷](#), S. Kazakos [ID¹³](#), V.F. Kazanin [ID³⁷](#), Y. Ke [ID¹⁴⁴](#), J.M. Keaveney [ID^{33a}](#), R. Keeler [ID¹⁶⁴](#), G.V. Kehris [ID⁶¹](#), J.S. Keller [ID³⁴](#), A.S. Kelly [ID⁹⁵](#), D. Kelsey [ID¹⁴⁵](#), J.J. Kempster [ID²⁰](#), K.E. Kennedy [ID⁴¹](#), O. Kepka [ID¹³⁰](#), B.P. Kerridge [ID¹⁶⁶](#), S. Kersten [ID¹⁷⁰](#), B.P. Kerševan [ID⁹²](#), S. Keshri [ID⁶⁶](#), L. Keszeghova [ID^{28a}](#), S. Ketabchi Haghigat [ID¹⁵⁴](#), M. Khandoga [ID¹²⁶](#),

A. Khanov **ID**¹²⁰, A.G. Kharlamov **ID**³⁷, T. Kharlamova **ID**³⁷, E.E. Khoda **ID**¹³⁷, T.J. Khoo **ID**¹⁸,
 G. Khoriauli **ID**¹⁶⁵, J. Khubua **ID**^{148b}, Y.A.R. Khwaira **ID**⁶⁶, M. Kiehn **ID**³⁶, A. Kilgallon **ID**¹²²,
 D.W. Kim **ID**^{47a,47b}, E. Kim **ID**¹⁵³, Y.K. Kim **ID**³⁹, N. Kimura **ID**⁹⁵, A. Kirchhoff **ID**⁵⁵, D. Kirchmeier **ID**⁵⁰,
 C. Kirfel **ID**²⁴, J. Kirk **ID**¹³³, A.E. Kiryunin **ID**¹⁰⁹, T. Kishimoto **ID**¹⁵², D.P. Kisliuk **ID**¹⁵⁴, C. Kitsaki **ID**¹⁰,
 O. Kivernyk **ID**²⁴, M. Klassen **ID**^{63a}, C. Klein **ID**³⁴, L. Klein **ID**¹⁶⁵, M.H. Klein **ID**¹⁰⁵, M. Klein **ID**⁹¹,
 S.B. Klein **ID**⁵⁶, U. Klein **ID**⁹¹, P. Klimek **ID**³⁶, A. Klimentov **ID**²⁹, F. Klimpel **ID**¹⁰⁹, T. Klingl **ID**²⁴,
 T. Klioutchnikova **ID**³⁶, F.F. Klitzner **ID**¹⁰⁸, P. Kluit **ID**¹¹³, S. Kluth **ID**¹⁰⁹, E. Kneringer **ID**⁷⁸,
 T.M. Knight **ID**¹⁵⁴, A. Knue **ID**⁵⁴, D. Kobayashi ⁸⁸, R. Kobayashi **ID**⁸⁶, M. Kocian **ID**¹⁴², P. Kodyš **ID**¹³²,
 D.M. Koeck **ID**¹⁴⁵, P.T. Koenig **ID**²⁴, T. Koffas **ID**³⁴, N.M. Köhler **ID**³⁶, M. Kolb **ID**¹³⁴, I. Koletsou **ID**⁴,
 T. Komarek **ID**¹²¹, K. Köneke **ID**⁵⁴, A.X.Y. Kong **ID**¹, T. Kono **ID**¹¹⁷, N. Konstantinidis **ID**⁹⁵, B. Konya **ID**⁹⁷,
 R. Kopeliansky **ID**⁶⁷, S. Koperny **ID**^{84a}, K. Korcyl **ID**⁸⁵, K. Kordas **ID**¹⁵¹, G. Koren **ID**¹⁵⁰, A. Korn **ID**⁹⁵,
 S. Korn **ID**⁵⁵, I. Korolkov **ID**¹³, N. Korotkova **ID**³⁷, B. Kortman **ID**¹¹³, O. Kortner **ID**¹⁰⁹, S. Kortner **ID**¹⁰⁹,
 W.H. Kostecka **ID**¹¹⁴, V.V. Kostyukhin **ID**¹⁴⁰, A. Kotsokechagia **ID**¹³⁴, A. Kotwal **ID**⁵¹, A. Koulouris **ID**³⁶,
 A. Kourkoumeli-Charalampidi **ID**^{72a,72b}, C. Kourkoumelis **ID**⁹, E. Kourlitis **ID**⁶, O. Kovanda **ID**¹⁴⁵,
 R. Kowalewski **ID**¹⁶⁴, W. Kozanecki **ID**¹³⁴, A.S. Kozhin **ID**³⁷, V.A. Kramarenko **ID**³⁷, G. Kramberger **ID**⁹²,
 P. Kramer **ID**⁹⁹, M.W. Krasny **ID**¹²⁶, A. Krasznahorkay **ID**³⁶, J.A. Kremer **ID**⁹⁹, T. Kresse **ID**⁵⁰,
 J. Kretzschmar **ID**⁹¹, K. Kreul **ID**¹⁸, P. Krieger **ID**¹⁵⁴, F. Krieter **ID**¹⁰⁸, S. Krishnamurthy **ID**¹⁰²,
 A. Krishnan **ID**^{63b}, M. Krivos **ID**¹³², K. Krizka **ID**^{17a}, K. Kroeninger **ID**⁴⁹, H. Kroha **ID**¹⁰⁹, J. Kroll **ID**¹³⁰,
 J. Kroll **ID**¹²⁷, K.S. Krowpman **ID**¹⁰⁶, U. Kruchonak **ID**³⁸, H. Krüger **ID**²⁴, N. Krumnack ⁸⁰, M.C. Kruse **ID**⁵¹,
 J.A. Krzysiak **ID**⁸⁵, A. Kubota **ID**¹⁵³, O. Kuchinskaia **ID**³⁷, S. Kuday **ID**^{3a}, D. Kuechler **ID**⁴⁸,
 J.T. Kuechler **ID**⁴⁸, S. Kuehn **ID**³⁶, T. Kuhl **ID**⁴⁸, V. Kukhtin **ID**³⁸, Y. Kulchitsky **ID**^{37,a},
 S. Kuleshov **ID**^{136d,136b}, M. Kumar **ID**^{33g}, N. Kumari **ID**¹⁰¹, M. Kuna **ID**⁶⁰, A. Kupco **ID**¹³⁰, T. Kupfer ⁴⁹,
 A. Kupich **ID**³⁷, O. Kuprash **ID**⁵⁴, H. Kurashige **ID**⁸³, L.L. Kurchaninov **ID**^{155a}, Y.A. Kurochkin **ID**³⁷,
 A. Kurova **ID**³⁷, E.S. Kuwertz **ID**³⁶, M. Kuze **ID**¹⁵³, A.K. Kvam **ID**¹⁰², J. Kvita **ID**¹²¹, T. Kwan **ID**¹⁰³,
 K.W. Kwok **ID**^{64a}, N.G. Kyriacou **ID**¹⁰⁵, L.A.O. Laatu **ID**¹⁰¹, C. Lacasta **ID**¹⁶², F. Lacava **ID**^{74a,74b},
 H. Lacker **ID**¹⁸, D. Lacour **ID**¹²⁶, N.N. Lad **ID**⁹⁵, E. Ladygin **ID**³⁸, B. Laforge **ID**¹²⁶, T. Lagouri **ID**^{136e},
 S. Lai **ID**⁵⁵, I.K. Lakomiec **ID**^{84a}, N. Lalloue **ID**⁶⁰, J.E. Lambert **ID**¹¹⁹, S. Lammers **ID**⁶⁷, W. Lampl **ID**⁷,
 C. Lampoudis **ID**¹⁵¹, A.N. Lancaster **ID**¹¹⁴, E. Lançon **ID**²⁹, U. Landgraf **ID**⁵⁴, M.P.J. Landon **ID**⁹³,
 V.S. Lang **ID**⁵⁴, R.J. Langenberg **ID**¹⁰², A.J. Lankford **ID**¹⁵⁹, F. Lanni **ID**³⁶, K. Lantzsch **ID**²⁴, A. Lanza **ID**^{72a},
 A. Lapertosa **ID**^{57b,57a}, J.F. Laporte **ID**¹³⁴, T. Lari **ID**^{70a}, F. Lasagni Manghi **ID**^{23b}, M. Lassnig **ID**³⁶,
 V. Latonova **ID**¹³⁰, T.S. Lau **ID**^{64a}, A. Laudrain **ID**⁹⁹, A. Laurier **ID**³⁴, S.D. Lawlor **ID**⁹⁴, Z. Lawrence **ID**¹⁰⁰,
 M. Lazzaroni **ID**^{70a,70b}, B. Le ¹⁰⁰, B. Leban **ID**⁹², A. Lebedev **ID**⁸⁰, M. LeBlanc **ID**³⁶, T. LeCompte **ID**⁶,
 F. Ledroit-Guillon **ID**⁶⁰, A.C.A. Lee ⁹⁵, G.R. Lee **ID**¹⁶, L. Lee **ID**⁶¹, S.C. Lee **ID**¹⁴⁷, S. Lee **ID**^{47a,47b},
 T.F. Lee **ID**⁹¹, L.L. Leeuw **ID**^{33c}, H.P. Lefebvre **ID**⁹⁴, M. Lefebvre **ID**¹⁶⁴, C. Leggett **ID**^{17a}, K. Lehmann **ID**¹⁴¹,
 G. Lehmann Miotto **ID**³⁶, M. Leigh **ID**⁵⁶, W.A. Leight **ID**¹⁰², A. Leisos **ID**^{151,u}, M.A.L. Leite **ID**^{81c},
 C.E. Leitgeb **ID**⁴⁸, R. Leitner **ID**¹³², K.J.C. Leney **ID**⁴⁴, T. Lenz **ID**²⁴, S. Leone **ID**^{73a}, C. Leonidopoulos **ID**⁵²,
 A. Leopold **ID**¹⁴³, C. Leroy **ID**¹⁰⁷, R. Les **ID**¹⁰⁶, C.G. Lester **ID**³², M. Levchenko **ID**³⁷, J. Levêque **ID**⁴,
 D. Levin **ID**¹⁰⁵, L.J. Levinson **ID**¹⁶⁸, M.P. Lewicki **ID**⁸⁵, D.J. Lewis **ID**²⁰, B. Li **ID**^{14b}, B. Li **ID**^{62b}, C. Li **ID**^{62a},
 C-Q. Li **ID**^{62c}, H. Li **ID**^{62a}, H. Li **ID**^{62b}, H. Li **ID**^{14c}, H. Li **ID**^{62b}, J. Li **ID**^{62c}, K. Li **ID**¹³⁷, L. Li **ID**^{62c},
 M. Li **ID**^{14a,14d}, Q.Y. Li **ID**^{62a}, S. Li **ID**^{62d,62c,e}, T. Li **ID**^{62b}, X. Li **ID**¹⁰³, Z. Li **ID**^{62b}, Z. Li **ID**¹²⁵, Z. Li **ID**¹⁰³,
 Z. Li **ID**⁹¹, Z. Liang **ID**^{14a}, M. Liberatore **ID**⁴⁸, B. Liberti **ID**^{75a}, K. Lie **ID**^{64c}, J. Lieber Marin **ID**^{81b},
 K. Lin **ID**¹⁰⁶, R.A. Linck **ID**⁶⁷, R.E. Lindley **ID**⁷, J.H. Lindon **ID**², A. Linss **ID**⁴⁸, E. Lipeles **ID**¹²⁷,
 A. Lipniacka **ID**¹⁶, A. Lister **ID**¹⁶³, J.D. Little **ID**⁴, B. Liu **ID**^{14a}, B.X. Liu **ID**¹⁴¹, D. Liu **ID**^{62d,62c},
 J.B. Liu **ID**^{62a}, J.K.K. Liu **ID**³², K. Liu **ID**^{62d,62c}, M. Liu **ID**^{62a}, M.Y. Liu **ID**^{62a}, P. Liu **ID**^{14a},
 Q. Liu **ID**^{62d,137,62c}, X. Liu **ID**^{62a}, Y. Liu **ID**⁴⁸, Y. Liu **ID**^{14c,14d}, Y.L. Liu **ID**¹⁰⁵, Y.W. Liu **ID**^{62a},
 M. Livan **ID**^{72a,72b}, J. Llorente Merino **ID**¹⁴¹, S.L. Lloyd **ID**⁹³, E.M. Lobodzinska **ID**⁴⁸, P. Loch **ID**⁷,
 S. Loffredo **ID**^{75a,75b}, T. Lohse **ID**¹⁸, K. Lohwasser **ID**¹³⁸, M. Lokajicek **ID**^{130,*}, J.D. Long **ID**¹⁶¹,

I. Longarini $\text{id}^{74a,74b}$, L. Longo $\text{id}^{69a,69b}$, R. Longo id^{161} , I. Lopez Paz id^{36} , A. Lopez Solis id^{48} ,
 J. Lorenz id^{108} , N. Lorenzo Martinez id^4 , A.M. Lory id^{108} , A. Lösle id^{54} , X. Lou $\text{id}^{47a,47b}$, X. Lou $\text{id}^{14a,14d}$,
 A. Lounis id^{66} , J. Love id^6 , P.A. Love id^{90} , J.J. Lozano Bahilo id^{162} , G. Lu $\text{id}^{14a,14d}$, M. Lu id^{79} ,
 S. Lu id^{127} , Y.J. Lu id^{65} , H.J. Lubatti id^{137} , C. Luci $\text{id}^{74a,74b}$, F.L. Lucio Alves id^{14c} , A. Lucotte id^{60} ,
 F. Luehring id^{67} , I. Luise id^{144} , O. Lukianchuk id^{66} , O. Lundberg id^{143} , B. Lund-Jensen id^{143} ,
 N.A. Luongo id^{122} , M.S. Lutz id^{150} , D. Lynn id^{29} , H. Lyons id^{91} , R. Lysak id^{130} , E. Lytken id^{97} , F. Lyu id^{14a} ,
 V. Lyubushkin id^{38} , T. Lyubushkina id^{38} , H. Ma id^{29} , L.L. Ma id^{62b} , Y. Ma id^{95} , D.M. Mac Donell id^{164} ,
 G. Maccarrone id^{53} , J.C. MacDonald id^{138} , R. Madar id^{40} , W.F. Mader id^{50} , J. Maeda id^{83} , T. Maeno id^{29} ,
 M. Maerker id^{50} , V. Magerl id^{54} , J. Magro $\text{id}^{68a,68c}$, H. Maguire id^{138} , D.J. Mahon id^{41} ,
 C. Maidantchik id^{81b} , A. Maio $\text{id}^{129a,129b,129d}$, K. Maj id^{84a} , O. Majersky id^{28a} , S. Majewski id^{122} ,
 N. Makovec id^{66} , V. Maksimovic id^{15} , B. Malaescu id^{126} , Pa. Malecki id^{85} , V.P. Maleev id^{37} ,
 F. Malek id^{60} , D. Malito $\text{id}^{43b,43a}$, U. Mallik id^{79} , C. Malone id^{32} , S. Maltezos id^{10} , S. Malyukov id^{38} ,
 J. Mamuzic id^{13} , G. Mancini id^{53} , G. Manco $\text{id}^{72a,72b}$, J.P. Mandalia id^{93} , I. Mandić id^{92} ,
 L. Manhaes de Andrade Filho id^{81a} , I.M. Maniatis id^{151} , M. Manisha id^{134} , J. Manjarres Ramos id^{50} ,
 D.C. Mankad id^{168} , A. Mann id^{108} , B. Mansoulie id^{134} , S. Manzoni id^{36} , A. Marantis $\text{id}^{151,u}$,
 G. Marchiori id^5 , M. Marcisovsky id^{130} , L. Marcoccia $\text{id}^{75a,75b}$, C. Marcon $\text{id}^{70a,70b}$, M. Marinescu id^{20} ,
 M. Marjanovic id^{119} , Z. Marshall id^{17a} , S. Marti-Garcia id^{162} , T.A. Martin id^{166} , V.J. Martin id^{52} ,
 B. Martin dit Latour id^{16} , L. Martinelli $\text{id}^{74a,74b}$, M. Martinez $\text{id}^{13,v}$, P. Martinez Agullo id^{162} ,
 V.I. Martinez Outschoorn id^{102} , P. Martinez Suarez id^{13} , S. Martin-Haugh id^{133} , V.S. Martoiu id^{27b} ,
 A.C. Martyniuk id^{95} , A. Marzin id^{36} , S.R. Maschek id^{109} , L. Masetti id^{99} , T. Mashimo id^{152} ,
 J. Masik id^{100} , A.L. Maslenikov id^{37} , L. Massa id^{23b} , P. Massarotti $\text{id}^{71a,71b}$, P. Mastrandrea $\text{id}^{73a,73b}$,
 A. Mastroberardino $\text{id}^{43b,43a}$, T. Masubuchi id^{152} , T. Mathisen id^{160} , N. Matsuzawa id^{152} , J. Maurer id^{27b} ,
 B. Maček id^{92} , D.A. Maximov id^{37} , R. Mazini id^{147} , I. Maznás id^{151} , M. Mazza id^{106} , S.M. Mazza id^{135} ,
 C. Mc Ginn id^{29} , J.P. Mc Gowan id^{103} , S.P. Mc Kee id^{105} , T.G. McCarthy id^{109} , W.P. McCormack id^{17a} ,
 E.F. McDonald id^{104} , A.E. McDougall id^{113} , J.A. McFayden id^{145} , G. McHedlidze id^{148b} ,
 R.P. Mckenzie id^{33g} , T.C. McLachlan id^{48} , D.J. McLaughlin id^{95} , K.D. McLean id^{164} , S.J. McMahon id^{133} ,
 P.C. McNamara id^{104} , C.M. Mcpartland id^{91} , R.A. McPherson $\text{id}^{164,x}$, T. Megy id^{40} , S. Mehlhase id^{108} ,
 A. Mehta id^{91} , B. Meirose id^{45} , D. Melini id^{149} , B.R. Mellado Garcia id^{33g} , A.H. Melo id^{55} ,
 F. Meloni id^{48} , E.D. Mendes Gouveia id^{129a} , A.M. Mendes Jacques Da Costa id^{20} , H.Y. Meng id^{154} ,
 L. Meng id^{90} , S. Menke id^{109} , M. Mentink id^{36} , E. Meoni $\text{id}^{43b,43a}$, C. Merlassino id^{125} ,
 L. Merola $\text{id}^{71a,71b}$, C. Meroni id^{70a} , G. Merz id^{105} , O. Meshkov id^{37} , J.K.R. Meshreki id^{140} , J. Metcalfe id^6 ,
 A.S. Mete id^6 , C. Meyer id^{67} , J-P. Meyer id^{134} , M. Michetti id^{18} , R.P. Middleton id^{133} , L. Mijović id^{52} ,
 G. Mikenberg id^{168} , M. Mikestikova id^{130} , M. Mikuž id^{92} , H. Mildner id^{138} , A. Milic id^{154} ,
 C.D. Milke id^{44} , D.W. Miller id^{39} , L.S. Miller id^{34} , A. Milov id^{168} , D.A. Milstead $\text{id}^{47a,47b}$, T. Min id^{14c} ,
 A.A. Minaenko id^{37} , I.A. Minashvili id^{148b} , L. Mince id^{59} , A.I. Mincer id^{116} , B. Mindur id^{84a} ,
 M. Mineev id^{38} , Y. Mino id^{86} , L.M. Mir id^{13} , M. Miralles Lopez id^{162} , M. Mironova id^{125} , T. Mitani id^{167} ,
 A. Mitra id^{166} , V.A. Mitsou id^{162} , O. Miu id^{154} , P.S. Miyagawa id^{93} , Y. Miyazaki id^{88} , A. Mizukami id^{82} ,
 J.U. Mjörnmark id^{97} , T. Mkrtchyan id^{63a} , T. Mlinarevic id^{95} , M. Mlynarikova id^{36} , T. Moa $\text{id}^{47a,47b}$,
 S. Mobius id^{55} , K. Mochizuki id^{107} , P. Moder id^{48} , P. Mogg id^{108} , A.F. Mohammed $\text{id}^{14a,14d}$,
 S. Mohapatra id^{41} , G. Mokgatitswane id^{33g} , B. Mondal id^{140} , S. Mondal id^{131} , K. Möning id^{48} ,
 E. Monnier id^{101} , L. Monsonis Romero id^{162} , J. Montejo Berlingen id^{36} , M. Montella id^{118} ,
 F. Monticelli id^{89} , N. Morange id^{66} , A.L. Moreira De Carvalho id^{129a} , M. Moreno Llácer id^{162} ,
 C. Moreno Martinez id^{13} , P. Morettini id^{57b} , S. Morgenstern id^{166} , M. Morii id^{61} , M. Morinaga id^{152} ,
 V. Morisbak id^{124} , A.K. Morley id^{36} , F. Morodei $\text{id}^{74a,74b}$, L. Morvaj id^{36} , P. Moschovakos id^{36} ,
 B. Moser id^{36} , M. Mosidze id^{148b} , T. Moskalets id^{54} , P. Moskvitina id^{112} , J. Moss $\text{id}^{31,o}$, E.J.W. Moyse id^{102} ,
 S. Muanza id^{101} , J. Mueller id^{128} , D. Muenstermann id^{90} , R. Müller id^{19} , G.A. Mullier id^{97} , J.J. Mullin id^{127} ,
 D.P. Mungo $\text{id}^{70a,70b}$, J.L. Munoz Martinez id^{13} , D. Munoz Perez id^{162} , F.J. Munoz Sanchez id^{100} ,

M. Murin [ID¹⁰⁰](#), W.J. Murray [ID^{166,133}](#), A. Murrone [ID^{70a,70b}](#), J.M. Muse [ID¹¹⁹](#), M. Muškinja [ID^{17a}](#), C. Mwewa [ID²⁹](#), A.G. Myagkov [ID^{37,a}](#), A.J. Myers [ID⁸](#), A.A. Myers [ID¹²⁸](#), G. Myers [ID⁶⁷](#), M. Myska [ID¹³¹](#), B.P. Nachman [ID^{17a}](#), O. Nackenhorst [ID⁴⁹](#), A. Nag [ID⁵⁰](#), K. Nagai [ID¹²⁵](#), K. Nagano [ID⁸²](#), J.L. Nagle [ID^{29,ai}](#), E. Nagy [ID¹⁰¹](#), A.M. Nairz [ID³⁶](#), Y. Nakahama [ID⁸²](#), K. Nakamura [ID⁸²](#), H. Nanjo [ID¹²³](#), R. Narayan [ID⁴⁴](#), E.A. Narayanan [ID¹¹¹](#), I. Naryshkin [ID³⁷](#), M. Naseri [ID³⁴](#), C. Nass [ID²⁴](#), G. Navarro [ID^{22a}](#), J. Navarro-Gonzalez [ID¹⁶²](#), R. Nayak [ID¹⁵⁰](#), A. Nayaz [ID¹⁸](#), P.Y. Nechaeva [ID³⁷](#), F. Nechansky [ID⁴⁸](#), L. Nedic [ID¹²⁵](#), T.J. Neep [ID²⁰](#), A. Negri [ID^{72a,72b}](#), M. Negrini [ID^{23b}](#), C. Nellist [ID¹¹²](#), C. Nelson [ID¹⁰³](#), K. Nelson [ID¹⁰⁵](#), S. Nemecek [ID¹³⁰](#), M. Nessi [ID^{36,h}](#), M.S. Neubauer [ID¹⁶¹](#), F. Neuhaus [ID⁹⁹](#), J. Neundorf [ID⁴⁸](#), R. Newhouse [ID¹⁶³](#), P.R. Newman [ID²⁰](#), C.W. Ng [ID¹²⁸](#), Y.S. Ng [ID¹⁸](#), Y.W.Y. Ng [ID¹⁵⁹](#), B. Ngair [ID^{35e}](#), H.D.N. Nguyen [ID¹⁰⁷](#), R.B. Nickerson [ID¹²⁵](#), R. Nicolaidou [ID¹³⁴](#), J. Nielsen [ID¹³⁵](#), M. Niemeyer [ID⁵⁵](#), N. Nikiforou [ID³⁶](#), V. Nikolaenko [ID^{37,a}](#), I. Nikolic-Audit [ID¹²⁶](#), K. Nikolopoulos [ID²⁰](#), P. Nilsson [ID²⁹](#), H.R. Nindhito [ID⁵⁶](#), A. Nisati [ID^{74a}](#), N. Nishu [ID²](#), R. Nisius [ID¹⁰⁹](#), J-E. Nitschke [ID⁵⁰](#), E.K. Nkadameng [ID^{33g}](#), S.J. Noacco Rosende [ID⁸⁹](#), T. Nobe [ID¹⁵²](#), D.L. Noel [ID³²](#), Y. Noguchi [ID⁸⁶](#), T. Nommensen [ID¹⁴⁶](#), M.A. Nomura [ID²⁹](#), M.B. Norfolk [ID¹³⁸](#), R.R.B. Norisam [ID⁹⁵](#), B.J. Norman [ID³⁴](#), J. Novak [ID⁹²](#), T. Novak [ID⁴⁸](#), O. Novgorodova [ID⁵⁰](#), L. Novotny [ID¹³¹](#), R. Novotny [ID¹¹¹](#), L. Nozka [ID¹²¹](#), K. Ntekas [ID¹⁵⁹](#), E. Nurse [ID⁹⁵](#), F.G. Oakham [ID^{34,af}](#), J. Ocariz [ID¹²⁶](#), A. Ochi [ID⁸³](#), I. Ochoa [ID^{129a}](#), S. Oerdek [ID¹⁶⁰](#), A. Ogronik [ID^{84a}](#), A. Oh [ID¹⁰⁰](#), C.C. Ohm [ID¹⁴³](#), H. Oide [ID¹⁵³](#), R. Oishi [ID¹⁵²](#), M.L. Ojeda [ID⁴⁸](#), Y. Okazaki [ID⁸⁶](#), M.W. O'Keefe [ID⁹¹](#), Y. Okumura [ID¹⁵²](#), A. Olariu [ID^{27b}](#), L.F. Oleiro Seabra [ID^{129a}](#), S.A. Olivares Pino [ID^{136e}](#), D. Oliveira Damazio [ID²⁹](#), D. Oliveira Goncalves [ID^{81a}](#), J.L. Oliver [ID¹⁵⁹](#), M.J.R. Olsson [ID¹⁵⁹](#), A. Olszewski [ID⁸⁵](#), J. Olszowska [ID^{85,*}](#), Ö.O. Öncel [ID⁵⁴](#), D.C. O'Neil [ID¹⁴¹](#), A.P. O'Neill [ID¹⁹](#), A. Onofre [ID^{129a,129e}](#), P.U.E. Onyisi [ID¹¹](#), M.J. Oreglia [ID³⁹](#), G.E. Orellana [ID⁸⁹](#), D. Orestano [ID^{76a,76b}](#), N. Orlando [ID¹³](#), R.S. Orr [ID¹⁵⁴](#), V. O'Shea [ID⁵⁹](#), R. Ospanov [ID^{62a}](#), G. Otero y Garzon [ID³⁰](#), H. Otono [ID⁸⁸](#), P.S. Ott [ID^{63a}](#), G.J. Ottino [ID^{17a}](#), M. Ouchrif [ID^{35d}](#), J. Ouellette [ID^{29,ai}](#), F. Ould-Saada [ID¹²⁴](#), M. Owen [ID⁵⁹](#), R.E. Owen [ID¹³³](#), K.Y. Oyulmaz [ID^{21a}](#), V.E. Ozcan [ID^{21a}](#), N. Ozturk [ID⁸](#), S. Ozturk [ID^{21d}](#), J. Pacalt [ID¹²¹](#), H.A. Pacey [ID³²](#), K. Pachal [ID⁵¹](#), A. Pacheco Pages [ID¹³](#), C. Padilla Aranda [ID¹³](#), G. Padovano [ID^{74a,74b}](#), S. Pagan Griso [ID^{17a}](#), G. Palacino [ID⁶⁷](#), A. Palazzo [ID^{69a,69b}](#), S. Palazzo [ID⁵²](#), S. Palestini [ID³⁶](#), M. Palka [ID^{84b}](#), J. Pan [ID¹⁷¹](#), T. Pan [ID^{64a}](#), D.K. Panchal [ID¹¹](#), C.E. Pandini [ID¹¹³](#), J.G. Panduro Vazquez [ID⁹⁴](#), H. Pang [ID^{14b}](#), P. Pani [ID⁴⁸](#), G. Panizzo [ID^{68a,68c}](#), L. Paolozzi [ID⁵⁶](#), C. Papadatos [ID¹⁰⁷](#), S. Parajuli [ID⁴⁴](#), A. Paramonov [ID⁶](#), C. Paraskevopoulos [ID¹⁰](#), D. Paredes Hernandez [ID^{64b}](#), T.H. Park [ID¹⁵⁴](#), M.A. Parker [ID³²](#), F. Parodi [ID^{57b,57a}](#), E.W. Parrish [ID¹¹⁴](#), V.A. Parrish [ID⁵²](#), J.A. Parsons [ID⁴¹](#), U. Parzefall [ID⁵⁴](#), B. Pascual Dias [ID¹⁰⁷](#), L. Pascual Dominguez [ID¹⁵⁰](#), V.R. Pascuzzi [ID^{17a}](#), F. Pasquali [ID¹¹³](#), E. Pasqualucci [ID^{74a}](#), S. Passaggio [ID^{57b}](#), F. Pastore [ID⁹⁴](#), P. Pasuwan [ID^{47a,47b}](#), P. Patel [ID⁸⁵](#), J.R. Pater [ID¹⁰⁰](#), J. Patton [ID⁹¹](#), T. Pauly [ID³⁶](#), J. Pearkes [ID¹⁴²](#), M. Pedersen [ID¹²⁴](#), R. Pedro [ID^{129a}](#), S.V. Peleganchuk [ID³⁷](#), O. Penc [ID³⁶](#), E.A. Pender [ID⁵²](#), C. Peng [ID^{64b}](#), H. Peng [ID^{62a}](#), K.E. Penski [ID¹⁰⁸](#), M. Penzin [ID³⁷](#), B.S. Peralva [ID^{81d}](#), A.P. Pereira Peixoto [ID⁶⁰](#), L. Pereira Sanchez [ID^{47a,47b}](#), D.V. Perepelitsa [ID^{29,ai}](#), E. Perez Codina [ID^{155a}](#), M. Perganti [ID¹⁰](#), L. Perini [ID^{70a,70b,*}](#), H. Pernegger [ID³⁶](#), S. Perrella [ID³⁶](#), A. Perrevoort [ID¹¹²](#), O. Perrin [ID⁴⁰](#), K. Peters [ID⁴⁸](#), R.F.Y. Peters [ID¹⁰⁰](#), B.A. Petersen [ID³⁶](#), T.C. Petersen [ID⁴²](#), E. Petit [ID¹⁰¹](#), V. Petousis [ID¹³¹](#), C. Petridou [ID¹⁵¹](#), A. Petrukhin [ID¹⁴⁰](#), M. Pettee [ID^{17a}](#), N.E. Pettersson [ID³⁶](#), A. Petukhov [ID³⁷](#), K. Petukhova [ID¹³²](#), A. Peyaud [ID¹³⁴](#), R. Pezoa [ID^{136f}](#), L. Pezzotti [ID³⁶](#), G. Pezzullo [ID¹⁷¹](#), T.M. Pham [ID¹⁶⁹](#), T. Pham [ID¹⁰⁴](#), P.W. Phillips [ID¹³³](#), M.W. Phipps [ID¹⁶¹](#), G. Piacquadio [ID¹⁴⁴](#), E. Pianori [ID^{17a}](#), F. Piazza [ID^{70a,70b}](#), R. Piegaia [ID³⁰](#), D. Pietreanu [ID^{27b}](#), A.D. Pilkington [ID¹⁰⁰](#), M. Pinamonti [ID^{68a,68c}](#), J.L. Pinfold [ID²](#), B.C. Pinheiro Pereira [ID^{129a}](#), C. Pitman Donaldson [ID⁹⁵](#), D.A. Pizzi [ID³⁴](#), L. Pizzimento [ID^{75a,75b}](#), A. Pizzini [ID¹¹³](#), M.-A. Pleier [ID²⁹](#), V. Plesanovs [ID⁵⁴](#), V. Pleskot [ID¹³²](#), E. Plotnikova [ID³⁸](#), G. Poddar [ID⁴](#), R. Poettgen [ID⁹⁷](#), L. Poggiali [ID¹²⁶](#), I. Pogrebnyak [ID¹⁰⁶](#), D. Pohl [ID²⁴](#), I. Pokharel [ID⁵⁵](#), S. Polacek [ID¹³²](#), G. Polesello [ID^{72a}](#), A. Poley [ID^{141,155a}](#), R. Polifka [ID¹³¹](#), A. Polini [ID^{23b}](#), C.S. Pollard [ID¹²⁵](#), Z.B. Pollock [ID¹¹⁸](#), V. Polychronakos [ID²⁹](#), E. Pompa Pacchi [ID^{74a,74b}](#), D. Ponomarenko [ID³⁷](#),

L. Pontecorvo [ID³⁶](#), S. Popa [ID^{27a}](#), G.A. Popeneciu [ID^{27d}](#), D.M. Portillo Quintero [ID^{155a}](#), S. Pospisil [ID¹³¹](#),
 P. Postolache [ID^{27c}](#), K. Potamianos [ID¹²⁵](#), I.N. Potrap [ID³⁸](#), C.J. Potter [ID³²](#), H. Potti [ID¹](#), T. Poulsen [ID⁴⁸](#),
 J. Poveda [ID¹⁶²](#), M.E. Pozo Astigarraga [ID³⁶](#), A. Prades Ibanez [ID¹⁶²](#), M.M. Prapa [ID⁴⁶](#), J. Pretel [ID⁵⁴](#),
 D. Price [ID¹⁰⁰](#), M. Primavera [ID^{69a}](#), M.A. Principe Martin [ID⁹⁸](#), M.L. Proffitt [ID¹³⁷](#), N. Proklova [ID¹²⁷](#),
 K. Prokofiev [ID^{64c}](#), G. Proto [ID^{75a,75b}](#), S. Protopopescu [ID²⁹](#), J. Proudfoot [ID⁶](#), M. Przybycien [ID^{84a}](#),
 J.E. Puddefoot [ID¹³⁸](#), D. Pudzha [ID³⁷](#), P. Puzo [ID⁶⁶](#), D. Pyatiizbyantseva [ID³⁷](#), J. Qian [ID¹⁰⁵](#), Y. Qin [ID¹⁰⁰](#),
 T. Qiu [ID⁹³](#), A. Quadt [ID⁵⁵](#), M. Queitsch-Maitland [ID¹⁰⁰](#), G. Quetant [ID⁵⁶](#), G. Rabanal Bolanos [ID⁶¹](#),
 D. Rafanoharana [ID⁵⁴](#), F. Ragusa [ID^{70a,70b}](#), J.L. Rainbolt [ID³⁹](#), J.A. Raine [ID⁵⁶](#), S. Rajagopalan [ID²⁹](#),
 E. Ramakoti [ID³⁷](#), K. Ran [ID^{48,14d}](#), V. Raskina [ID¹²⁶](#), D.F. Rassloff [ID^{63a}](#), S. Rave [ID⁹⁹](#), B. Ravina [ID⁵⁵](#),
 I. Ravinovich [ID¹⁶⁸](#), M. Raymond [ID³⁶](#), A.L. Read [ID¹²⁴](#), N.P. Readioff [ID¹³⁸](#), D.M. Rebuzzi [ID^{72a,72b}](#),
 G. Redlinger [ID²⁹](#), K. Reeves [ID⁴⁵](#), J.A. Reidelsturz [ID¹⁷⁰](#), D. Reikher [ID¹⁵⁰](#), A. Reiss [ID⁹⁹](#), A. Rej [ID¹⁴⁰](#),
 C. Rembser [ID³⁶](#), A. Renardi [ID⁴⁸](#), M. Renda [ID^{27b}](#), M.B. Rendel [ID¹⁰⁹](#), A.G. Rennie [ID⁵⁹](#), S. Resconi [ID^{70a}](#),
 M. Ressegotti [ID^{57b,57a}](#), E.D. Ressegue [ID^{17a}](#), S. Rettie [ID⁹⁵](#), B. Reynolds [ID¹¹⁸](#), E. Reynolds [ID^{17a}](#),
 M. Rezaei Estabragh [ID¹⁷⁰](#), O.L. Rezanova [ID³⁷](#), P. Reznicek [ID¹³²](#), E. Ricci [ID^{77a,77b}](#), R. Richter [ID¹⁰⁹](#),
 S. Richter [ID^{47a,47b}](#), E. Richter-Was [ID^{84b}](#), M. Ridel [ID¹²⁶](#), P. Rieck [ID¹¹⁶](#), P. Riedler [ID³⁶](#),
 M. Rijssenbeek [ID¹⁴⁴](#), A. Rimoldi [ID^{72a,72b}](#), M. Rimoldi [ID⁴⁸](#), L. Rinaldi [ID^{23b,23a}](#), T.T. Rinn [ID²⁹](#),
 M.P. Rinnagel [ID¹⁰⁸](#), G. Ripellino [ID¹⁴³](#), I. Riu [ID¹³](#), P. Rivadeneira [ID⁴⁸](#), J.C. Rivera Vergara [ID¹⁶⁴](#),
 F. Rizatdinova [ID¹²⁰](#), E. Rizvi [ID⁹³](#), C. Rizzi [ID⁵⁶](#), B.A. Roberts [ID¹⁶⁶](#), B.R. Roberts [ID^{17a}](#),
 S.H. Robertson [ID^{103,x}](#), M. Robin [ID⁴⁸](#), D. Robinson [ID³²](#), C.M. Robles Gajardo [ID^{136f}](#),
 M. Robles Manzano [ID⁹⁹](#), A. Robson [ID⁵⁹](#), A. Rocchi [ID^{75a,75b}](#), C. Roda [ID^{73a,73b}](#), S. Rodriguez Bosca [ID^{63a}](#),
 Y. Rodriguez Garcia [ID^{22a}](#), A. Rodriguez Rodriguez [ID⁵⁴](#), A.M. Rodríguez Vera [ID^{155b}](#), S. Roe [ID³⁶](#),
 J.T. Roemer [ID¹⁵⁹](#), A.R. Roepe-Gier [ID¹¹⁹](#), J. Roggel [ID¹⁷⁰](#), O. Røhne [ID¹²⁴](#), R.A. Rojas [ID¹⁶⁴](#), B. Roland [ID⁵⁴](#),
 C.P.A. Roland [ID⁶⁷](#), J. Roloff [ID²⁹](#), A. Romaniouk [ID³⁷](#), E. Romano [ID^{72a,72b}](#), M. Romano [ID^{23b}](#),
 A.C. Romero Hernandez [ID¹⁶¹](#), N. Rompotis [ID⁹¹](#), L. Roos [ID¹²⁶](#), S. Rosati [ID^{74a}](#), B.J. Rosser [ID³⁹](#),
 E. Rossi [ID⁴](#), E. Rossi [ID^{71a,71b}](#), L.P. Rossi [ID^{57b}](#), L. Rossini [ID⁴⁸](#), R. Rosten [ID¹¹⁸](#), M. Rotaru [ID^{27b}](#),
 B. Rottler [ID⁵⁴](#), D. Rousseau [ID⁶⁶](#), D. Rousso [ID³²](#), G. Rovelli [ID^{72a,72b}](#), A. Roy [ID¹⁶¹](#), A. Rozanova [ID¹⁰¹](#),
 Y. Rozen [ID¹⁴⁹](#), X. Ruan [ID^{33g}](#), A. Rubio Jimenez [ID¹⁶²](#), A.J. Ruby [ID⁹¹](#), V.H. Ruelas Rivera [ID¹⁸](#),
 T.A. Ruggeri [ID¹](#), F. Rühr [ID⁵⁴](#), A. Ruiz-Martinez [ID¹⁶²](#), A. Rummler [ID³⁶](#), Z. Rurikova [ID⁵⁴](#),
 N.A. Rusakovich [ID³⁸](#), H.L. Russell [ID¹⁶⁴](#), J.P. Rutherford [ID⁷](#), K. Rybacki [ID⁹⁰](#), M. Rybar [ID¹³²](#),
 E.B. Rye [ID¹²⁴](#), A. Ryzhov [ID³⁷](#), J.A. Sabater Iglesias [ID⁵⁶](#), P. Sabatini [ID¹⁶²](#), L. Sabetta [ID^{74a,74b}](#),
 H.F-W. Sadrozinski [ID¹³⁵](#), F. Safai Tehrani [ID^{74a}](#), B. Safarzadeh Samani [ID¹⁴⁵](#), M. Safdari [ID¹⁴²](#),
 S. Saha [ID¹⁰³](#), M. Sahinsoy [ID¹⁰⁹](#), M. Saimpert [ID¹³⁴](#), M. Saito [ID¹⁵²](#), T. Saito [ID¹⁵²](#), D. Salamani [ID³⁶](#),
 G. Salamanna [ID^{76a,76b}](#), A. Salnikov [ID¹⁴²](#), J. Salt [ID¹⁶²](#), A. Salvador Salas [ID¹³](#), D. Salvatore [ID^{43b,43a}](#),
 F. Salvatore [ID¹⁴⁵](#), A. Salzburger [ID³⁶](#), D. Sammel [ID⁵⁴](#), D. Sampsonidis [ID¹⁵¹](#), D. Sampsonidou [ID^{62d,62c}](#),
 J. Sánchez [ID¹⁶²](#), A. Sanchez Pineda [ID⁴](#), V. Sanchez Sebastian [ID¹⁶²](#), H. Sandaker [ID¹²⁴](#), C.O. Sander [ID⁴⁸](#),
 J.A. Sandesara [ID¹⁰²](#), M. Sandhoff [ID¹⁷⁰](#), C. Sandoval [ID^{22b}](#), D.P.C. Sankey [ID¹³³](#), A. Sansoni [ID⁵³](#),
 L. Santi [ID^{74a,74b}](#), C. Santoni [ID⁴⁰](#), H. Santos [ID^{129a,129b}](#), S.N. Santpur [ID^{17a}](#), A. Santra [ID¹⁶⁸](#),
 K.A. Saoucha [ID¹³⁸](#), J.G. Saraiva [ID^{129a,129d}](#), J. Sardain [ID⁷](#), O. Sasaki [ID⁸²](#), K. Sato [ID¹⁵⁶](#), C. Sauer [ID^{63b}](#),
 F. Sauerburger [ID⁵⁴](#), E. Sauvan [ID⁴](#), P. Savard [ID^{154,af}](#), R. Sawada [ID¹⁵²](#), C. Sawyer [ID¹³³](#), L. Sawyer [ID⁹⁶](#),
 I. Sayago Galvan [ID¹⁶²](#), C. Sbarra [ID^{23b}](#), A. Sbrizzi [ID^{23b,23a}](#), T. Scanlon [ID⁹⁵](#), J. Schaarschmidt [ID¹³⁷](#),
 P. Schacht [ID¹⁰⁹](#), D. Schaefer [ID³⁹](#), U. Schäfer [ID⁹⁹](#), A.C. Schaffer [ID⁶⁶](#), D. Schaile [ID¹⁰⁸](#),
 R.D. Schamberger [ID¹⁴⁴](#), E. Schanet [ID¹⁰⁸](#), C. Scharf [ID¹⁸](#), V.A. Schegelsky [ID³⁷](#), D. Scheirich [ID¹³²](#),
 F. Schenck [ID¹⁸](#), M. Schernau [ID¹⁵⁹](#), C. Scheulen [ID⁵⁵](#), C. Schiavi [ID^{57b,57a}](#), Z.M. Schillaci [ID²⁶](#),
 E.J. Schioppa [ID^{69a,69b}](#), M. Schioppa [ID^{43b,43a}](#), B. Schlag [ID⁹⁹](#), K.E. Schleicher [ID⁵⁴](#), S. Schlenker [ID³⁶](#),
 K. Schmieden [ID⁹⁹](#), C. Schmitt [ID⁹⁹](#), S. Schmitt [ID⁴⁸](#), L. Schoeffel [ID¹³⁴](#), A. Schoening [ID^{63b}](#),
 P.G. Scholer [ID⁵⁴](#), E. Schopf [ID¹²⁵](#), M. Schott [ID⁹⁹](#), J. Schovancova [ID³⁶](#), S. Schramm [ID⁵⁶](#),
 F. Schroeder [ID¹⁷⁰](#), H-C. Schultz-Coulon [ID^{63a}](#), M. Schumacher [ID⁵⁴](#), B.A. Schumm [ID¹³⁵](#), Ph. Schune [ID¹³⁴](#),

A. Schwartzman [ID¹⁴²](#), T.A. Schwarz [ID¹⁰⁵](#), Ph. Schwemling [ID¹³⁴](#), R. Schwienhorst [ID¹⁰⁶](#),
 A. Sciandra [ID¹³⁵](#), G. Sciolla [ID²⁶](#), F. Scuri [ID^{73a}](#), F. Scutti [ID¹⁰⁴](#), C.D. Sebastiani [ID⁹¹](#), K. Sedlaczek [ID⁴⁹](#),
 P. Seema [ID¹⁸](#), S.C. Seidel [ID¹¹¹](#), A. Seiden [ID¹³⁵](#), B.D. Seidlitz [ID⁴¹](#), T. Seiss [ID³⁹](#), C. Seitz [ID⁴⁸](#),
 J.M. Seixas [ID^{81b}](#), G. Sekhniaidze [ID^{71a}](#), S.J. Sekula [ID⁴⁴](#), L. Selem [ID⁴](#), N. Semprini-Cesari [ID^{23b,23a}](#),
 S. Sen [ID⁵¹](#), D. Sengupta [ID⁵⁶](#), V. Senthilkumar [ID¹⁶²](#), L. Serin [ID⁶⁶](#), L. Serkin [ID^{68a,68b}](#), M. Sessa [ID^{76a,76b}](#),
 H. Severini [ID¹¹⁹](#), S. Sevova [ID¹⁴²](#), F. Sforza [ID^{57b,57a}](#), A. Sfyrla [ID⁵⁶](#), E. Shabalina [ID⁵⁵](#), R. Shaheen [ID¹⁴³](#),
 J.D. Shahinian [ID¹²⁷](#), N.W. Shaikh [ID^{47a,47b}](#), D. Shaked Renous [ID¹⁶⁸](#), L.Y. Shan [ID^{14a}](#), M. Shapiro [ID^{17a}](#),
 A. Sharma [ID³⁶](#), A.S. Sharma [ID¹⁶³](#), P. Sharma [ID⁷⁹](#), S. Sharma [ID⁴⁸](#), P.B. Shatalov [ID³⁷](#), K. Shaw [ID¹⁴⁵](#),
 S.M. Shaw [ID¹⁰⁰](#), Q. Shen [ID^{62c,5}](#), P. Sherwood [ID⁹⁵](#), L. Shi [ID⁹⁵](#), C.O. Shimmin [ID¹⁷¹](#), Y. Shimogama [ID¹⁶⁷](#),
 J.D. Shinner [ID⁹⁴](#), I.P.J. Shipsey [ID¹²⁵](#), S. Shirabe [ID⁶⁰](#), M. Shiyakova [ID³⁸](#), J. Shlomi [ID¹⁶⁸](#),
 M.J. Shochet [ID³⁹](#), J. Shojaei [ID¹⁰⁴](#), D.R. Shope [ID¹²⁴](#), S. Shrestha [ID^{118,aj}](#), E.M. Shrif [ID^{33g}](#),
 M.J. Shroff [ID¹⁶⁴](#), P. Sicho [ID¹³⁰](#), A.M. Sickles [ID¹⁶¹](#), E. Sideras Haddad [ID^{33g}](#), A. Sidoti [ID^{23b}](#),
 F. Siegert [ID⁵⁰](#), Dj. Sijacki [ID¹⁵](#), R. Sikora [ID^{84a}](#), F. Sili [ID⁸⁹](#), J.M. Silva [ID²⁰](#), M.V. Silva Oliveira [ID³⁶](#),
 S.B. Silverstein [ID^{47a}](#), S. Simion [ID⁶⁶](#), R. Simoniello [ID³⁶](#), E.L. Simpson [ID⁵⁹](#), N.D. Simpson [ID⁹⁷](#),
 S. Simsek [ID^{21d}](#), S. Sindhu [ID⁵⁵](#), P. Sinervo [ID¹⁵⁴](#), V. Sinetckii [ID³⁷](#), S. Singh [ID¹⁴¹](#), S. Singh [ID¹⁵⁴](#),
 S. Sinha [ID⁴⁸](#), S. Sinha [ID^{33g}](#), M. Sioli [ID^{23b,23a}](#), I. Siral [ID¹²²](#), S.Yu. Sivoklokov [ID^{37,*}](#), J. Sjölin [ID^{47a,47b}](#),
 A. Skaf [ID⁵⁵](#), E. Skorda [ID⁹⁷](#), P. Skubic [ID¹¹⁹](#), M. Slawinska [ID⁸⁵](#), V. Smakhtin [ID¹⁶⁸](#), B.H. Smart [ID¹³³](#),
 J. Smiesko [ID³⁶](#), S.Yu. Smirnov [ID³⁷](#), Y. Smirnov [ID³⁷](#), L.N. Smirnova [ID^{37,a}](#), O. Smirnova [ID⁹⁷](#),
 A.C. Smith [ID⁴¹](#), E.A. Smith [ID³⁹](#), H.A. Smith [ID¹²⁵](#), J.L. Smith [ID⁹¹](#), R. Smith [ID¹⁴²](#), M. Smizanska [ID⁹⁰](#),
 K. Smolek [ID¹³¹](#), A. Smykiewicz [ID⁸⁵](#), A.A. Snesarev [ID³⁷](#), H.L. Snoek [ID¹¹³](#), S. Snyder [ID²⁹](#),
 R. Sobie [ID^{164,x}](#), A. Soffer [ID¹⁵⁰](#), C.A. Solans Sanchez [ID³⁶](#), E.Yu. Soldatov [ID³⁷](#), U. Soldevila [ID¹⁶²](#),
 A.A. Solodkov [ID³⁷](#), S. Solomon [ID⁵⁴](#), A. Soloshenko [ID³⁸](#), K. Solovieva [ID⁵⁴](#), O.V. Solovyanov [ID³⁷](#),
 V. Solovyev [ID³⁷](#), P. Sommer [ID³⁶](#), A. Sonay [ID¹³](#), W.Y. Song [ID^{155b}](#), A. Sopczak [ID¹³¹](#), A.L. Sopio [ID⁹⁵](#),
 F. Sopkova [ID^{28b}](#), V. Sothilingam [ID^{63a}](#), S. Sottocornola [ID^{72a,72b}](#), R. Soualah [ID^{115b}](#), Z. Soumaimi [ID^{35e}](#),
 D. South [ID⁴⁸](#), S. Spagnolo [ID^{69a,69b}](#), M. Spalla [ID¹⁰⁹](#), F. Spanò [ID⁹⁴](#), D. Sperlich [ID⁵⁴](#), G. Spigo [ID³⁶](#),
 M. Spina [ID¹⁴⁵](#), S. Spinali [ID⁹⁰](#), D.P. Spiteri [ID⁵⁹](#), M. Spousta [ID¹³²](#), E.J. Staats [ID³⁴](#), A. Stabile [ID^{70a,70b}](#),
 R. Stamen [ID^{63a}](#), M. Stamenkovic [ID¹¹³](#), A. Stampekitis [ID²⁰](#), M. Standke [ID²⁴](#), E. Stanecka [ID⁸⁵](#),
 M.V. Stange [ID⁵⁰](#), B. Stanislaus [ID^{17a}](#), M.M. Stanitzki [ID⁴⁸](#), M. Stankaityte [ID¹²⁵](#), B. Stapf [ID⁴⁸](#),
 E.A. Starchenko [ID³⁷](#), G.H. Stark [ID¹³⁵](#), J. Stark [ID^{101,aa}](#), D.M. Starko [ID^{155b}](#), P. Staroba [ID¹³⁰](#),
 P. Starovoitov [ID^{63a}](#), S. Stärz [ID¹⁰³](#), R. Staszewski [ID⁸⁵](#), G. Stavropoulos [ID⁴⁶](#), J. Steentoft [ID¹⁶⁰](#),
 P. Steinberg [ID²⁹](#), A.L. Steinhebel [ID¹²²](#), B. Stelzer [ID^{141,155a}](#), H.J. Stelzer [ID¹²⁸](#), O. Stelzer-Chilton [ID^{155a}](#),
 H. Stenzel [ID⁵⁸](#), T.J. Stevenson [ID¹⁴⁵](#), G.A. Stewart [ID³⁶](#), M.C. Stockton [ID³⁶](#), G. Stoicea [ID^{27b}](#),
 M. Stolarski [ID^{129a}](#), S. Stonjek [ID¹⁰⁹](#), A. Straessner [ID⁵⁰](#), J. Strandberg [ID¹⁴³](#), S. Strandberg [ID^{47a,47b}](#),
 M. Strauss [ID¹¹⁹](#), T. Strebler [ID¹⁰¹](#), P. Strizenec [ID^{28b}](#), R. Ströhmer [ID¹⁶⁵](#), D.M. Strom [ID¹²²](#), L.R. Strom [ID⁴⁸](#),
 R. Stroynowski [ID⁴⁴](#), A. Strubig [ID^{47a,47b}](#), S.A. Stucci [ID²⁹](#), B. Stugu [ID¹⁶](#), J. Stupak [ID¹¹⁹](#), N.A. Styles [ID⁴⁸](#),
 D. Su [ID¹⁴²](#), S. Su [ID^{62a}](#), W. Su [ID^{62d,137,62c}](#), X. Su [ID^{62a,66}](#), K. Sugizaki [ID¹⁵²](#), V.V. Sulin [ID³⁷](#),
 M.J. Sullivan [ID⁹¹](#), D.M.S. Sultan [ID^{77a,77b}](#), L. Sultanaliyeva [ID³⁷](#), S. Sultansoy [ID^{3b}](#), T. Sumida [ID⁸⁶](#),
 S. Sun [ID¹⁰⁵](#), S. Sun [ID¹⁶⁹](#), O. Sunneborn Gudnadottir [ID¹⁶⁰](#), M.R. Sutton [ID¹⁴⁵](#), M. Svatos [ID¹³⁰](#),
 M. Swiatlowski [ID^{155a}](#), T. Swirski [ID¹⁶⁵](#), I. Sykora [ID^{28a}](#), M. Sykora [ID¹³²](#), T. Sykora [ID¹³²](#), D. Ta [ID⁹⁹](#),
 K. Tackmann [ID^{48,w}](#), A. Taffard [ID¹⁵⁹](#), R. Tafirout [ID^{155a}](#), J.S. Tafoya Vargas [ID⁶⁶](#), R.H.M. Taibah [ID¹²⁶](#),
 R. Takashima [ID⁸⁷](#), K. Takeda [ID⁸³](#), E.P. Takeva [ID⁵²](#), Y. Takubo [ID⁸²](#), M. Talby [ID¹⁰¹](#), A.A. Talyshев [ID³⁷](#),
 K.C. Tam [ID^{64b}](#), N.M. Tamir [ID¹⁵⁰](#), A. Tanaka [ID¹⁵²](#), J. Tanaka [ID¹⁵²](#), R. Tanaka [ID⁶⁶](#), M. Tanasini [ID^{57b,57a}](#),
 J. Tang [ID^{62c}](#), Z. Tao [ID¹⁶³](#), S. Tapia Araya [ID⁸⁰](#), S. Tapprogge [ID⁹⁹](#), A. Tarek Abouelfadl Mohamed [ID¹⁰⁶](#),
 S. Tarem [ID¹⁴⁹](#), K. Tariq [ID^{62b}](#), G. Tarna [ID^{27b}](#), G.F. Tartarelli [ID^{70a}](#), P. Tas [ID¹³²](#), M. Tasevsky [ID¹³⁰](#),
 E. Tassi [ID^{43b,43a}](#), A.C. Tate [ID¹⁶¹](#), G. Tateno [ID¹⁵²](#), Y. Tayalati [ID^{35e}](#), G.N. Taylor [ID¹⁰⁴](#), W. Taylor [ID^{155b}](#),
 H. Teagle [ID⁹¹](#), A.S. Tee [ID¹⁶⁹](#), R. Teixeira De Lima [ID¹⁴²](#), P. Teixeira-Dias [ID⁹⁴](#), J.J. Teoh [ID¹⁵⁴](#),
 K. Terashi [ID¹⁵²](#), J. Terron [ID⁹⁸](#), S. Terzo [ID¹³](#), M. Testa [ID⁵³](#), R.J. Teuscher [ID^{154,x}](#), A. Thaler [ID⁷⁸](#),

O. Theiner [ID⁵⁶](#), N. Themistokleous [ID⁵²](#), T. Theveneaux-Pelzer [ID¹⁸](#), O. Thielmann [ID¹⁷⁰](#), D.W. Thomas ⁹⁴, J.P. Thomas [ID²⁰](#), E.A. Thompson [ID⁴⁸](#), P.D. Thompson [ID²⁰](#), E. Thomson [ID¹²⁷](#), E.J. Thorpe [ID⁹³](#), Y. Tian [ID⁵⁵](#), V. Tikhomirov [ID^{37,a}](#), Yu.A. Tikhonov [ID³⁷](#), S. Timoshenko ³⁷, E.X.L. Ting [ID¹](#), P. Tipton [ID¹⁷¹](#), S. Tisserant [ID¹⁰¹](#), S.H. Tlou [ID^{33g}](#), A. Tnourji [ID⁴⁰](#), K. Todome [ID^{23b,23a}](#), S. Todorova-Nova [ID¹³²](#), S. Todt ⁵⁰, M. Togawa [ID⁸²](#), J. Tojo [ID⁸⁸](#), S. Tokár [ID^{28a}](#), K. Tokushuku [ID⁸²](#), R. Tombs [ID³²](#), M. Tomoto [ID^{82,110}](#), L. Tompkins [ID^{142,q}](#), K.W. Topolnicki [ID^{84b}](#), P. Tornambe [ID¹⁰²](#), E. Torrence [ID¹²²](#), H. Torres [ID⁵⁰](#), E. Torró Pastor [ID¹⁶²](#), M. Toscani [ID³⁰](#), C. Tosciri [ID³⁹](#), D.R. Tovey [ID¹³⁸](#), A. Traeet ¹⁶, I.S. Trandafir [ID^{27b}](#), T. Trefzger [ID¹⁶⁵](#), A. Tricoli [ID²⁹](#), I.M. Trigger [ID^{155a}](#), S. Trincaz-Duvold [ID¹²⁶](#), D.A. Trischuk [ID²⁶](#), B. Trocmé [ID⁶⁰](#), A. Trofymov [ID⁶⁶](#), C. Troncon [ID^{70a}](#), L. Truong [ID^{33c}](#), M. Trzebinski [ID⁸⁵](#), A. Trzupek [ID⁸⁵](#), F. Tsai [ID¹⁴⁴](#), M. Tsai [ID¹⁰⁵](#), A. Tsiamis [ID¹⁵¹](#), P.V. Tsiareshka ³⁷, S. Tsigaridas [ID^{155a}](#), A. Tsirigotis [ID^{151,u}](#), V. Tsiskaridze [ID¹⁴⁴](#), E.G. Tskhadadze ^{148a}, M. Tsopoulou [ID¹⁵¹](#), Y. Tsujikawa [ID⁸⁶](#), I.I. Tsukerman [ID³⁷](#), V. Tsulaia [ID^{17a}](#), S. Tsuno [ID⁸²](#), O. Tsur ¹⁴⁹, D. Tsybychev [ID¹⁴⁴](#), Y. Tu [ID^{64b}](#), A. Tudorache [ID^{27b}](#), V. Tudorache [ID^{27b}](#), A.N. Tuna [ID³⁶](#), S. Turchikhin [ID³⁸](#), I. Turk Cakir [ID^{3a}](#), R. Turra [ID^{70a}](#), T. Turtuvshin [ID³⁸](#), P.M. Tuts [ID⁴¹](#), S. Tzamarias [ID¹⁵¹](#), P. Tzanis [ID¹⁰](#), E. Tzovara [ID⁹⁹](#), K. Uchida ¹⁵², F. Ukegawa [ID¹⁵⁶](#), P.A. Ulloa Poblete [ID^{136c}](#), G. Unal [ID³⁶](#), M. Unal [ID¹¹](#), A. Undrus [ID²⁹](#), G. Unel [ID¹⁵⁹](#), J. Urban [ID^{28b}](#), P. Urquijo [ID¹⁰⁴](#), G. Usai [ID⁸](#), R. Ushioda [ID¹⁵³](#), M. Usman [ID¹⁰⁷](#), Z. Uysal [ID^{21b}](#), V. Vacek [ID¹³¹](#), B. Vachon [ID¹⁰³](#), K.O.H. Vadla [ID¹²⁴](#), T. Vafeiadis [ID³⁶](#), C. Valderanis [ID¹⁰⁸](#), E. Valdes Santurio [ID^{47a,47b}](#), M. Valente [ID^{155a}](#), S. Valentini [ID^{23b,23a}](#), A. Valero [ID¹⁶²](#), A. Vallier [ID^{101,aa}](#), J.A. Valls Ferrer [ID¹⁶²](#), T.R. Van Daalen [ID¹³⁷](#), P. Van Gemmeren [ID⁶](#), M. Van Rijnbach [ID^{124,36}](#), S. Van Stroud [ID⁹⁵](#), I. Van Vulpen [ID¹¹³](#), M. Vanadia [ID^{75a,75b}](#), W. Vandelli [ID³⁶](#), M. Vandebroucke [ID¹³⁴](#), E.R. Vandewall [ID¹²⁰](#), D. Vannicola [ID¹⁵⁰](#), L. Vannoli [ID^{57b,57a}](#), R. Vari [ID^{74a}](#), E.W. Varnes [ID⁷](#), C. Varni [ID^{17a}](#), T. Varol [ID¹⁴⁷](#), D. Varouchas [ID⁶⁶](#), L. Varriale [ID¹⁶²](#), K.E. Varvell [ID¹⁴⁶](#), M.E. Vasile [ID^{27b}](#), L. Vaslin ⁴⁰, G.A. Vasquez [ID¹⁶⁴](#), F. Vazeille [ID⁴⁰](#), T. Vazquez Schroeder [ID³⁶](#), J. Veatch [ID³¹](#), V. Vecchio [ID¹⁰⁰](#), M.J. Veen [ID¹⁰²](#), I. Veliscek [ID¹²⁵](#), L.M. Veloce [ID¹⁵⁴](#), F. Veloso [ID^{129a,129c}](#), S. Veneziano [ID^{74a}](#), A. Ventura [ID^{69a,69b}](#), A. Verbytskyi [ID¹⁰⁹](#), M. Verducci [ID^{73a,73b}](#), C. Vergis [ID²⁴](#), M. Verissimo De Araujo [ID^{81b}](#), W. Verkerke [ID¹¹³](#), J.C. Vermeulen [ID¹¹³](#), C. Vernieri [ID¹⁴²](#), P.J. Verschuuren [ID⁹⁴](#), M. Vessella [ID¹⁰²](#), M.C. Vetterli [ID^{141,af}](#), A. Vgenopoulos [ID¹⁵¹](#), N. Viaux Maira [ID^{136f}](#), T. Vickey [ID¹³⁸](#), O.E. Vickey Boeriu [ID¹³⁸](#), G.H.A. Viehhauser [ID¹²⁵](#), L. Vigani [ID^{63b}](#), M. Villa [ID^{23b,23a}](#), M. Villaplana Perez [ID¹⁶²](#), E.M. Villhauer ⁵², E. Vilucchi [ID⁵³](#), M.G. Vincter [ID³⁴](#), G.S. Virdee [ID²⁰](#), A. Vishwakarma [ID⁵²](#), C. Vittori [ID^{23b,23a}](#), I. Vivarelli [ID¹⁴⁵](#), V. Vladimirov ¹⁶⁶, E. Voevodina [ID¹⁰⁹](#), F. Vogel [ID¹⁰⁸](#), P. Vokac [ID¹³¹](#), J. Von Ahnen [ID⁴⁸](#), E. Von Toerne [ID²⁴](#), B. Vormwald [ID³⁶](#), V. Vorobel [ID¹³²](#), K. Vorobev [ID³⁷](#), M. Vos [ID¹⁶²](#), J.H. Vossebeld [ID⁹¹](#), M. Vozak [ID¹¹³](#), L. Vozdecky [ID⁹³](#), N. Vranjes [ID¹⁵](#), M. Vranjes Milosavljevic [ID¹⁵](#), M. Vreeswijk [ID¹¹³](#), R. Vuillermet [ID³⁶](#), O. Vujinovic [ID⁹⁹](#), I. Vukotic [ID³⁹](#), S. Wada [ID¹⁵⁶](#), C. Wagner ¹⁰², W. Wagner [ID¹⁷⁰](#), S. Wahdan [ID¹⁷⁰](#), H. Wahlberg [ID⁸⁹](#), R. Wakasa [ID¹⁵⁶](#), M. Wakida [ID¹¹⁰](#), V.M. Walbrecht [ID¹⁰⁹](#), J. Walder [ID¹³³](#), R. Walker [ID¹⁰⁸](#), W. Walkowiak [ID¹⁴⁰](#), A.M. Wang [ID⁶¹](#), A.Z. Wang [ID¹⁶⁹](#), C. Wang [ID^{62a}](#), C. Wang [ID^{62c}](#), H. Wang [ID^{17a}](#), J. Wang [ID^{64a}](#), P. Wang [ID⁴⁴](#), R.-J. Wang [ID⁹⁹](#), R. Wang [ID⁶¹](#), R. Wang [ID⁶](#), S.M. Wang [ID¹⁴⁷](#), S. Wang [ID^{62b}](#), T. Wang [ID^{62a}](#), W.T. Wang [ID⁷⁹](#), W.X. Wang [ID^{62a}](#), X. Wang [ID^{14c}](#), X. Wang [ID¹⁶¹](#), X. Wang [ID^{62c}](#), Y. Wang [ID^{62d}](#), Y. Wang [ID^{14c}](#), Z. Wang [ID¹⁰⁵](#), Z. Wang [ID^{62d,51,62c}](#), Z. Wang [ID¹⁰⁵](#), A. Warburton [ID¹⁰³](#), R.J. Ward [ID²⁰](#), N. Warrack [ID⁵⁹](#), A.T. Watson [ID²⁰](#), M.F. Watson [ID²⁰](#), G. Watts [ID¹³⁷](#), B.M. Waugh [ID⁹⁵](#), A.F. Webb [ID¹¹](#), C. Weber [ID²⁹](#), M.S. Weber [ID¹⁹](#), S.M. Weber [ID^{63a}](#), C. Wei [ID^{62a}](#), Y. Wei [ID¹²⁵](#), A.R. Weidberg [ID¹²⁵](#), J. Weingarten [ID⁴⁹](#), M. Weirich [ID⁹⁹](#), C. Weiser [ID⁵⁴](#), C.J. Wells [ID⁴⁸](#), T. Wenaus [ID²⁹](#), B. Wendland [ID⁴⁹](#), T. Wengler [ID³⁶](#), N.S. Wenke ¹⁰⁹, N. Wermes [ID²⁴](#), M. Wessels [ID^{63a}](#), K. Whalen [ID¹²²](#), A.M. Wharton [ID⁹⁰](#), A.S. White [ID⁶¹](#), A. White [ID⁸](#), M.J. White [ID¹](#), D. Whiteson [ID¹⁵⁹](#), L. Wickremasinghe [ID¹²³](#), W. Wiedenmann [ID¹⁶⁹](#), C. Wiel [ID⁵⁰](#), M. Wielers [ID¹³³](#), N. Wieseotte ⁹⁹, C. Wiglesworth [ID⁴²](#), L.A.M. Wiik-Fuchs [ID⁵⁴](#), D.J. Wilbern ¹¹⁹, H.G. Wilkens [ID³⁶](#), D.M. Williams [ID⁴¹](#), H.H. Williams ¹²⁷, S. Williams [ID³²](#), S. Willocq [ID¹⁰²](#), P.J. Windischhofer [ID¹²⁵](#), F. Winklmeier [ID¹²²](#), B.T. Winter [ID⁵⁴](#),

M. Wittgen¹⁴², M. Wobisch  ⁹⁶, R. Wölker  ¹²⁵, J. Wollrath¹⁵⁹, M.W. Wolter  ⁸⁵, H. Wolters  ^{129a,129c}, V.W.S. Wong  ¹⁶³, A.F. Wongel  ⁴⁸, S.D. Worm  ⁴⁸, B.K. Wosiek ⁸⁵, K.W. Woźniak ⁸⁵, K. Wright ⁵⁹, B.M. Wright ¹⁶⁴, J. Wu ^{14a,14d}, M. Wu ^{64a}, M. Wu ¹¹², S.L. Wu ¹⁶⁹, X. Wu ⁵⁶, Y. Wu ^{62a}, Z. Wu ^{134,62a}, J. Wuerzinger ¹²⁵, T.R. Wyatt ¹⁰⁰, B.M. Wynne ⁵², S. Xella ⁴², L. Xia ^{14c}, M. Xia ^{14b}, J. Xiang ^{64c}, X. Xiao ¹⁰⁵, M. Xie ^{62a}, X. Xie ^{62a}, J. Xiong ^{17a}, I. Xiotidis ¹⁴⁵, D. Xu ^{14a}, H. Xu ^{62a}, L. Xu ^{62a}, R. Xu ¹²⁷, T. Xu ¹⁰⁵, W. Xu ¹⁰⁵, Y. Xu ^{14b}, Z. Xu ^{62b}, Z. Xu ¹⁴², B. Yabsley ¹⁴⁶, S. Yacoob ^{33a}, N. Yamaguchi ⁸⁸, Y. Yamaguchi ¹⁵³, H. Yamauchi ¹⁵⁶, T. Yamazaki ^{17a}, Y. Yamazaki ⁸³, J. Yan ^{62c}, S. Yan ¹²⁵, Z. Yan ²⁵, H.J. Yang ^{62c,62d}, H.T. Yang ^{17a}, S. Yang ^{62a}, T. Yang ^{64c}, X. Yang ^{62a}, X. Yang ^{14a}, Y. Yang ⁴⁴, Z. Yang ^{62a,105}, W-M. Yao ^{17a}, Y.C. Yap ⁴⁸, H. Ye ^{14c}, J. Ye ⁴⁴, S. Ye ²⁹, X. Ye ^{62a}, Y. Yeh ⁹⁵, I. Yeletskikh ³⁸, M.R. Yexley ⁹⁰, P. Yin ⁴¹, K. Yorita ¹⁶⁷, C.J.S. Young ⁵⁴, C. Young ¹⁴², M. Yuan ¹⁰⁵, R. Yuan ^{62b,k}, L. Yue ⁹⁵, X. Yue ^{63a}, M. Zaazoua ^{35e}, B. Zabinski ⁸⁵, E. Zaid ⁵², T. Zakareishvili ^{148b}, N. Zakharchuk ³⁴, S. Zambito ⁵⁶, J.A. Zamora Saa ^{136d}, J. Zang ¹⁵², D. Zanzi ⁵⁴, O. Zaplatilek ¹³¹, S.V. Zeißner ⁴⁹, C. Zeitnitz ¹⁷⁰, J.C. Zeng ¹⁶¹, D.T. Zenger Jr ²⁶, O. Zenin ³⁷, T. Ženiš ^{28a}, S. Zenz ⁹³, S. Zerradi ^{35a}, D. Zerwas ⁶⁶, B. Zhang ^{14c}, D.F. Zhang ¹³⁸, G. Zhang ^{14b}, J. Zhang ^{62b}, J. Zhang ⁶, K. Zhang ^{14a,14d}, L. Zhang ^{14c}, P. Zhang ^{14a,14d}, R. Zhang ¹⁶⁹, S. Zhang ¹⁰⁵, T. Zhang ¹⁵², X. Zhang ^{62c}, X. Zhang ^{62b}, Z. Zhang ^{17a}, Z. Zhang ⁶⁶, H. Zhao ¹³⁷, P. Zhao ⁵¹, T. Zhao ^{62b}, Y. Zhao ¹³⁵, Z. Zhao ^{62a}, A. Zhemchugov ³⁸, X. Zheng ^{62a}, Z. Zheng ¹⁴², D. Zhong ¹⁶¹, B. Zhou ¹⁰⁵, C. Zhou ¹⁶⁹, H. Zhou ⁷, N. Zhou ^{62c}, Y. Zhou ⁷, C.G. Zhu ^{62b}, C. Zhu ^{14a,14d}, H.L. Zhu ^{62a}, H. Zhu ^{14a}, J. Zhu ¹⁰⁵, Y. Zhu ^{62c}, Y. Zhu ^{62a}, X. Zhuang ^{14a}, K. Zhukov ³⁷, V. Zhulanov ³⁷, N.I. Zimine ³⁸, J. Zinsser ^{63b}, M. Ziolkowski ¹⁴⁰, L. Živković ¹⁵, A. Zoccoli ^{23b,23a}, K. Zoch ⁵⁶, T.G. Zorbas ¹³⁸, O. Zormpa ⁴⁶, W. Zou ⁴¹, L. Zwalinski ³⁶.

¹Department of Physics, University of Adelaide, Adelaide; Australia.

²Department of Physics, University of Alberta, Edmonton AB; Canada.

^{3(a)}Department of Physics, Ankara University, Ankara; ^(b)Division of Physics, TOBB University of Economics and Technology, Ankara; Türkiye.

⁴LAPP, Université Savoie Mont Blanc, CNRS/IN2P3, Annecy; France.

⁵APC, Université Paris Cité, CNRS/IN2P3, Paris; France.

⁶High Energy Physics Division, Argonne National Laboratory, Argonne IL; United States of America.

⁷Department of Physics, University of Arizona, Tucson AZ; United States of America.

⁸Department of Physics, University of Texas at Arlington, Arlington TX; United States of America.

⁹Physics Department, National and Kapodistrian University of Athens, Athens; Greece.

¹⁰Physics Department, National Technical University of Athens, Zografou; Greece.

¹¹Department of Physics, University of Texas at Austin, Austin TX; United States of America.

¹²Institute of Physics, Azerbaijan Academy of Sciences, Baku; Azerbaijan.

¹³Institut de Física d'Altes Energies (IFAE), Barcelona Institute of Science and Technology, Barcelona; Spain.

^{14(a)}Institute of High Energy Physics, Chinese Academy of Sciences, Beijing; ^(b)Physics Department, Tsinghua University, Beijing; ^(c)Department of Physics, Nanjing University, Nanjing; ^(d)University of Chinese Academy of Science (UCAS), Beijing; China.

¹⁵Institute of Physics, University of Belgrade, Belgrade; Serbia.

¹⁶Department for Physics and Technology, University of Bergen, Bergen; Norway.

^{17(a)}Physics Division, Lawrence Berkeley National Laboratory, Berkeley CA; ^(b)University of California, Berkeley CA; United States of America.

¹⁸Institut für Physik, Humboldt Universität zu Berlin, Berlin; Germany.

- ¹⁹Albert Einstein Center for Fundamental Physics and Laboratory for High Energy Physics, University of Bern, Bern; Switzerland.
- ²⁰School of Physics and Astronomy, University of Birmingham, Birmingham; United Kingdom.
- ²¹^(a)Department of Physics, Bogazici University, Istanbul;^(b)Department of Physics Engineering, Gaziantep University, Gaziantep;^(c)Department of Physics, Istanbul University, Istanbul;^(d)Istinye University, Sariyer, Istanbul; Türkiye.
- ²²^(a)Facultad de Ciencias y Centro de Investigaciones, Universidad Antonio Nariño, Bogotá;^(b)Departamento de Física, Universidad Nacional de Colombia, Bogotá; Colombia.
- ²³^(a)Dipartimento di Fisica e Astronomia A. Righi, Università di Bologna, Bologna;^(b)INFN Sezione di Bologna; Italy.
- ²⁴Physikalisches Institut, Universität Bonn, Bonn; Germany.
- ²⁵Department of Physics, Boston University, Boston MA; United States of America.
- ²⁶Department of Physics, Brandeis University, Waltham MA; United States of America.
- ²⁷^(a)Transilvania University of Brasov, Brasov;^(b)Horia Hulubei National Institute of Physics and Nuclear Engineering, Bucharest;^(c)Department of Physics, Alexandru Ioan Cuza University of Iasi, Iasi;^(d)National Institute for Research and Development of Isotopic and Molecular Technologies, Physics Department, Cluj-Napoca;^(e)University Politehnica Bucharest, Bucharest;^(f)West University in Timisoara, Timisoara;^(g)Faculty of Physics, University of Bucharest, Bucharest; Romania.
- ²⁸^(a)Faculty of Mathematics, Physics and Informatics, Comenius University, Bratislava;^(b)Department of Subnuclear Physics, Institute of Experimental Physics of the Slovak Academy of Sciences, Kosice; Slovak Republic.
- ²⁹Physics Department, Brookhaven National Laboratory, Upton NY; United States of America.
- ³⁰Universidad de Buenos Aires, Facultad de Ciencias Exactas y Naturales, Departamento de Física, y CONICET, Instituto de Física de Buenos Aires (IFIBA), Buenos Aires; Argentina.
- ³¹California State University, CA; United States of America.
- ³²Cavendish Laboratory, University of Cambridge, Cambridge; United Kingdom.
- ³³^(a)Department of Physics, University of Cape Town, Cape Town;^(b)iThemba Labs, Western Cape;^(c)Department of Mechanical Engineering Science, University of Johannesburg, Johannesburg;^(d)National Institute of Physics, University of the Philippines Diliman (Philippines);^(e)University of South Africa, Department of Physics, Pretoria;^(f)University of Zululand, KwaDlangezwa;^(g)School of Physics, University of the Witwatersrand, Johannesburg; South Africa.
- ³⁴Department of Physics, Carleton University, Ottawa ON; Canada.
- ³⁵^(a)Faculté des Sciences Ain Chock, Réseau Universitaire de Physique des Hautes Energies - Université Hassan II, Casablanca;^(b)Faculté des Sciences, Université Ibn-Tofail, Kénitra;^(c)Faculté des Sciences Semlalia, Université Cadi Ayyad, LPHEA-Marrakech;^(d)LPMR, Faculté des Sciences, Université Mohamed Premier, Oujda;^(e)Faculté des sciences, Université Mohammed V, Rabat;^(f)Institute of Applied Physics, Mohammed VI Polytechnic University, Ben Guerir; Morocco.
- ³⁶CERN, Geneva; Switzerland.
- ³⁷Affiliated with an institute covered by a cooperation agreement with CERN.
- ³⁸Affiliated with an international laboratory covered by a cooperation agreement with CERN.
- ³⁹Enrico Fermi Institute, University of Chicago, Chicago IL; United States of America.
- ⁴⁰LPC, Université Clermont Auvergne, CNRS/IN2P3, Clermont-Ferrand; France.
- ⁴¹Nevis Laboratory, Columbia University, Irvington NY; United States of America.
- ⁴²Niels Bohr Institute, University of Copenhagen, Copenhagen; Denmark.
- ⁴³^(a)Dipartimento di Fisica, Università della Calabria, Rende;^(b)INFN Gruppo Collegato di Cosenza, Laboratori Nazionali di Frascati; Italy.
- ⁴⁴Physics Department, Southern Methodist University, Dallas TX; United States of America.

- ⁴⁵Physics Department, University of Texas at Dallas, Richardson TX; United States of America.
- ⁴⁶National Centre for Scientific Research "Demokritos", Agia Paraskevi; Greece.
- ^{47(a)}Department of Physics, Stockholm University;^(b)Oskar Klein Centre, Stockholm; Sweden.
- ⁴⁸Deutsches Elektronen-Synchrotron DESY, Hamburg and Zeuthen; Germany.
- ⁴⁹Fakultät Physik , Technische Universität Dortmund, Dortmund; Germany.
- ⁵⁰Institut für Kern- und Teilchenphysik, Technische Universität Dresden, Dresden; Germany.
- ⁵¹Department of Physics, Duke University, Durham NC; United States of America.
- ⁵²SUPA - School of Physics and Astronomy, University of Edinburgh, Edinburgh; United Kingdom.
- ⁵³INFN e Laboratori Nazionali di Frascati, Frascati; Italy.
- ⁵⁴Physikalisches Institut, Albert-Ludwigs-Universität Freiburg, Freiburg; Germany.
- ⁵⁵II. Physikalisches Institut, Georg-August-Universität Göttingen, Göttingen; Germany.
- ⁵⁶Département de Physique Nucléaire et Corpusculaire, Université de Genève, Genève; Switzerland.
- ^{57(a)}Dipartimento di Fisica, Università di Genova, Genova;^(b)INFN Sezione di Genova; Italy.
- ⁵⁸II. Physikalisches Institut, Justus-Liebig-Universität Giessen, Giessen; Germany.
- ⁵⁹SUPA - School of Physics and Astronomy, University of Glasgow, Glasgow; United Kingdom.
- ⁶⁰LPSC, Université Grenoble Alpes, CNRS/IN2P3, Grenoble INP, Grenoble; France.
- ⁶¹Laboratory for Particle Physics and Cosmology, Harvard University, Cambridge MA; United States of America.
- ^{62(a)}Department of Modern Physics and State Key Laboratory of Particle Detection and Electronics, University of Science and Technology of China, Hefei;^(b)Institute of Frontier and Interdisciplinary Science and Key Laboratory of Particle Physics and Particle Irradiation (MOE), Shandong University, Qingdao;^(c)School of Physics and Astronomy, Shanghai Jiao Tong University, Key Laboratory for Particle Astrophysics and Cosmology (MOE), SKLPPC, Shanghai;^(d)Tsung-Dao Lee Institute, Shanghai; China.
- ^{63(a)}Kirchhoff-Institut für Physik, Ruprecht-Karls-Universität Heidelberg, Heidelberg;^(b)Physikalisches Institut, Ruprecht-Karls-Universität Heidelberg, Heidelberg; Germany.
- ^{64(a)}Department of Physics, Chinese University of Hong Kong, Shatin, N.T., Hong Kong;^(b)Department of Physics, University of Hong Kong, Hong Kong;^(c)Department of Physics and Institute for Advanced Study, Hong Kong University of Science and Technology, Clear Water Bay, Kowloon, Hong Kong; China.
- ⁶⁵Department of Physics, National Tsing Hua University, Hsinchu; Taiwan.
- ⁶⁶IJCLab, Université Paris-Saclay, CNRS/IN2P3, 91405, Orsay; France.
- ⁶⁷Department of Physics, Indiana University, Bloomington IN; United States of America.
- ^{68(a)}INFN Gruppo Collegato di Udine, Sezione di Trieste, Udine;^(b)ICTP, Trieste;^(c)Dipartimento Politecnico di Ingegneria e Architettura, Università di Udine, Udine; Italy.
- ^{69(a)}INFN Sezione di Lecce;^(b)Dipartimento di Matematica e Fisica, Università del Salento, Lecce; Italy.
- ^{70(a)}INFN Sezione di Milano;^(b)Dipartimento di Fisica, Università di Milano, Milano; Italy.
- ^{71(a)}INFN Sezione di Napoli;^(b)Dipartimento di Fisica, Università di Napoli, Napoli; Italy.
- ^{72(a)}INFN Sezione di Pavia;^(b)Dipartimento di Fisica, Università di Pavia, Pavia; Italy.
- ^{73(a)}INFN Sezione di Pisa;^(b)Dipartimento di Fisica E. Fermi, Università di Pisa, Pisa; Italy.
- ^{74(a)}INFN Sezione di Roma;^(b)Dipartimento di Fisica, Sapienza Università di Roma, Roma; Italy.
- ^{75(a)}INFN Sezione di Roma Tor Vergata;^(b)Dipartimento di Fisica, Università di Roma Tor Vergata, Roma; Italy.
- ^{76(a)}INFN Sezione di Roma Tre;^(b)Dipartimento di Matematica e Fisica, Università Roma Tre, Roma; Italy.
- ^{77(a)}INFN-TIFPA;^(b)Università degli Studi di Trento, Trento; Italy.
- ⁷⁸Universität Innsbruck, Department of Astro and Particle Physics, Innsbruck; Austria.
- ⁷⁹University of Iowa, Iowa City IA; United States of America.
- ⁸⁰Department of Physics and Astronomy, Iowa State University, Ames IA; United States of America.

- ⁸¹^(a) Departamento de Engenharia Elétrica, Universidade Federal de Juiz de Fora (UFJF), Juiz de Fora; ^(b) Universidade Federal do Rio De Janeiro COPPE/EE/IF, Rio de Janeiro; ^(c) Instituto de Física, Universidade de São Paulo, São Paulo; ^(d) Rio de Janeiro State University, Rio de Janeiro; Brazil.
- ⁸² KEK, High Energy Accelerator Research Organization, Tsukuba; Japan.
- ⁸³ Graduate School of Science, Kobe University, Kobe; Japan.
- ⁸⁴^(a) AGH University of Science and Technology, Faculty of Physics and Applied Computer Science, Krakow; ^(b) Marian Smoluchowski Institute of Physics, Jagiellonian University, Krakow; Poland.
- ⁸⁵ Institute of Nuclear Physics Polish Academy of Sciences, Krakow; Poland.
- ⁸⁶ Faculty of Science, Kyoto University, Kyoto; Japan.
- ⁸⁷ Kyoto University of Education, Kyoto; Japan.
- ⁸⁸ Research Center for Advanced Particle Physics and Department of Physics, Kyushu University, Fukuoka ; Japan.
- ⁸⁹ Instituto de Física La Plata, Universidad Nacional de La Plata and CONICET, La Plata; Argentina.
- ⁹⁰ Physics Department, Lancaster University, Lancaster; United Kingdom.
- ⁹¹ Oliver Lodge Laboratory, University of Liverpool, Liverpool; United Kingdom.
- ⁹² Department of Experimental Particle Physics, Jožef Stefan Institute and Department of Physics, University of Ljubljana, Ljubljana; Slovenia.
- ⁹³ School of Physics and Astronomy, Queen Mary University of London, London; United Kingdom.
- ⁹⁴ Department of Physics, Royal Holloway University of London, Egham; United Kingdom.
- ⁹⁵ Department of Physics and Astronomy, University College London, London; United Kingdom.
- ⁹⁶ Louisiana Tech University, Ruston LA; United States of America.
- ⁹⁷ Fysiska institutionen, Lunds universitet, Lund; Sweden.
- ⁹⁸ Departamento de Física Teorica C-15 and CIAFF, Universidad Autónoma de Madrid, Madrid; Spain.
- ⁹⁹ Institut für Physik, Universität Mainz, Mainz; Germany.
- ¹⁰⁰ School of Physics and Astronomy, University of Manchester, Manchester; United Kingdom.
- ¹⁰¹ CPPM, Aix-Marseille Université, CNRS/IN2P3, Marseille; France.
- ¹⁰² Department of Physics, University of Massachusetts, Amherst MA; United States of America.
- ¹⁰³ Department of Physics, McGill University, Montreal QC; Canada.
- ¹⁰⁴ School of Physics, University of Melbourne, Victoria; Australia.
- ¹⁰⁵ Department of Physics, University of Michigan, Ann Arbor MI; United States of America.
- ¹⁰⁶ Department of Physics and Astronomy, Michigan State University, East Lansing MI; United States of America.
- ¹⁰⁷ Group of Particle Physics, University of Montreal, Montreal QC; Canada.
- ¹⁰⁸ Fakultät für Physik, Ludwig-Maximilians-Universität München, München; Germany.
- ¹⁰⁹ Max-Planck-Institut für Physik (Werner-Heisenberg-Institut), München; Germany.
- ¹¹⁰ Graduate School of Science and Kobayashi-Maskawa Institute, Nagoya University, Nagoya; Japan.
- ¹¹¹ Department of Physics and Astronomy, University of New Mexico, Albuquerque NM; United States of America.
- ¹¹² Institute for Mathematics, Astrophysics and Particle Physics, Radboud University/Nikhef, Nijmegen; Netherlands.
- ¹¹³ Nikhef National Institute for Subatomic Physics and University of Amsterdam, Amsterdam; Netherlands.
- ¹¹⁴ Department of Physics, Northern Illinois University, DeKalb IL; United States of America.
- ¹¹⁵^(a) New York University Abu Dhabi, Abu Dhabi; ^(b) University of Sharjah, Sharjah; United Arab Emirates.
- ¹¹⁶ Department of Physics, New York University, New York NY; United States of America.
- ¹¹⁷ Ochanomizu University, Otsuka, Bunkyo-ku, Tokyo; Japan.

- ¹¹⁸Ohio State University, Columbus OH; United States of America.
- ¹¹⁹Homer L. Dodge Department of Physics and Astronomy, University of Oklahoma, Norman OK; United States of America.
- ¹²⁰Department of Physics, Oklahoma State University, Stillwater OK; United States of America.
- ¹²¹Palacký University, Joint Laboratory of Optics, Olomouc; Czech Republic.
- ¹²²Institute for Fundamental Science, University of Oregon, Eugene, OR; United States of America.
- ¹²³Graduate School of Science, Osaka University, Osaka; Japan.
- ¹²⁴Department of Physics, University of Oslo, Oslo; Norway.
- ¹²⁵Department of Physics, Oxford University, Oxford; United Kingdom.
- ¹²⁶LPNHE, Sorbonne Université, Université Paris Cité, CNRS/IN2P3, Paris; France.
- ¹²⁷Department of Physics, University of Pennsylvania, Philadelphia PA; United States of America.
- ¹²⁸Department of Physics and Astronomy, University of Pittsburgh, Pittsburgh PA; United States of America.
- ^{129(a)}Laboratório de Instrumentação e Física Experimental de Partículas - LIP, Lisboa;^(b)Departamento de Física, Faculdade de Ciências, Universidade de Lisboa, Lisboa;^(c)Departamento de Física, Universidade de Coimbra, Coimbra;^(d)Centro de Física Nuclear da Universidade de Lisboa, Lisboa;^(e)Departamento de Física, Universidade do Minho, Braga;^(f)Departamento de Física Teórica y del Cosmos, Universidad de Granada, Granada (Spain);^(g)Departamento de Física, Instituto Superior Técnico, Universidade de Lisboa, Lisboa; Portugal.
- ¹³⁰Institute of Physics of the Czech Academy of Sciences, Prague; Czech Republic.
- ¹³¹Czech Technical University in Prague, Prague; Czech Republic.
- ¹³²Charles University, Faculty of Mathematics and Physics, Prague; Czech Republic.
- ¹³³Particle Physics Department, Rutherford Appleton Laboratory, Didcot; United Kingdom.
- ¹³⁴IRFU, CEA, Université Paris-Saclay, Gif-sur-Yvette; France.
- ¹³⁵Santa Cruz Institute for Particle Physics, University of California Santa Cruz, Santa Cruz CA; United States of America.
- ^{136(a)}Departamento de Física, Pontificia Universidad Católica de Chile, Santiago;^(b)Millennium Institute for Subatomic physics at high energy frontier (SAPHIR), Santiago;^(c)Instituto de Investigación Multidisciplinario en Ciencia y Tecnología, y Departamento de Física, Universidad de La Serena;^(d)Universidad Andres Bello, Department of Physics, Santiago;^(e)Instituto de Alta Investigación, Universidad de Tarapacá, Arica;^(f)Departamento de Física, Universidad Técnica Federico Santa María, Valparaíso; Chile.
- ¹³⁷Department of Physics, University of Washington, Seattle WA; United States of America.
- ¹³⁸Department of Physics and Astronomy, University of Sheffield, Sheffield; United Kingdom.
- ¹³⁹Department of Physics, Shinshu University, Nagano; Japan.
- ¹⁴⁰Department Physik, Universität Siegen, Siegen; Germany.
- ¹⁴¹Department of Physics, Simon Fraser University, Burnaby BC; Canada.
- ¹⁴²SLAC National Accelerator Laboratory, Stanford CA; United States of America.
- ¹⁴³Department of Physics, Royal Institute of Technology, Stockholm; Sweden.
- ¹⁴⁴Departments of Physics and Astronomy, Stony Brook University, Stony Brook NY; United States of America.
- ¹⁴⁵Department of Physics and Astronomy, University of Sussex, Brighton; United Kingdom.
- ¹⁴⁶School of Physics, University of Sydney, Sydney; Australia.
- ¹⁴⁷Institute of Physics, Academia Sinica, Taipei; Taiwan.
- ^{148(a)}E. Andronikashvili Institute of Physics, Iv. Javakhishvili Tbilisi State University, Tbilisi;^(b)High Energy Physics Institute, Tbilisi State University, Tbilisi;^(c)University of Georgia, Tbilisi; Georgia.
- ¹⁴⁹Department of Physics, Technion, Israel Institute of Technology, Haifa; Israel.

- ¹⁵⁰Raymond and Beverly Sackler School of Physics and Astronomy, Tel Aviv University, Tel Aviv; Israel.
- ¹⁵¹Department of Physics, Aristotle University of Thessaloniki, Thessaloniki; Greece.
- ¹⁵²International Center for Elementary Particle Physics and Department of Physics, University of Tokyo, Tokyo; Japan.
- ¹⁵³Department of Physics, Tokyo Institute of Technology, Tokyo; Japan.
- ¹⁵⁴Department of Physics, University of Toronto, Toronto ON; Canada.
- ¹⁵⁵^(a)TRIUMF, Vancouver BC; ^(b)Department of Physics and Astronomy, York University, Toronto ON; Canada.
- ¹⁵⁶Division of Physics and Tomonaga Center for the History of the Universe, Faculty of Pure and Applied Sciences, University of Tsukuba, Tsukuba; Japan.
- ¹⁵⁷Department of Physics and Astronomy, Tufts University, Medford MA; United States of America.
- ¹⁵⁸United Arab Emirates University, Al Ain; United Arab Emirates.
- ¹⁵⁹Department of Physics and Astronomy, University of California Irvine, Irvine CA; United States of America.
- ¹⁶⁰Department of Physics and Astronomy, University of Uppsala, Uppsala; Sweden.
- ¹⁶¹Department of Physics, University of Illinois, Urbana IL; United States of America.
- ¹⁶²Instituto de Física Corpuscular (IFIC), Centro Mixto Universidad de Valencia - CSIC, Valencia; Spain.
- ¹⁶³Department of Physics, University of British Columbia, Vancouver BC; Canada.
- ¹⁶⁴Department of Physics and Astronomy, University of Victoria, Victoria BC; Canada.
- ¹⁶⁵Fakultät für Physik und Astronomie, Julius-Maximilians-Universität Würzburg, Würzburg; Germany.
- ¹⁶⁶Department of Physics, University of Warwick, Coventry; United Kingdom.
- ¹⁶⁷Waseda University, Tokyo; Japan.
- ¹⁶⁸Department of Particle Physics and Astrophysics, Weizmann Institute of Science, Rehovot; Israel.
- ¹⁶⁹Department of Physics, University of Wisconsin, Madison WI; United States of America.
- ¹⁷⁰Fakultät für Mathematik und Naturwissenschaften, Fachgruppe Physik, Bergische Universität Wuppertal, Wuppertal; Germany.
- ¹⁷¹Department of Physics, Yale University, New Haven CT; United States of America.
- ^a Also Affiliated with an institute covered by a cooperation agreement with CERN.
- ^b Also at An-Najah National University, Nablus; Palestine.
- ^c Also at Borough of Manhattan Community College, City University of New York, New York NY; United States of America.
- ^d Also at Bruno Kessler Foundation, Trento; Italy.
- ^e Also at Center for High Energy Physics, Peking University; China.
- ^f Also at Centro Studi e Ricerche Enrico Fermi; Italy.
- ^g Also at CERN, Geneva; Switzerland.
- ^h Also at Département de Physique Nucléaire et Corpusculaire, Université de Genève, Genève; Switzerland.
- ⁱ Also at Departament de Fisica de la Universitat Autònoma de Barcelona, Barcelona; Spain.
- ^j Also at Department of Financial and Management Engineering, University of the Aegean, Chios; Greece.
- ^k Also at Department of Physics and Astronomy, Michigan State University, East Lansing MI; United States of America.
- ^l Also at Department of Physics and Astronomy, University of Louisville, Louisville, KY; United States of America.
- ^m Also at Department of Physics, Ben Gurion University of the Negev, Beer Sheva; Israel.
- ⁿ Also at Department of Physics, California State University, East Bay; United States of America.
- ^o Also at Department of Physics, California State University, Sacramento; United States of America.
- ^p Also at Department of Physics, King's College London, London; United Kingdom.

^q Also at Department of Physics, Stanford University, Stanford CA; United States of America.

^r Also at Department of Physics, University of Fribourg, Fribourg; Switzerland.

^s Also at Department of Physics, University of Thessaly; Greece.

^t Also at Department of Physics, Westmont College, Santa Barbara; United States of America.

^u Also at Hellenic Open University, Patras; Greece.

^v Also at Institutio Catalana de Recerca i Estudis Avancats, ICREA, Barcelona; Spain.

^w Also at Institut für Experimentalphysik, Universität Hamburg, Hamburg; Germany.

^x Also at Institute of Particle Physics (IPP); Canada.

^y Also at Institute of Physics, Azerbaijan Academy of Sciences, Baku; Azerbaijan.

^z Also at Institute of Theoretical Physics, Ilia State University, Tbilisi; Georgia.

^{aa} Also at L2IT, Université de Toulouse, CNRS/IN2P3, UPS, Toulouse; France.

^{ab} Also at Lawrence Livermore National Laboratory, Livermore; United States of America.

^{ac} Also at National Institute of Physics, University of the Philippines Diliman (Philippines); Philippines.

^{ad} Also at Technical University of Munich, Munich; Germany.

^{ae} Also at The Collaborative Innovation Center of Quantum Matter (CICQM), Beijing; China.

^{af} Also at TRIUMF, Vancouver BC; Canada.

^{ag} Also at Università di Napoli Parthenope, Napoli; Italy.

^{ah} Also at University of Chinese Academy of Sciences (UCAS), Beijing; China.

^{ai} Also at University of Colorado Boulder, Department of Physics, Colorado; United States of America.

^{aj} Also at Washington College, Maryland; United States of America.

^{ak} Also at Yeditepe University, Physics Department, Istanbul; Türkiye.

* Deceased